Dissertation for Doctor of Philosophy

Novel high-throughput approaches for transforming and improving filamentous fungus *Trichoderma reesei* using a droplet-based microfluidic platform

(糸状菌*Trichoderma reesei*における油中微小液滴を用い
形質転換体および変異株のハイスループットスクリーニング系の構築)

Luu Xuan Chinh

Department of Science of Technology Innovation,
Nagaoka University of Technology, Nagaoka, Japan

October 13, 2023

Table of Contents

Chapter 1: General Introduction

1. 1 Background

The United Nations estimates the global population will rise steadily and hit 8.5 billion in 2030 and 9.7 billion by 2050 [1]. Consequently, human activities such as deforestation, fossil fuel combustion, and raising livestock have led to releasing a significant amount of global warming gases or greenhouse gases (GHGs) into the atmosphere. The rising concentration of GHGs in the atmosphere has both direct and indirect impacts including: ocean warming and acidification (through uptake of CO_2), melting of the Greenland and Arctic ice sheets, sea level rise (1.5–1.9 mm/year), threatening coastal communities and ecosystems, decreased snow cover and increased permafrost temperature, reduction in precipitation and increased occurrence of drought, extreme and unpredictable weather events, and the spread of certain diseases [2]. In 2015, the United Nations (UN) Summit adopted "the Sustainable Development Agenda 2030" to meet the needs of the present while ensuring sustainable development that preserves the earth's resources for future generations [3]. With 17 Sustainable Development Goals (SDGs) containing 169 specific targets, the UN's blueprint for achieving a happier and healthier world by 2030 (**Figure 1-1**).

Figure 1-1. Sustainable Development Goals (SDGs)

One potential solution for achieving the SDGs is to transition from a reliance on fossil fuels to a bio-based economy. Implementing bioeconomy strategies has significant potential for positively impacting the progress toward the achievement of multiple SDGs (**Figure 1-2**) [4,5]. The bioeconomy is defined as the production, utilization and conservation of biological resources (biomass and waste), including related knowledge, science, technology, and innovation, to provide information, products, processes and services across all economic sectors aiming toward a sustainable economy [5,6]. Since 2015, the European Union has implemented the Economy Action Plan, which brought together bioeconomy approaches and circular economy strategies, resulting in a new concept called "circular bioeconomy" [7]. In the EU-28, the bioeconomy contributes to a turnover of €2,3 trillion EUR (approximately ¥343 trillion) , accounting for 4.2% of the gross national product and creating 18.1 million jobs, which is 8.2% of total employment [8].

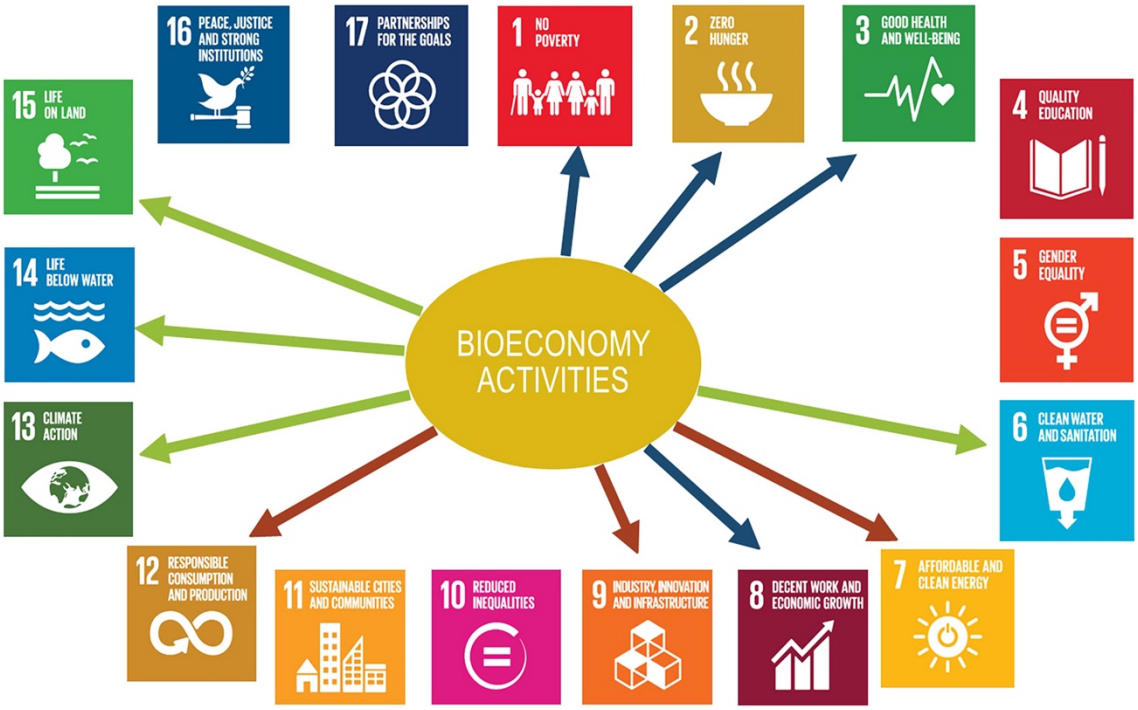

Figure 1-2: Sustainable Development Goals affected by bioeconomy activities. Blue arrow: socioeconomic targets; green arrow: ecological targets; red arrow: clean industry and economic targets [4].

1.2 Lignocellulosic biorefinery

The concept of biorefinery, which involves transforming biomass resources into valuable products such as biofuels and biochemicals, has emerged as a promising alternative to reduce the dependence on traditional fossil fuels (**Figure 1-3**). Biomass comprises both edible and non-edible sources. Edible biomass refers to starch, sugar, and oil-rich sources, while non-edible biomass includes lignocellulosic sources from crop production, residues, and organic waste [9]. When edible biomass is utilized, it may create competition with the supply chains for food and feed. On the other hand, using inedible biomass does not usually pose a significant threat to food security or have a major economic impact [10].

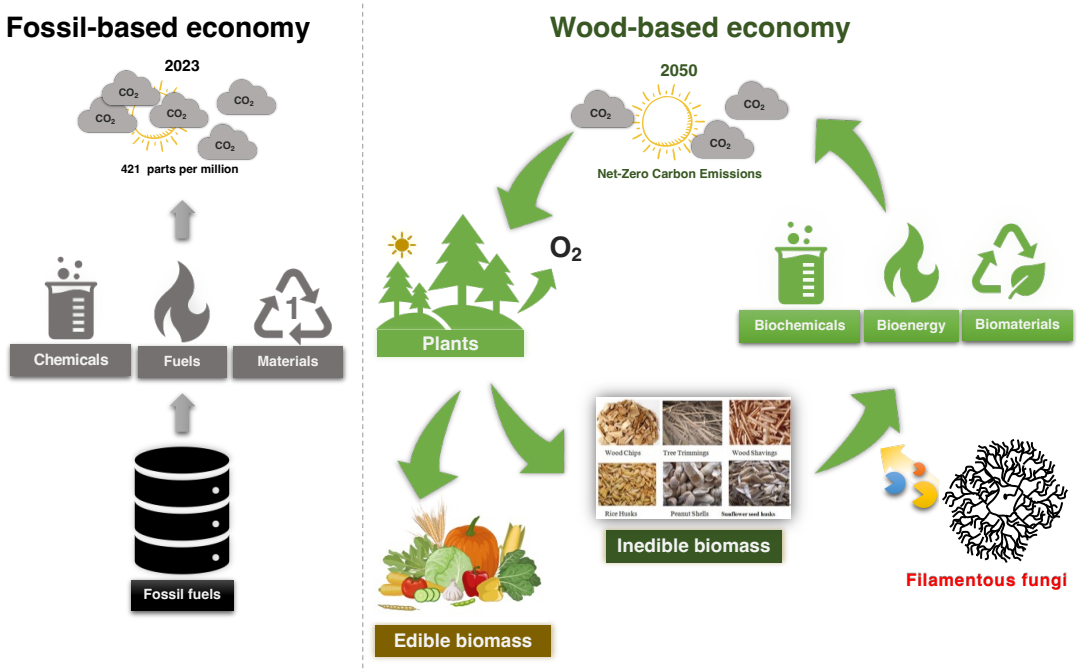

Figure 1-3. The concept of biorefinery.

Lignocellulosic biomass was reported to be the most abundant, cost-effective renewable, and sustainable bioresource for foreseeable biorefinery. Lignocellulose is a complex network of organic polymers, mainly composed of cellulose, hemicellulose, and lignin [11]. Cellulose, the main component of lignocellulosic biomass (30% - 50%), is a linear homopolysaccharide that consists of repeated glucose units linked by β-1,4 glycosidic linkages [12]. Hemicellulose contributes about 20–35% of lignocellulosic biomass and xylan is the most abundant hemicellulose in nature [12,13]. Xylan is a polysaccharide comprising d-xylose residues linked together through β-1,4 linkages [14].

Lignocellulose can be degraded to produce fermentable sugars used for the biorefinery industry as well as applied widely in food, animal feed, textile, pulp and paper, grain alcohol fermentation, starch processing, pharmaceutical, malting, and brewing industries. With these potentials, the chemical degradation of lignocellulose has been studied but not widely available because of its adverse environmental impacts. In this context, biodegradation stands out as a more efficient and environmentally friendly process in which the production of lignocellulosic biomass-degrading enzymes plays a vital role. Among biomass-degrading microorganisms, filamentous fungi have been attracted much due to their capability to produce high amounts of extracellular cellulases [15]. The study of filamentous fungi, both fundamental and applied science, presents promising solutions for the transition from the current petroleum-based economy to the circular bioeconomy. Additionally, it provides innovative approaches to address the increasing food demand for the continuously increasing global population [15].

1.3 Filamentous fungus *Trichoderma reesei* as cell factories for protein production

1.3.1 Filamentous fungus *T. reesei*

The filamentous fungus *T. reesei* (teleomorph *Hypocrea jecorina, Ascomycota*) is a well-known lignocellulolytic enzyme-producing strain in the industry [16]. Also, it is utilized as an efficient host for homologous and heterologous protein production. *T. reesei* strain QM6a was first isolated by the US Army on the Solomon Islands during the Second World War [17]. During the first oil crisis in the 1970s, *T. reesei* was employed for commercial cellulase production for bioethanol formation from lignocellulose, which is a part of the solution to the world's growing dependence on fossil fuels [18]. At the time, some cellulase-overproducing strains, such as RUT-C30 and QM9414, have been isolated and used till now [16]. Several lineages of hyper-cellulolytic mutant strains have since been generated from RUT-C30 and QM9414 (**Figure 1-4**). In 2008, the whole genome sequencing of *T. reesei* QM6a provided a comprehensive understanding of gene functions and highlighted the genetic differences between the wild-type and its improved mutants [19,20]. The *T. reesei* genome is available at the Joint Genome Institute website (http://genome.jgi psf.org/Trire2/Trire2.home.html). In 2015, there were approximately 243 commercial enzyme produced through microbial fermentations [18]. Out of these, 30 were created using *Trichoderma* as a host. These *Trichoderma*-based products have been approved for use in various industries such as bio-ethanol production, textile processing,

the chemical sector, and food and feed production [18]. With the advancement of genetic transformation techniques and genome-manipulating tools for *T. reesei*, the industrial enzyme market will continue to expand, accelerating the switch from the fossil fuel-based economy into the bio-based economy.

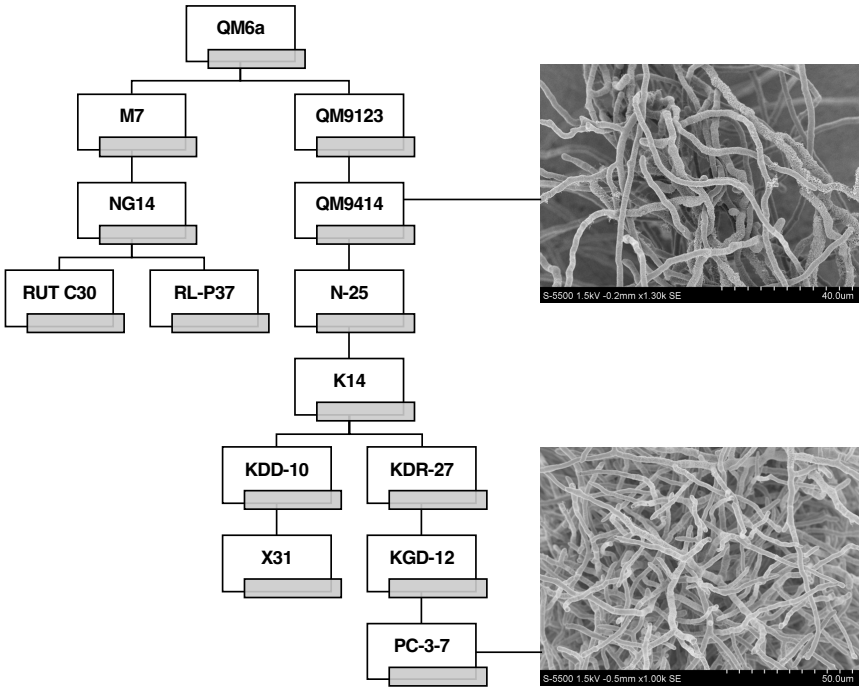

Figure 1-4. The lineages of mutants derived from QM6a [21,22]**.**

1.3.1 Extracellular protein secretion by *T. reesei*

The *T. reesei* genome contains approximately 200 genes that encode glycoside hydrolases (GHs). The expression of these genes is influenced by environmental factors such as the carbon source, pH, and temperature. It has been observed that this strain yields approximately 100 g of secreted proteins per liter during industrial fermentation [23]. The secretome has a high concentration of endo-glucanases (CEL7B/EGI, CEL5A/EG II, CEL5B, CEL12A/ EG III, CEL45A/EG V) that cleaves internal β-1,4-glucosidic bonds and exo-glucanases (CEL7A/CBHI and CEL6A/CBHII) that remove the disaccharide cellobiose from the non-reducing end of the cellulose polymer chain. These enzymes make up about 80% of the total secreted protein [24]. It has been found that the secretome contains a high percentage (over 75%) of cellobiohydrolase (CBH), with around 50-60% being CBHI and approximately 20% being CBHII [25,26]. Its β-glucosidase (CEL3A/BGLI, CEL1A, CEL3B, CEL3D, CEL1B, CEL3C, CEL3E), which hydrolyzes

the cellobiose and oligosaccharides to glucose, remains very low [24]. In addition to the traditional cellulases, *T. reesei* has recently revealed new effective auxiliary enzymes in cellulose degradation, including expansin-like proteins (SWOI, EEL1, EEL2, and EEL3) and lytic polysaccharide monooxygenases (LPMOs) [22,24].

During the cultivation of *T. reesei* on lignocellulose, various hemicellulose hydrolyzing enzyme or hemicellulases were quantified using iTRAQ [27]. These enzymes included xylanases (GH11 and GH30), arabinofuranosidases (GH54 and GH62), β-xylosidases (GH52, GH43), β-glucuronidase (GH79), acetyl xylan esterase (AXE, EC 3.1.1.72), and acetyl esterase. Endo-β-1,4-xylanase, which catalyzes the hydrolysis of 1,4-β-D-xylosidic linkages in xylan to short xylooligosaccharides of varying length, is the most prominent hemicellulose of *T. reesei* [27].

Lignin degradation mechanism is reliant on H_2O_2 as oxidant in the peroxidative reactions [24]. It has been observed that the secretome of *T. reesei* and other *Trichoderma* strains contain laccase that oxidizes various phenolic compounds [28,29]. In addition to major lignin-degrading peroxidases, a group of oxidoreductase family plays a significant role in generating highly reactive free radicals. When *T. reesei* was cultured with lignocellulosic biomasses, it resulted in the expression of the oxidoreductase family (peroxidase/catalase, glyoxal oxidase, glutathione reductase, and glutathione S-transferase glyoxalase) [30].

Apart from cellulases, hemicellulases, and lignin-degrading proteins, the secretome of *T. reesei* QM6a and its mutant strains contain peptidases, chitinases, phosphatase, transport proteins, and hypothetical proteins [24].

1.3.2 Heterologous protein production in *T. reesei*

T. reesei has been utilized as a host for expressing heterologous proteins for many years. The genetic transformation system for this fungus was first reported by Pentillä et al. in 1987 [31]. In the following two years, the production of the first heterologous protein (calf chymosin) was accomplished an reported in *T. reesei* [32]. From 1971 to 1981, high protein-secreting strains were discovered and used as hosts for recombinant protein production. A significant achievement in the progression of the *T. reesei* expression system was using the strong *cbh1* promoter for expressing recombinant proteins. Besides, the fusions of recombinant proteins and efficiently secreted native proteins like CBHI is another approach for the heterologous protein expression in *T.*

reesei. With various approaches, many mammalian and microbial products were successfully produced by this fungus (**Table 1-1**) [24]. It has been reported that *T. reesei* has achieved impressive yields of heterologous proteins, with *Melanocarpus albomyces* cellulase Cel5A production reaching up to 7.7 g L^{-1} [33].

Table 1-1. Heterologous Proteins Expressed in *T. reesei* [24].

Heterologous Protein	Host Strain	Culture Mode	Yield (g/l)	References
Fungal				
Cel5A from *Melanocarpus albomyces*	ALKO3620	Shake flask	7.7	[33]
XynVI from *Acrophialophora nainiana*	RUT-C30	Shake flask	0.17	[34]
Lipase from *Aspergillus niger*	TU6 (ATCC MYA-256)	Shake flask	0.30	[35]
Bacterial				
Xyn11A from *Nonomuraea flexuosa*	ALKO3620	1 L Fermenter	0.82	[36]
Truncated Xyn11A from *Nonomuraea flexuosa*	ALKO3620	2 L Fermenter	1.8	[37]
Plant				
Barley endopeptidase B	ALKO2221	1 L Fermenter	0.5	[36]
Mammalian				
Calf chymosin	RUT-C30	10 L Fermenter	0.04	[36]
Human erythropoetin	RUT-C30 M3	Shake flask	0.10	[38]

1.3.3 Cellulase regulation mechanisms in *T. reesei*

Cellulase production in *T. reesei* is regulated by a sophisticated regulation system at the transcriptional level, depending on the available carbon source. Generally, *T. reesei* cellulase biosynthesis is induced by a small compound released or formed during cellulose degradation. Certain enzyme cascades are expressed constitutively at low levels, serving as scavengers or scouts. Once these enzymes encounter cellulose, the inducers are released from the polymer, triggering the secretion of the complete cellulase [39]. The inducers consist of several disaccharides such as cellobiose, cellobiono-1,5-lactone, lactose and sophorose [40]. Sophorose (2-O-β-D-glucopyranosyl-α-D-glucose), a transglycosylation product of cellobiose, is the strongest inducer for the cellulolytic system and considered to be a possible natural inducer [22,39]. Other low-molecular-weight compounds, such as arabitol and sorbose, have previously been assumed to stimulate cellulase gene expression [41]. In contrast, the presence of easily metabolizable carbon sources like glucose and fructose represses cellulase gene expression (**Figure 1-5**) [40]. Glucose inhibits cellobiose uptake and triggers carbon catabolite repression (CCR) of cellulase expression.

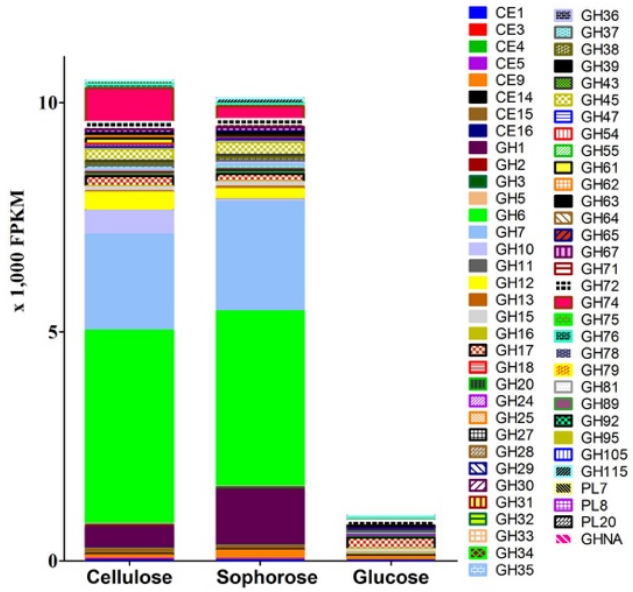

Figure 1-5. Carbohydrate active enZymes (CAZy) genes and expression data from RNA-seq analysis. Fragments per kilobase of exon per million fragments mapped (FPKM) means for each glycolic hydrase (GH) family when cultured in glucose, cellulose and sophorose [40].

Recently, other environmental factors such as light, nitrogen source, pH and metal ion responsive system in *T. reesei* received attention for its glycoside hydrolase induction mechanisms (**Figure 1-6**).

1.3.4 Transcription factors involved in cellulase gene expression in *T. reesei*

With intensive efforts in elucidating the molecular mechanisms that control the cellulase gene expression in *T. reesei*, several transcriptional activators and repressors have been identified [42]. In the *T. reesei* genome, there are around 700 transcription factors, but only a few (including at least three transcriptional activators XYR1, ACE2, the HAP2/3/5 and two repressors CRE1 and ACE1) have been studied so far.

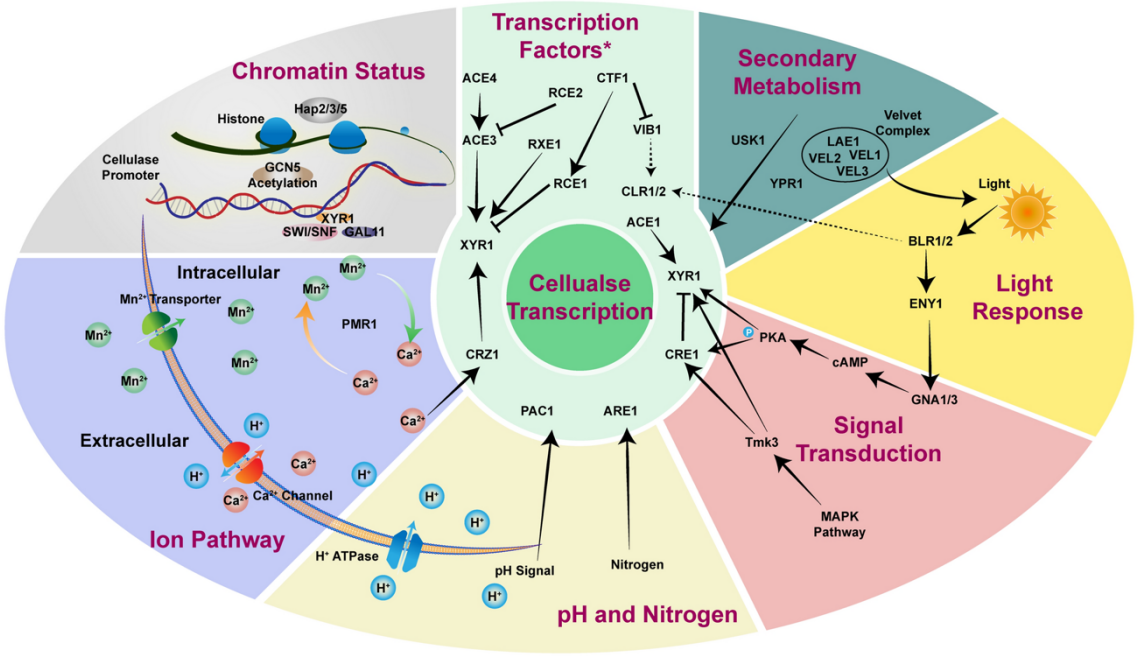

Figure 1-6. Cellulase regulation at the transcription level. In *T. reesei*, transcription of cellulase is under complicated and coordinated regulation networks including transcription factors, signal transduction, chromatin status, secondary metabolism and environmental factors such as light, nitrogen source, pH and metal ion, which are depicted in different areas with diverse colors. Only the factors involved in the crosstalk with other factors and pathways are depicted in the picture. The inter-regulation of different factors and regulators is shown by black arrows and lines. The dashed lines indicate characterized regulation mechanism in other fungi but not in *T. reesei* [42].

a. XYR1(xylanase regulator 1)

XYR1 (xylanase regulator 1) is the main activator for cellulase and xylanase genes in *T. reesei*. The transcription factor contains an N-terminal Zn_2-Cys_6 DNA binding domain, followed by an adjacent dimerization domain and a complex middle and C-terminal region with 934 amino acids and a predicted molecular mass of 102 kDa [22,39]. The functional XYR1-binding site (XBS) is the sequence 5'-GGCWWW-3'. Several XBSs were found on the upstream regulatory regions of main cellulase and xylanase genes. Xyr1-deletion strains are not expressing any of the major cellulolytic genes (*cbh1*, *cbh2*, *egl1*, and *bgl1*) and xylanolytic genes (*xyn1*, *xyn2*, and *bxl1*) [43]. Furthermore, XYR1 also regulates the gene expression of D-xylose reductase, which is responsible for the first step in metabolizing D-xylose, D-galactose, and L-arabinose. The *xyr1* gene expression is downregulated by CRE1 and ACE1 repressors but upregulated by xylanase promoter-binding protein 1 (XPP1) [22].

b. ACE2 (activator of cellulase expression 2)

ACE2 is a specific transcriptional activator for *T. reesei* cellulase and xylanase gene expressions. The DNA-binding domain of ACE2 is 5'-GGCTAATAA-3' sequences in the *cbh1* promoter region and 5'- GGGTAA-3' sequences in the *cbh2* and *xyn2* promoter region [22]. Disruption of the *ace2* gene led to 30–70% reduced cellulase activity when the fungus was grown on a cellulose medium. However, there was no effect on cellulase activity when grown on sophorose [44]. This suggested the cellulase and xylanase gene expressions controlled by at least two different induction systems in this fungus.

c. ACE3 (activator of cellulase expression 3)

ACE3 is another essential transcriptional activator for cellulolytic genes in *T. reesei*. The activator binds to the specific motifs 5'-CGGAN$(T/A)_3$-3', which were found in the promoters of the CBHI-encoding gene, transcription factor-encoding genes (*xyr1* and *ace3*), and the cellulose response transporter gene *crt1* [45]. Overexpression of the *ace3* gene led to improvements in cellulase and hemicellulase production. In contrast, the *ace3* deletion completely abrogates cellulase production and merely reduces the hemicellulose expressions [45].

d. BGLR (β-glucosidase regulator)

BGLR was identified as a new Zn_2Cys_6-type fungal-specific transcription factor. One function is to upregulate specific β-glucosidase genes (except for *bgl1*) on cellobiose cultivation, promoting glucose production in the cell and triggering CCR in cellobiose culture. The *bglr* gene disruptant showed increased cellulase production during cellobiose growth but delayed expression of genes encoding BGL2 and CEL3B [46]. The two β-glucosidase play essential roles in cellulase induction on lactose [47]. To better understand other functions of BGLR, it is necessary to perform the detailed analysis and characterize the transcription factor on different lignocellulosic sources.

e. ACE1

ACE1, a Cys_2-His_2 transcription factor, activated the *cbh1* promoter in *Saccharomyces cerevisiae* [48]. However, it repressed expressions of all the major *T. reesei* cellulase genes (*cbh1*, *cbh2* and *egl1*) and xylanase genes (*xyn1* and *xyn2*) on both sophorose and cellulose. The ACE1-binding domain is 5'-AGGCA-3' sequences in the *cbh1* promoter region [22]. An *ace1*-disrupting *T. reesei* strain showed slow growth on a cellulase-inducing medium but had high cellulase yields [48]. This suggested that ACE1 may have another general regulatory role besides the repressor function.

f. CRE1

In *T. reesei*, when glucose or other carbon sources that are easily metabolized in large quantities are present, secretions of cellulases and hemicellulases that catalyze the hydrolysis of complex compounds are repressed through a process called carbon catabolite repression (CCR). This ensures the fungus does not waste energy and material for enzyme biosynthesis and secretion. CCR is mediated by the transcription factor CRE1, which directly and indirectly repressed the cellulase- and hemicellulases-related gene expressions by binding to specific sites in the promoter region of the target genes [49]. The CRE1 protein bears an N-terminal DNA-binding domain containing two Cys_2His_2 zinc fingers. The CRE1-binding sequences are the 5'-SYGGRG-3' motifs in the promoters of *cbh1*, *xyn1*, and *xyr1* [39].

1. 3. Fugal strain modifications and improvements

1.3.1 Genetic transformation techniques of filamentous fungi

Developing genetic transformation techniques is considered a breakthrough in modifying fungal strains genetically. The methods have been widely applied for revealing the functions of targeted genes, overexpressing native proteins, and expressing heterologous proteins. They aid in gaining a deeper comprehension of the fungal molecular mechanisms and constructing desired strains for industrial applications. The main genetic transformation methods of filamentous fungi include the protoplast-mediated transformation method, the *Agrobacterium*-mediated transformation method, and the electroporation method [50].

1.3.1.1 Protoplast-mediated transformation

Protoplast-mediated transformation is the most used method for fungal transformation because of its simplicity and effectiveness without requiring costly equipment. The process of genetically transforming *T. reesei* was initially established in 1987 [31]. The basic steps of the method include fungal protoplast preparation, exogenous DNA uptake, and protoplast regeneration and selection [50,51]. The first step in protoplast preparation is removing the cell wall through enzymatic digestion. In the procedure of *T. reesei*, the protoplasts are prepared by hydrolyzing the hyphae (culture for 24 h under 28-30 °C). To ensure the stability of protoplasts, a solution containing sorbitol with a concentration range of 0.8-1.2 M is utilized due to its sensitivity to osmotic pressure. During the process of DNA uptake, exogenous DNA can enter the fungal cell using calcium ions. These ions are believed to open channels in the cytomembrane, allowing exogenous DNA entry into the cell. Additionally, polyethylene glycol (PEG) helps promote adhesion by forming a molecular bridge between cells or between the cytomembrane and the donor DNA. During the regeneration and selection, protoplasts are recovered on double-layer agar plates under selection pressure. This ensures that only the protoplasts carrying the desired DNA can grow on the selective medium. The transformation efficiency varied between 150 to 1500 transformants per μg of external DNA [31,52].

1.3.1.2 *Agrobacterium tumefacient*-mediated transformation (ATM)

The *Agrobacterium tumefaciens*-mediated transformation (ATM), a method for introducing genes into plant cells, could be applied to filamentous fungal transformation [51]. In plant infection, *A. tumefaciens* enters the plant through the wound and randomly integrates part of the Ti plasmid into the plant genome as a single copy. Similarly, the bacterium could integrate the target gene into the fungal genome. The basic steps of the ATM transformation include pre-cultivation of *Agrobacterium* and fungi, co-culture at a ratio of fungi to bacteria at a certain temperature, and cultivation of transformed fungi in a selection medium [50]. This transformation method allows for achieving high levels of efficiency in both transformation and homologous recombination. In 2007, a highly efficient AMT protocol was established for *T. reesei* with a transformation efficiency of approximately 200 to 9,000 transformants per 10^7 conidia, depending on the starting fungal material (conidia or protoplasts) [53].

1.3.1.3 Electroporation transformation

Electroporation is a simple, rapid, and efficient transformation method for filamentous fungi. The host cells and the exogenous nucleic acid are suspended in a conductive solution. After the electric shock, the fungal plasma membrane will change temporarily, creating microscopic pores which allow exogenous DNA to enter the cell [51]. The fungal membrane can restore the original structure with appropriate voltage, pulse time, and pulse frequency. However, high-voltage electric shocks are detrimental to the cell membrane and can cause irreversible damage, ultimately leading to cell death. The electroporation transformation of filamentous fungi is performed with 200–800 Ω resistance, 25 mF capacitance, and 2–15 $kVcm^{-1}$ field strength [54]. The electroporation transformation protocol for *T. reesei* was derived from the patent application US2010/0304468 [55].

1.3.2 Random mutagenesis

In the 1970s, random mutagenesis was the primary method to obtain several mutants that improved cellulase productivity from the wild-type QM6a (**Figure 1-4**). The first attempt at Natick laboratories by irradiating electric beam to conidia using a linear accelerator generated the cellulase-overproducing strain QM9414 [56]. This strain exhibited a notable increase in cellulase production with extracellular protein levels two to four times higher than those of QM6a but remained CCR. QM9414 has been the standard for developing further mutagenesis lineages of new hyper-cellulolytic strains. In a separate mutagenesis program at Rutgers University, a high cellulase-producing and catabolite-derepressed mutant RUT-C30 strain was obtained by three mutagenesis steps, including UV mutagenesis, N-nitrosoguanidine (NTG) mutagenesis, and UV mutagenesis [30]. Numerous research institutes have investigated the RUT-C30 strain, resulting in the creation of various modified strains. In Japan, a lineage of new mutant strains has been developed in the Research Association for Petroleum Alternatives Development (RAPAD), a national project [22,57]. One of the obtained mutants, the PC-3-7 strain, showed improved cellulase production on a broad range of carbon sources: microcrystalline cellulose, sophorose, bagasse, whey, L-sorbose, and cellobiose [57]. In 2021, a *T. reesei* hyper-cellulase producer T1281, obtained through 12 different rounds of UV/NTG mutation generations, exhibited remarkable outperformance over PC-3-7 in protein and cellulase productivities on lactose [58].

Currently, 21 out of 30 commercial *T. reesei* enzymes are recombinant proteins [18]. However, the recombinant productions must adhere to strict non-proliferation regulations outlined by the Cartagena Protocol on Biosafety, resulting in higher production costs [58]. However, the bioproducts created by mutants resulting from random mutagenesis techniques are an exception to this regulation.

1. 5. Droplet-based microfluidic technology

Droplet microfluidics, one of the major branches of microfluidic techniques, has rapidly emerged as a critical technology. The technology opens up new possibilities in various life science applications, including single-cell sequencing, microbial identification, drug discovery, directed evolution and biotechnological applications [59]. Water-in-oil droplet (WODL) microfluidic technologies use two immiscible phases [59]. One is the continuous phase with oil containing a surfactant, which preferentially wets the microfluidic channel walls. Another is the dispersed phase, typically aqueous, which is introduced into the system and split into droplets. WODLs can be generated in microfluidic channels using T-junction, flow-focusing, and co-flow [60]. The flow-focusing is a widely used method for forming WODLs. This involves pumping the oil phase perpendicularly from two side channels to split the aqueous phase into monodisperse WODLs ranging in volume from pico- to microliters.

The current state of the art allows droplet generation with frequencies of up to15,000 droplets s^{-1} with a polydispersity of less than 2% [61]. In the single-cell encapsulation in droplets, the aqueous phase is often a mixture of cell suspension and medium. The number of cells in droplets is dictated by a Poisson distribution (**Figure 1-7a**). The possibility of single-cell compartmentalization is one of the outstanding advantages of droplet microfluidics over classical culture methods. This opens up opportunities for biological processes, including DNA amplification, cell growth, enzymatic reactions, and protein expression (**Figure 1-7b**). The second most important feature of droplet microfluidics is the feasibility of screening million droplets per round. The screening speed could reach up to 30,000 droplets s^{-1} [61]. This feature enables high throughput selections from large pools of cells or populations. In addition to the high-speed droplet generation and high-throughput screening, droplet microfluidic techniques offer various modules for manipulating droplets, such as mixing and generation, fusion, stationary storage, detection, sorting, re-injection, splitting, on-chip incubation, and off-chip incubation [60]. Each module can be combined to suit the requirements of specific biological experiments. The detailed benefits will be discussed in the following chapters.

This versatile and powerful platform has contributed significantly to studies on bacteria, yeasts, and algae, but negligibly to fungal research. When cultivating fungi in droplets, the biggest challenge is the fast growth of the branched mycelia over the droplets, resulting in the formation of fungal clumps and blockage of microfluidic channels.

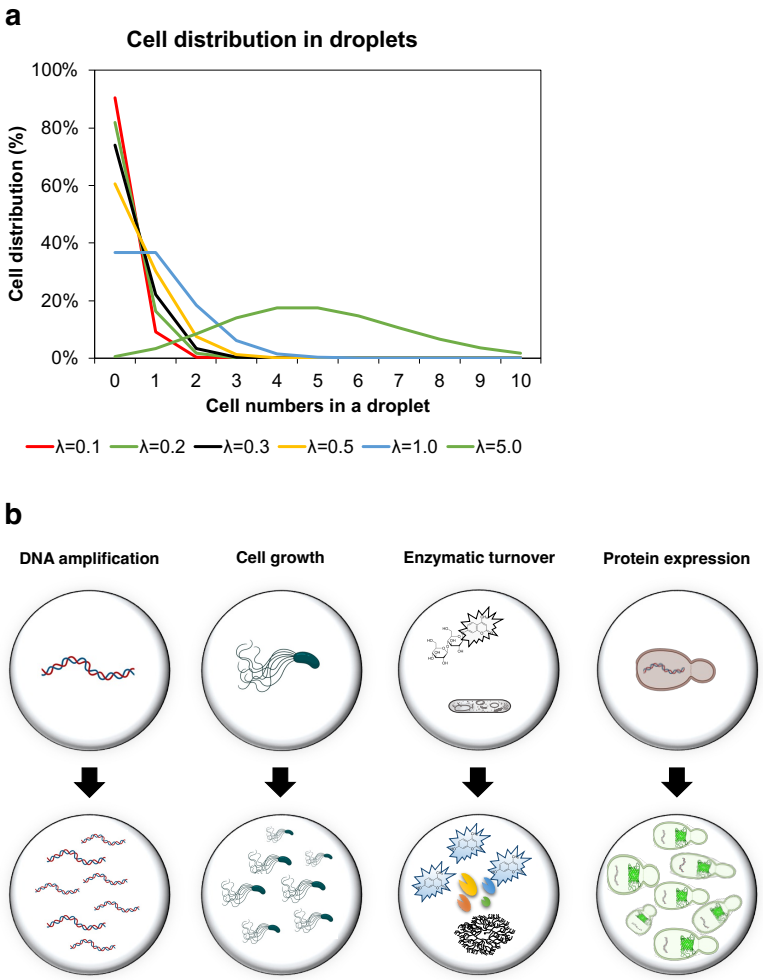

Figure 1-7. Applications of WODL encapsulations. (a) Poisson distribution simulated the probability of the number of cells per droplet at varying λ values (representing the average number of cells per droplet) [62]. (b) WODLs are being used for various biological investigations.

1. 6 Purpose of the study

This study aimed to develop novel high-throughput workflows for genetic engineering and random mutagenesis of the filamentous fungus *T. reesei* employing a droplet-base microfluidic platform. The proposed workflows are expected to open up opportunities for accelerating the genetic modifications and strain improvements of filamentous fungi in research and practical applications. In this field of research, studies on the molecular mechanisms involved in gene function and expression should become rapid and insightful. By means of this novel method, industrial fungal strains can be generated in a short period and used to produce bioactive compounds, hydrolytic enzymes, or recombinant proteins.

For the genetic engineering, a novel droplet-based method for *T. reesei* expressing green fluorescent protein (GFP) as a marker has been developed. This strategy enabled the encapsulation of single fungal spores and protoplasts, the induction of gene expression, and the rapid detection and enrichment of either growing fungi or regenerating fungal transformants from a large candidate library. It presented several outstanding advantages over the traditional transformation method, including a 7-fold reduction in time for *T. reesei* protoplast regeneration, an 8-fold increase in regeneration frequency, and a screening speed of up to 8,000 droplets·min^{-1}. The gfp-transformed *T. reesei* protoplasts were successfully encapsulated, incubated in droplets for 24 h, and screened in a high-throughput assay. Eventually, a transformant library with over 96 % of the desirable candidates was collected. The total time for the approach is about two weeks, with one round of droplet cultivation and screening, two rounds of genomic evaluation, and one round of single-spore separation.

For the fungal strain improvement using random mutagenesis, a microfluidic droplet platform for ultraviolet (UV) mutagenesis was employed to construct high-yielding fungal strains capable of producing cellulase in repression conditions. Several generations of hypercellulase producers with carbon catabolite repression resistance were rapidly generated and isolated from an extensive mutagenized library. Several isolated mutants exhibited more excellent protein and cellulase productivity on repression conditions than the parent strain. Furthermore, cellulase and transcription factor gene expressions and genomic sequencing of those mutants have been evaluated to get a deeper insight into the regulatory mechanisms of cellulase hyper-producing strains.

1. 7 Reference

[1] Nations U. World population prospects 2019. 2019.

[2] Lewandowski I, Gaudet N, Lask J, Maier J, Tchouga B, Vargas-Carpintero R. Context BT - Bioeconomy: Shaping the Transition to a Sustainable, Biobased Economy. In: Lewandowski I, editor., Cham: Springer International Publishing; 2018, p. 5–16. https://doi.org/10.1007/978-3-319-68152-8_2.

[3] Nations U. Transforming our world: the 2030 agenda for sustainable development n.d.

[4] Heimann T. Bioeconomy and SDGs: Does the Bioeconomy Support the Achievement of the SDGs? Earth's Futur 2019;7:43–57. https://doi.org/10.1029/2018EF001014.

[5] Calicioglu Ö, Bogdanski A. Linking the bioeconomy to the 2030 sustainable development agenda: Can SDG indicators be used to monitor progress towards a sustainable bioeconomy? N Biotechnol 2021;61:40–9. https://doi.org/10.1016/j.nbt.2020.10.010.

[6] Birner R. Bioeconomy Concepts BT - Bioeconomy: Shaping the Transition to a Sustainable, Biobased Economy. In: Lewandowski I, editor., Cham: Springer International Publishing; 2018, p. 17–38. https://doi.org/10.1007/978-3-319-68152-8_3.

[7] Singh R, Paritosh K, Pareek N, Vivekanand V. Integrated system of anaerobic digestion and pyrolysis for valorization of agricultural and food waste towards circular bioeconomy: Review. Bioresour Technol 2022;360:127596. https://doi.org/10.1016/j.biortech.2022.127596.

[8] Kircher M. Bioeconomy – present status and future needs of industrial value chains. N Biotechnol 2021;60:96–104. https://doi.org/10.1016/j.nbt.2020.09.005.

[9] Zörb C, Lewandowski I, Kindervater R, Göttert U, Patzelt D. Biobased Resources and Value Chains BT - Bioeconomy: Shaping the Transition to a Sustainable, Biobased Economy. In: Lewandowski I, editor., Cham: Springer International Publishing; 2018, p. 75–95. https://doi.org/10.1007/978-3-319-68152-8_5.

[10] Yadav A, Sharma V, Tsai ML, Chen CW, Sun PP, Nargotra P, et al. Development of lignocellulosic biorefineries for the sustainable production of biofuels: Towards circular bioeconomy. Bioresour Technol 2023;381:129145. https://doi.org/10.1016/j.biortech.2023.129145.

[11] Sharma V, Tsai M-L, Nargotra P, Chen C-W, Kuo C-H, Sun P-P, et al. Agro-Industrial Food Waste as a Low-Cost Substrate for Sustainable Production of Industrial Enzymes: A Critical Review. Catalysts 2022;12. https://doi.org/10.3390/catal12111373.

[12] Marakana PG, Dey A, Saini B. Isolation of nanocellulose from lignocellulosic biomass: Synthesis, characterization, modification, and potential applications. J Environ Chem Eng 2021;9:106606. https://doi.org/https://doi.org/10.1016/j.jece.2021.106606.

[13] Popp J, Kovács S, Oláh J, Divéki Z, Balázs E. Bioeconomy: Biomass and biomass-based energy supply and demand. N Biotechnol 2021;60:76–84. https://doi.org/10.1016/j.nbt.2020.10.004.

[14] Madeira JV, Contesini FJ, Calzado F, Rubio MV, Zubieta MP, Lopes DB, et al. Chapter 18 - Agro-Industrial Residues and Microbial Enzymes: An Overview on the Eco-Friendly Bioconversion into High Value-Added Products. In: Brahmachari GBT-B of ME, editor., Academic Press; 2017, p. 475–511. https://doi.org/https://doi.org/10.1016/B978-0-12-803725-6.00018-2.

[15] Meyer V, Basenko EY, Benz JP, Braus GH, Caddick MX, Csukai M, et al. Growing a circular economy with fungal biotechnology: A white paper. Fungal Biol Biotechnol 2020;7:1–23. https://doi.org/10.1186/s40694-020-00095-z.

[16] Ma C, Liu J, Tang J, Sun Y, Jiang X, Zhang T, et al. Current genetic strategies to investigate gene functions in Trichoderma reesei. Microb Cell Fact 2023;22:97. https://doi.org/10.1186/s12934-023-02104-3.

[17] Gupta VK, O'Donovan A, Tuohy MG, Sharma GD. Trichoderma in Bioenergy Research: An Overview. Elsevier; 2014. https://doi.org/10.1016/B978-0-444-59576-8.00023-0.

[18] Fischer AJ, Maiyuran S, Yaver DS. Industrial Relevance of *Trichoderma reesei* as an Enzyme Producer BT - *Trichoderma reesei:* Methods and Protocols. In: Mach-Aigner AR, Martzy R, editors., New York, NY: Springer US; 2021, p. 23–43. https://doi.org/10.1007/978-1-0716-1048-0_2.

[19] Chenthamara K, Druzhinina IS, Rahimi MJ, Grujic M, Cai F. Ecological Genomics and Evolution of *Trichoderma reesei* BT - *Trichoderma reesei*: Methods and Protocols. In: Mach-Aigner AR, Martzy R, editors., New York, NY: Springer US; 2021, p. 1–21. https://doi.org/10.1007/978-1-0716-1048-0_1.

[20] Peterson R, Nevalainen H. *Trichoderma reesei* RUT-C30 - Thirty years of strain improvement. Microbiology 2012;158:58–68. https://doi.org/10.1099/mic.0.054031-0.

[21] Vitikainen M, Arvas M, Pakula T, Oja M, Penttilä M, Saloheimo M. Array comparative genomic hybridization analysis of *Trichoderma reesei* strains with enhanced cellulase production properties. BMC Genomics 2010;11:441. https://doi.org/10.1186/1471-2164-11-441.

[22] Shida Y, Furukawa T, Ogasawara W. Deciphering the molecular mechanisms behind cellulase production in *Trichoderma reesei*, the hyper-cellulolytic filamentous fungus. Biosci Biotechnol Biochem 2016;80:1712–29. https://doi.org/10.1080/09168451.2016.1171701.

[23] Saloheimo M, Pakula TM. The cargo and the transport system: Secreted proteins and protein secretion in *Trichoderma reesei* (*Hypocrea jecorina*). Microbiology 2012;158:46–57. https://doi.org/10.1099/mic.0.053132-0.

[24] Adav SS, Sze SK. *Trichoderma* Secretome. Biotechnol Biol Trichoderma, Elsevier; 2014, p. 103–14. https://doi.org/10.1016/b978-0-444-59576-8.00008-4.

[25] Gusakov A V. Alternatives to *Trichoderma reesei* in biofuel production. Trends Biotechnol 2011;29:419–25. https://doi.org/https://doi.org/10.1016/j.tibtech.2011.04.004.

[26] Margeot A, Hahn-Hagerdal B, Edlund M, Slade R, Monot F. New improvements for lignocellulosic ethanol. Curr Opin Biotechnol 2009;20:372–80. https://doi.org/https://doi.org/10.1016/j.copbio.2009.05.009.

[27] Chundawat SPS, Lipton MS, Purvine SO, Uppugundla N, Gao D, Balan V, et al. Proteomics-based compositional analysis of complex cellulase-hemicellulase mixtures. J Proteome Res 2011;10:4365–72. https://doi.org/10.1021/pr101234z.

[28] Hölker U, Dohse J, Höfer M. Extracellular laccases in ascomycetes *Trichoderma atroviride* and *Trichoderma harzianum*. Folia Microbiol (Praha) 2002;47:423–7. https://doi.org/10.1007/BF02818702.

[29] Gianfreda L, Xu F, Bollag J-M. Laccases: A Useful Group of Oxidoreductive Enzymes. Bioremediat J 1999;3:1–26. https://doi.org/10.1080/10889869991219163.

[30] Adav SS, Chao LT, Sze SK. Quantitative secretomic analysis of *Trichoderma reesei* strains reveals enzymatic composition for lignocellulosic biomass

degradation. Mol Cell Proteomics 2012;11:M111.012419-1-M111.012419-15. https://doi.org/10.1074/mcp.M111.012419.

[31] Penttilä M, Nevalainen H, Rättö M, Salminen E, Knowles J. A versatile transformation system for the cellulolytic filamentous fungus *Trichoderma reesei*. Gene 1987;61:155–64. https://doi.org/10.1016/0378-1119(87)90110-7.

[32] Harkki A, Uusitalo J, Bailey M, Penttilä M, Knowles JKC. A Novel Fungal Expression System: Secretion of Active Calf Chymosin from the Filamentous Fungus *Trichoderma reesei*. Bio/Technology 1989;7:596–603. https://doi.org/10.1038/nbt0689-596.

[33] Arumugam Mahadevan S, Gon Wi S, Lee D-S, Bae H-J. Site-directed mutagenesis and CBM engineering of Cel5A (*Thermotoga maritima*). FEMS Microbiol Lett 2008;287:205–11. https://doi.org/10.1111/j.1574-6968.2008.01324.x.

[34] Salles BC, Te'o VSJ, Gibbs MD, Bergquist PL, Filho EXF, Ximenes EA, et al. Identification of two novel xylanase-encoding genes (*xyn5* and *xyn6*) from Acrophialophora nainiana and heterologous expression of *xyn6* in *Trichoderma reesei*. Biotechnol Lett 2007;29:1195–201. https://doi.org/10.1007/s10529-007-9380-z.

[35] Qin L-N, Cai F-R, Dong X-R, Huang Z-B, Tao Y, Huang J-Z, et al. Improved production of heterologous lipase in Trichoderma reesei by RNAi mediated gene silencing of an endogenic highly expressed gene. Bioresour Technol 2012;109:116–22. https://doi.org/https://doi.org/10.1016/j.biortech.2012.01.013.

[36] Paloheimo M, Mäntylä A, Kallio J, Suominen P. High-Yield Production of a Bacterial Xylanase in the Filamentous Fungus *Trichoderma reesei* Requires a Carrier Polypeptide with an Intact Domain Structure. Appl Environ Microbiol 2003;69:7073–82. https://doi.org/10.1128/AEM.69.12.7073-7082.2003.

[37] Paloheimo M, Mäntylä A, Kallio J, Puranen T, Suominen P. Increased production of xylanase by expression of a truncated version of the *xyn11A* gene from *Nonomuraea flexuosa* in *Trichoderma reesei*. Appl Environ Microbiol 2007;73:3215–24. https://doi.org/10.1128/AEM.02967-06.

[38] Zhong Y, Liu X, Xiao P, Wei S, Wang T. Expression and Secretion of the Human Erythropoietin Using an Optimized *cbh1* Promoter and the Native CBH I Signal Sequence in the Industrial Fungus *Trichoderma reesei*. Appl Biochem Biotechnol 2011;165:1169–77. https://doi.org/10.1007/s12010-011-9334-8.

[39] Zimmermann C, Till P, Danner C, Mach-Aigner AR. Genetic Regulation Networks in Cellulase and Hemicellulase Production in an Industrially Applied Cellulase Producer *Trichoderma reesei*. Handb Biorefinery Res Technol 2023:1–23. https://doi.org/10.1007/978-94-007-6724-9_25-1.

[40] Dos Santos Castro L, Pedersoli WR, Antoniêto ACC, Steindorff AS, Silva-Rocha R, Martinez-Rossi NM, et al. Comparative metabolism of cellulose, sophorose and glucose in *Trichoderma reesei* using high-throughput genomic and proteomic analyses. Biotechnol Biofuels 2014;7. https://doi.org/10.1186/1754-6834-7-41.

[41] Nogawa M, Goto M, Okada H, Morikawa Y. l-Sorbose induces cellulase gene transcription in the cellulolytic fungus *Trichoderma reesei*. Curr Genet 2001;38:329–34. https://doi.org/10.1007/s002940000165.

[42] Yan S, Xu Y, Yu XW. From induction to secretion: a complicated route for cellulase production in *Trichoderma reesei*. Bioresour Bioprocess 2021;8. https://doi.org/10.1186/s40643-021-00461-8.

[43] Stricker AR, Grosstessner-Hain K, Würleitner E, Mach RL. Xyr1 (Xylanase Regulator 1) regulates both the hydrolytic enzyme system and D-xylose metabolism in *Hypocrea jecorina*. Eukaryot Cell 2006;5:2128–37. https://doi.org/10.1128/EC.00211-06.

[44] Aro N, Saloheimo A, Ilmén M, Penttilä M. ACEII, a Novel Transcriptional Activator Involved in Regulation of Cellulase and Xvlanase Genes of *Trichoderma reesei*. J Biol Chem 2001;276:24309–14. https://doi.org/10.1074/jbc.M003624200.

[45] Zhang J, Chen Y, Wu C, Liu P, Wang W, Wei D. The transcription factor ACE3 controls cellulase activities and lactose metabolism via two additional regulators in the fungus *Trichoderma reesei*. J Biol Chem 2019;294:18435–50. https://doi.org/https://doi.org/10.1074/jbc.RA119.008497.

[46] Nitta M, Furukawa T, Shida Y, Mori K, Kuhara S, Morikawa Y, et al. A new Zn(II)2Cys6-type transcription factor BglR regulates β-glucosidase expression in *Trichoderma reesei*. Fungal Genet Biol 2012;49:388–97. https://doi.org/https://doi.org/10.1016/j.fgb.2012.02.009.

[47] Shida Y, Yamaguchi K, Nitta M, Nakamura A, Takahashi M, Kidokoro SI, et al. The impact of a single-nucleotide mutation of bgl2 on cellulase induction in a *Trichoderma reesei* mutant. Biotechnol Biofuels 2015;8:1–18. https://doi.org/10.1186/s13068-015-0420-y.

[48] Saloheimo A, Aro N, Ilmén M, Penttilä M. Isolation of the ace1 Gene Encoding a Cys2-His2 Transcription Factor Involved in Regulation of Activity of the Cellulase Promoter *cbh1* of *Trichoderma reesei*. J Biol Chem 2000;275:5817–25. https://doi.org/https://doi.org/10.1074/jbc.275.8.5817.

[49] Antoniêto ACC, dos Santos Castro L, Silva-Rocha R, Persinoti GF, Silva RN. Defining the genome-wide role of CRE1 during carbon catabolite repression in Trichoderma reesei using RNA-Seq analysis. Fungal Genet Biol 2014;73:93–103. https://doi.org/https://doi.org/10.1016/j.fgb.2014.10.009.

[50] Li D, Tang Y, Lin J, Cai W. Methods for genetic transformation of filamentous fungi. Microb Cell Fact 2017;16:1–13. https://doi.org/10.1186/s12934-017-0785-7.

[51] Shida Y, Ogasawara W. Genetic Engineering of *Trichoderma reesei* for Biomass Hydrolysis. Handb Biorefinery Res Technol 2023:1–30. https://doi.org/10.1007/978-94-007-6724-9_26-1.

[52] Gruber F, Visser J, Kubicek CP, de Graaff LH. The development of a heterologous transformation system for the cellulolytic fungus *Trichoderma reesei* based on a pyrG-negative mutant strain. Curr Genet 1990;18:71–6. https://doi.org/10.1007/BF00321118.

[53] Zhong YH, Wang XL, Wang TH, Jiang Q. Agrobacterium-mediated transformation (AMT) of *Trichoderma reesei* as an efficient tool for random insertional mutagenesis. Appl Microbiol Biotechnol 2007;73:1348–54. https://doi.org/10.1007/s00253-006-0603-3.

[54] Wanka F. Open the Pores: Electroporation for the Transformation of *Trichoderma reesei* BT - *Trichoderma reesei*: Methods and Protocols. In: Mach-Aigner AR, Martzy R, editors., New York, NY: Springer US; 2021, p. 73–8. https://doi.org/10.1007/978-1-0716-1048-0_6.

[55] Kim S, Miasnikov A. Method for introducing nucleic acids into fungal cells 2010;1.

[56] Gadgil NJ, Daginawala HF, Chakrabarti T, Khanna P. Enhanced cellulase production by a mutant of *Trichoderma reesei*. Enzyme Microb Technol 1995;17:942–6. https://doi.org/10.1016/0141-0229(94)00131-A.

[57] Hirasawa H, Shioya K, Mori K, Tashiro K, Aburatani S, Shida Y, et al. Cellulase productivity of *Trichoderma reesei* mutants developed in Japan varies with varying

pH conditions. J Biosci Bioeng 2019;xxx. https://doi.org/10.1016/j.jbiosc.2019.03.005.

[58] Noguchi T, Saito H, Nishiyama R, Yoshida N, Matsubayashi T, Teshima Y, et al. Isolation of a cellulase hyperproducing mutant strain of *Trichoderma reesei*. Bioresour Technol Reports 2021;15:100733. https://doi.org/10.1016/j.biteb.2021.100733.

[59] Kaminski TS, Scheler O, Garstecki P. Droplet microfluidics for microbiology: techniques, applications and challenges. Lab Chip 2016;16:2168. https://doi.org/10.1039/c6lc00367b.

[60] Kintses B, van Vliet LD, Devenish SRA, Hollfelder F. Microfluidic droplets: New integrated workflows for biological experiments. Curr Opin Chem Biol 2010;14:548–55. https://doi.org/10.1016/j.cbpa.2010.08.013.

[61] Neun S, Zurek PJ, Kaminski TS, Hollfelder F. Ultrahigh throughput screening for enzyme function in droplets. vol. 643. 1st ed. Elsevier Inc.; 2020. https://doi.org/10.1016/bs.mie.2020.06.002.

[62] Li P, Ma Z, Zhou Y, Collins DJ, Wang Z, Ai Y. Detachable Acoustophoretic System for Fluorescence-Activated Sorting at the Single-Droplet Level. Anal Chem 2019;91:9970–7. https://doi.org/10.1021/acs.analchem.9b01708.

Chapter 2: A novel high-throughput approach for transforming filamentous fungi employing a droplet-based microfluidic platform

2.1 Introduction

Currently, droplet-based microfluidic platforms are a powerful technology with numerous outstanding advantages. The first benefit of the technology is its ability to encapsulate single cells stochastically in separate water-in-oil droplets (WODLs). The confinement of single cells within these droplets enables microbes to grow and accumulate metabolites faster than in a bulk population in 96-well plates or flasks [1]. The second advantage is the possibility of miniaturizing volumes of culture medium, increasing cost efficiency and allowing the use of expensive substances. Compared with the smallest available volumes in multiwell plates, the microfluidic system allowed an approximately 11-fold reduction in medium volume and a 555-fold reduction in fluorogenic substrate use [2]. Another significant benefit is that the platform can produce a large number of droplets for high-throughput screening. The state-of-the-art technology generates 1,000-15,000 droplets per second and can screen 1,000-3,000 droplets per second [3], a 1,000-fold improvement of the screening speed of robotic microtiter plate-based systems [4]. Therefore, the platform is used widely for bacteria [5,6], yeasts [7,8], and algae [9,10] but rarely for filamentous fungi [3,11]. The main obstacle to fungal cultivation in droplets is the rapid expansion of branched mycelia, which causes uncontrolled coalescences between droplets, the formation of fungal clumps, and the blockage of the microfluidic channels as a result. Possible solutions include increasing droplet volumes, using an induction medium, or controlling droplet incubation time for the directed evolution and metagenomic screening of enzymes [2,12]. Despite the above efforts, the application of this technology in the cultivation, analysis, and isolation processes required for the genetic engineering of filamentous fungi remains limited and needs more profound research.

Filamentous fungi are widely exploited in many fields for their ability to produce extracellular proteins and synthesize bioactive natural compounds and other secondary metabolites [13]. Additionally, filamentous fungi are selected as production hosts for recombinant proteins due to their ability to synthesize eukaryotic proteins [14]. Despite

their excellent capacities, strain improvements with higher production yields are crucial for industrial applications using filamentous fungi. To date, scientific efforts have produced hyper-productive strains with the support of genetic transformation techniques. These techniques have been used to modify native genes efficiently or to insert heterologous genes into the genomes of filamentous fungi [15,16]. The protoplast-mediated transformation method is the most preferred protocol for its simplicity and minimal use of specialized equipment [13]. Generally, the basic steps for protoplast-mediated transformation include fungal protoplast preparation, DNA uptake, fungal regeneration onto bilayer-agar plates, and screening for targeted transformants. However, problems related to the considerable regeneration time, restrictions in transgenic line selection, limited use of expensive substances, and low-throughput screening have hindered using this method to transform filamentous fungi. Although multiwell plates can be used to culture fungal protoplasts to miniaturize the use of reagents required for protoplast regeneration [17], there are few reports on the successful isolation of transformed protoplasts following this culturing method. Auxotrophic complementation and drug resistance are often employed to isolate fungal transformants [13]; however, auxotrophic mutant complementation requires the generation of auxotrophic strains, and antibiotic resistance may inhibit the growth of fungal transformants [18]. Fluorescence-activated cell sorting (FACS) can separate transformed spores with a throughput of 1,000-20,000 spores per second [19–21] but cannot isolate fungal protoplasts due to their vulnerability [22].

To tackle these problems, a novel high-throughput method using a droplet-based microfluidic system to transform filamentous fungi genetically has been developed. Firstly, this study identified inducers with the greatest potential for green fluorescent protein (GFP) expression during the early fungal growth stages. The results revealed that GFP expression was detected only in droplets containing the sophorose medium from 18-h to 24-h cultivation. This study subsequently investigated the feasibility of droplet screening in the rapid isolation of GFP-expressing fungi from a mixed spore library. Single spores from the mixture were cultured in droplets containing sophorose for 24 h, then over 7.0×10^5 droplets were screened with a screening speed of up to 8,000 droplets·min^{-1} and 860 droplets were separated and plated for fungal strain recovery. Next, the study compared the regeneration of *T. reesei* protoplasts with the droplet cultivation approach and the traditional plate cultivation method. The droplet culture presents two

main advantages for fungal protoplast recovery: a faster regeneration time and a higher regeneration frequency than the plate culture. As a proof of concept, the study established and applied a high-throughput workflow for the heterologous GFP expression in *T. reesei*. A library of over 10^5 *gfp*-transformed protoplasts was confined and incubated in droplets for 24 h, 247 positive droplets were sorted within 1.5 h, and 28 fungal transformants were eventually recovered on agar plates. The success of this approach will lead to significant reductions in time, labour and reagent costs for fungal studies and industrial strain improvements.

2.2 Materials and methods

2.2.1 Filamentous fungal strains and culture conditions

T. reesei strains PC-3-7 (ATCC 66589) and QM9414 (ATCC26921) were provided from Kao Co., Ltd. (Tokyo, Japan). *T. reesei* PC-3-7ΔP, a uridine auxotroph of *T. reesei* PC-3-7, was previously described [23]. The fungal strains were cultured on Difco^{TM} Potato Dextrose Agar (PDA; BD Diagnostics, Franklin Lakes, NJ, USA) plates for sporulation. Spores were then collected and stored at −80 °C in a 0.9% NaCl solution containing 10% glycerol until use. Potato dextrose agar plates with the addition of 0.1% Triton X-100 (PDA-X) were used for streaking the regenerating fungi after cultivation in droplets.

For droplet culture of fungal spores, the cultural medium contained a 1% carbon source (sophorose, sorbose, cellobiose, lactose, carboxymethyl cellulose (CMC) , and glucose), 0.14% $(NH_4)_2SO_4$, 0.20% KH_2PO_4, 0.03% $CaCl_2{\cdot}2H_2O$, 0.03% $MgSO_4{\cdot}7H_2O$, 0.05% Bacto yeast extract, 0.10% Bacto peptone, and a 0.10% trace element solution [5 $g{\cdot}L^{-1}$ $FeSO_4$, 2 $g{\cdot}L^{-1}$ $MnSO_4{\cdot}H_2O$, 1 $g{\cdot}L^{-1}$ $CuSO_4{\cdot}5H_2O$, 2 $g{\cdot}L^{-1}$ $ZnSO_4{\cdot}7H_2O$, 1 $g{\cdot}L^{-1}$ $(NH_4)_6Mo_7O_{24}{\cdot}4H_2O$, 2 $g{\cdot}L^{-1}$ $CoCl_2{\cdot}6H_2O$, and 1 $g{\cdot}L^{-1}$ $NiCl_2{\cdot}6H_2O$] in 50 mM Na-tartrate buffer (pH 4.0).

For droplet and plate cultivation of fungal protoplasts and transformants, a minimal medium consisting of 2% glucose or sophorose, 1-1.2 M sorbitol, 0.50% $(NH_4)_2SO_4$, 1.50% KH_2PO_4, 0.06% $MgSO_4$, 0.06% $CaCl_2$ and a 0.10% trace element solution [5 $g{\cdot}L^{-1}$ $FeSO_4{\cdot}7H_2O$, 2 $g{\cdot}L^{-1}$ $CoCl_2$, 1.6 $g{\cdot}L^{-1}$ $MgSO_4{\cdot}H_2O$, 1.2 $g{\cdot}L^{-1}$ $ZnSO_4{\cdot}7H_2O$] was used. For plate cultivation, a top agar medium with 2% glucose, 1M sorbitol, and 1% agarose was maintained at 50 °C before being mixed with a fungal protoplast suspension and overlaid on a minimal medium plus 2% agar.

2.2.2 Construction of a DNA cassette for *T. reesei* transformation

Constructing a plasmid pU-cbh1-gfp-pyr4 containing the *T. reesei cbh1* promoter, *cbh1* (gene encoding *T. reesei* cellobiohydrolase I or CBHI, GenBank accession no. **XM_006969162**), *Aequorea coerulescens gfp (Acgfp* gene encoding *Aequorea coerulescens* GFP*)*, *T. reesei pyr4* (gene encoding orotidine-5'-monophosphate decarboxylase, GenBank accession no. **XM_006961640**), and the *T. reesei cbh1* terminator was designed. The *cbh1* gene with its promoter and terminator was amplified by polymerase chain reaction (PCR) using the *T. reesei* genomic DNA as a template and

a primer pair (Pro.cbh1_Fw and Ter.cbh1_Rv). The DNA fragment was cloned into the EcoRV site of pUC118 (Takara Bio, Shiga, Japan) using the In-Fusion Cloning Kit (Takara Bio, Shiga, Japan). Next, this plasmid was opened at − 318 bp downstream of *cbh1* using inverse PCR with a primer pair (Inv1_Fw and Inv1_Rv) and ligated to a selectable marker pyr4 derived from pUpyr4F [24] using a Gibson Assembly Cloning Kit. Then, the plasmid was opened at the site between *cbh1* and its terminator by inverse PCR with a primer pair (Inv.sCBHI_Fw and Inv.sCBHI_Rv) and ligated to the *Acgfp* gene derived from pU-gfp (Takara Bio). The constructed DNA cassette was introduced into *T. reesei* PC-3-7ΔP to obtain the strain PC-CBHI-GFP.

The plasmid pU-cbh1-gfp-pyr4 was used as a template to construct a new plasmid harbouring the *cbh1* promoter, the *gfp* gene, and the *cbh1* terminator. To eliminate the *pyr4* gene, inverse PCR with a primer pair (Inv1_Fw and Inv1_Rv) was conducted, and the resulting PCR product was self-ligated using a DNA Ligation Kit (Takara Bio). Similarly, the same process was conducted to remove the *cbh1* gene using another primer pair (Inv2_Fw and Inv2_Rv) and a DNA Ligation Kit. The resulting plasmid was named pU-P. cbh1-gfp. A DNA cassette was excised from the plasmid by digestion with PstI and XhoI and used to transform *T. reesei* QM9414.

All plasmids were introduced to *E. coli* DH5α for amplification and sequenced to confirm no errors were present in their sequences. All PCR primers are listed in Supplementary Table 2-1.

Supplementary Table 2-1. Primers used in this study

Primers	Primer sequence (5' → 3')	Note
Pro.cbh1_Fw	CAG TCC CGT GGA ATT CTC ACG GT	For construction of the plasmid pU-cbh1-gfp-pyr4
Ter.cbh1_Rv	GAA TTC CAG CCC TAG AAG CGC C	
Inv_sCBHI_Fw	TCG GCC TGC ACT CTC CAA TCG	
In_sCBHI_Rv	CTG AGC ACG AGC TGT GGC CA	

Inv1_Fw	GCT CTT CGT GTA TCC CAG TAC CAC	For construction of the plasmid pU-P.cbh1-gfp
Inv1_Rv	GGC GAT TCT ACG GGT TAT GAA CG	
Inv2_Fw	ATG GTG AGC AAG GGC GCC	
Inv2_Rv	GAT GCG CAG TCC GCG GTT	
Seq.cbh1_Fw	GCA CAG AAA CCC AAT AGT CAA CCG	For PCR validation of GFP-expressing transformants
Seq.cbh1_Rv	GTC ATG ATA CGG GCT CAC CAA GA	

2.2.3 Fungal protoplast preparation and transformation

Fungal protoplasts were prepared based on the protoplast-mediated transformation method with a modification using fungal cell wall digestion enzymes [23,25]. Briefly, after pre-cultivation in flasks containing 50 mL of 0.3% glucose medium for 22 h at 28 °C, the *T. reesei* mycelia were collected by filtering through Miracloth, washed with sterilized distilled water, suspended in 15 mL Yatalase (Takara Bio, Shiga, Japan) solution, and incubated for 2 h at 30 °C with mild agitation (70 strokes/min). The released protoplasts were separated from undigested mycelia by Miracloth filtration and diluted with an equal volume of solution D (0.6 M sorbitol and 0.1 M Tris·HCl - pH 7.0). The diluted suspension was centrifuged at 4000 × g for 15 min to collect fungal protoplasts at the interphase. The collected protoplasts were washed twice with solution B (1 M sorbitol and 10 mM Tris·HCl - pH 7.5) before being resuspended with solution C (1 M sorbitol, 10 mM CaCl, 10 mM Tris·HCl - pH 7.5) to a concentration of 6.4×10^7 protoplasts·mL^{-1}. To check the cell wall digestion, the lysis of protoplasts using a microscope was observed after changing the osmotic pressure.

For protoplast-mediated transformation reactions, 200 µL of protoplast suspension was mixed with the DNA cassette (in 20 µL TE buffer) and 50 µL of polyethylene glycol (PEG) solution (25% of PEG 6000, 50 mM CaCl, 10 mM Tris·HCl - pH 7.5). Next, the mixture was incubated on ice for 20 min before adding 2 mL of the PEG solution. After being kept at room temperature for 5 min, the PEG-treated protoplast

suspension was diluted with 4 mL of the solution C, centrifuged at 2500 rpm for 15 min at 4 °C, and resuspended in the solution C.

For *T. reesei* PC-CBHI-GFP strain construction, a DNA cassette was excised from the plasmid pU-cbh1-gfp-pyr4 and then transferred into *T. reesei* PC-3-7ΔP protoplasts. The transformed protoplasts were isolated on minimal medium plates without uridine. The regenerating transformants were streaked twice on the plates to obtain stable transformants. Homologous integrants were confirmed by PCR and Southern analysis (data not shown).

2.2.4 Droplet generation and microscopic observations

Fungal spores or protoplasts were encapsulated in uniformly sized water-in-oil droplets (WODLs) using DG8™ Cartridges, a flow-focusing microfluidic chip (Bio-Rad Laboratories, Inc., Hercules, CA, USA) with a droplet generator (On-chip Biotechnologies, Tokyo, Japan). Eighty microliters of the fluorocarbon oil HFE-7500 with 2% (w/w) FluoroSurfactant 008 (On-chip Biotechnologies) were dispensed into eight wells of the microfluidic chip. After that, 20 μL of the aqueous phase consisting of a mixture of *T. reesei* protoplast suspension and the minimal medium was loaded into eight sample wells. The microfluidic chip was then inserted into the droplet generator to form 1-nL droplets by regulating the pressure of the continuous and aqueous phases. The generator allows droplet formation in a chip well with a speed of about 20,000 droplets·min^{-1} (**Figure 2-1**) and a polydispersity of less than 1.0% in droplet volumes. Following Poisson statistics, the expected number of protoplasts per droplet was controlled by the initial density of the protoplast suspension. The generated droplets were transferred into Eppendorf tubes for incubation.

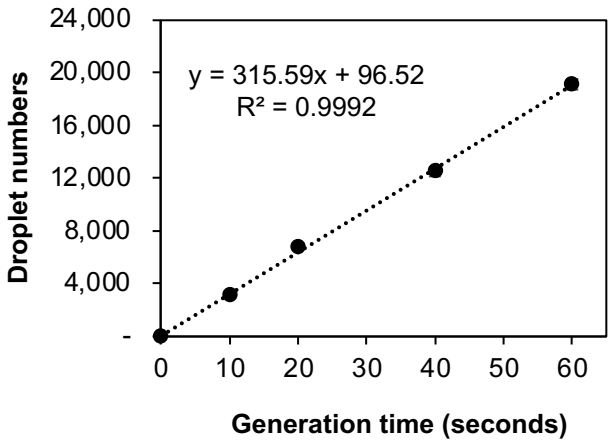

Supplementary Figure 2-1. Droplet formation using a single well of a DG8 cartridge and the droplet generator in different generation times. The aqueous phase contained minimal medium without fungal spores. The data represent an average of three independent experiments. Error bars indicate standard deviations.

For microscopic observations, after 40 μL of 008-FluoroSurfactant-0.1wtH in HFE-7500 (On-chip Biotechnologies) was prefilled into a channel of a micro-Slide VI flat (IBIDI, Martinsried, Germany), a 4 μL droplet sample was pipetted into each channel. The droplets in the micro-Slide VI flat were visualized with a Nikon Eclipse Ti2 microscope equipped with a Nis-element Ar software-operated camera (Nikon, Tokyo, Japan).

2.2.5 Enumeration, high-throughput screening, and PCR verification of sorted transformants

Enumeration and high-throughput screening of the WODLs were performed by a fluorescence-activated droplet sorting (FADS) system (On-chip Biotechnologies), following the manufacturer's instructions [26]. Before the enumeration or screening, the sheath, sorting, sample, collection, and reservoirs of a 150 μm-wide sorting chip (On-chip Biotechnologies) had 8 mL, 1.5 mL, 0.1 mL, and 0.1 mL of the fluorocarbon oil HFE-7500 (008-FluoroSurfactant-0.1wtH in HFE-7500) added, respectively. For droplet analysis, 20 μL of droplet sample was loaded into the sample reservoir. The sorting chip was then inserted into the On-chip sorter to measure the distributions of forward scatter (FSC) intensity and green fluorescence intensity (488 nm excitation and 543±22 nm detection) of the droplets. Data output was analyzed by FlowJoTM v10.6.2 (Tree Star, Inc, Ashland, OR, USA). Droplets with GFP-expressing fungal transformants were detected via green fluorescence intensity, and high-throughput screening sorted the targeted droplets. In addition to the fluorocarbon oil, 500 μL of mineral oil (Sigma Aldrich, Darmstadt, Germany) was supplied to each sample and collection reservoir, resulting in the protoplasts layering between two oil phases. At the interphase of the two oil layers in the sample reservoir, a 200 μL droplet sample was then injected. The sorting chip was also placed into the sorter to screen droplets with a throughput of up to 8,000 droplets·min^{-1}. The droplets with high green fluorescence intensity were sorted and

pushed into the collection reservoir. The sorted droplets were transferred onto PDA-X plates and incubated at 28 °C to form separate colonies.

The presence of the *gfp* gene in sorted transformants was verified using colony PCR with a pair of primers (Seq.cbh1_Fw and Seq.cbh1_Rv) (Supplementary Table S1). The PCR process was performed as follows: 1 cycle of 98 °C for 2 min, 30 cycles of 98 °C for 10 sec, 60 °C for 30 sec, and 68 °C for 2 min.

2.3 Results

2.3.1 Detection of marker gene expression in water-in-oil droplets (WODLs)

The feasibility of detecting target fungi in WODLs was an essential task for establishing a droplet-based microfluidic workflow for filamentous fungal transformation. A fluorescence-activated droplet sorting (FADS) system could theoretically identify a green fluorescent protein (GFP) expression and separate the GFP-expressing fungi from an extensive library. To investigate the task, the study selected *T. reesei* PC-CBHI-GFP strain as a target fungus because this strain harbours a fusion of the marker gene gfp and the native gene cbh1 under the control of the cbh1 promoter. Depending on the case, the marker gene expression could be enhanced or hidden when inducing or repressing substances were added to the culture medium. To address the impediment of the rapid expansion of fungal mycelia, the study investigated the best inducers of GFP expression during the early fungal growth stage and identified when the marker gene initiated expressing.

Firstly, various soluble inducers of the cbh1 promoter, including sorbose, cellobiose, lactose, CMC, and sophorose, were tested in the droplet culture of the GFP-expressing fungal strain. Glucose, a repressor of the *cbh1* promoter, served as a negative control for the investigation. The *T. reesei* PC-CBHI-GFP spores were mixed with induction or repression media before being encapsulated in droplets and incubated for 24 h. To ensure encapsulation of a strict single spore, an average number of fungal spores in droplets to 0.06 spore per droplet ($\lambda \sim 0.06$) with 6.41% of droplets containing single spores, 0.22% of droplets harbouring two or more spores, and 93.37% empty droplets was set up. Within the 24-h droplet cultivation period, fungal mycelia grew inside droplets regardless of the carbon source (**Figure 2-2a)**. The droplet size distribution analyzed via the forward scatters (FSC) intensity by a FADS system indicated that approximately 98% of the droplets were stable on average during fungal growth (**Figure 2-2b**). However, GFP expression was visualized and detected in only the sophorose induction medium. As a result, sophorose was selected as the sole carbon source to induce the early expression of genes driven by the *cbh1* promoter in the WODLs cultures of *T. reesei.*

Secondly, the study explored fungal growth and GFP expression in the sophorose-induction medium droplets (**Figure 2-2c**). The parental strain *T. reesei* PC-3-7 was used as a negative control. Spores germinated during the 12-h incubation period, and hyphae expanded within the droplets. After 18-h incubation, GFP expression started

to be observed in some droplets containing mycelia. Although some fungal hyphae exited the droplets, there was no evidence of droplet coalescence during this period. By 24-h cultivation, GFP expression levels had increased concurrently with fungal growth in the droplets. For extended cultivation periods of 36 h and 48 h, the encapsulated fungi quickly grew, punctured the droplets, and formed fungal clumps. Besides, significantly increased autofluorescence levels were observed in the negative control during the longer cultivation time, which could lead to the detection and isolation of false-positive droplets. These findings suggest that WODLs culture successfully induced marker gene expression in *T. reesei* during the growing period from 18 h to 24 h incubation with over 98% of the stable droplets.

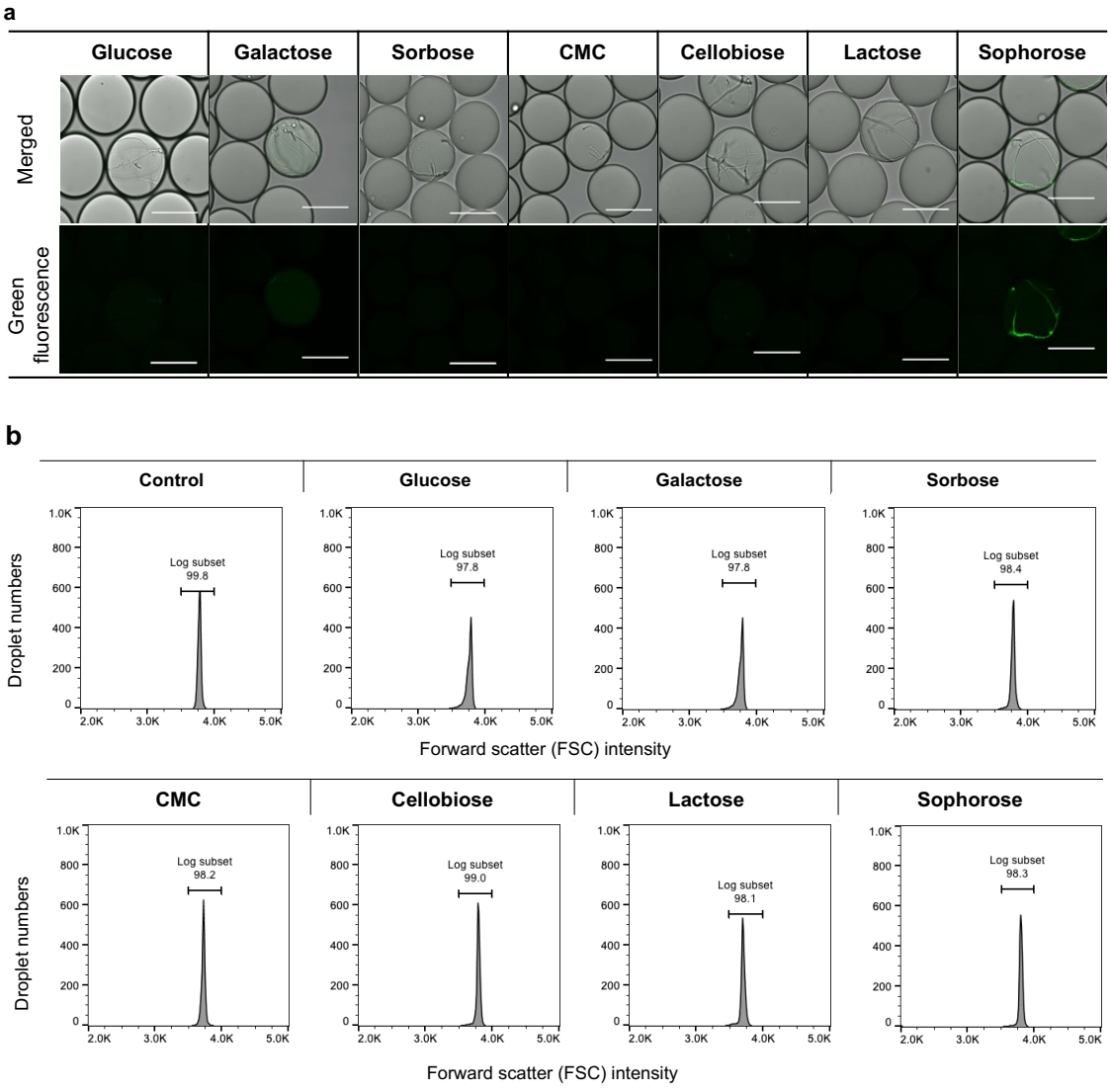

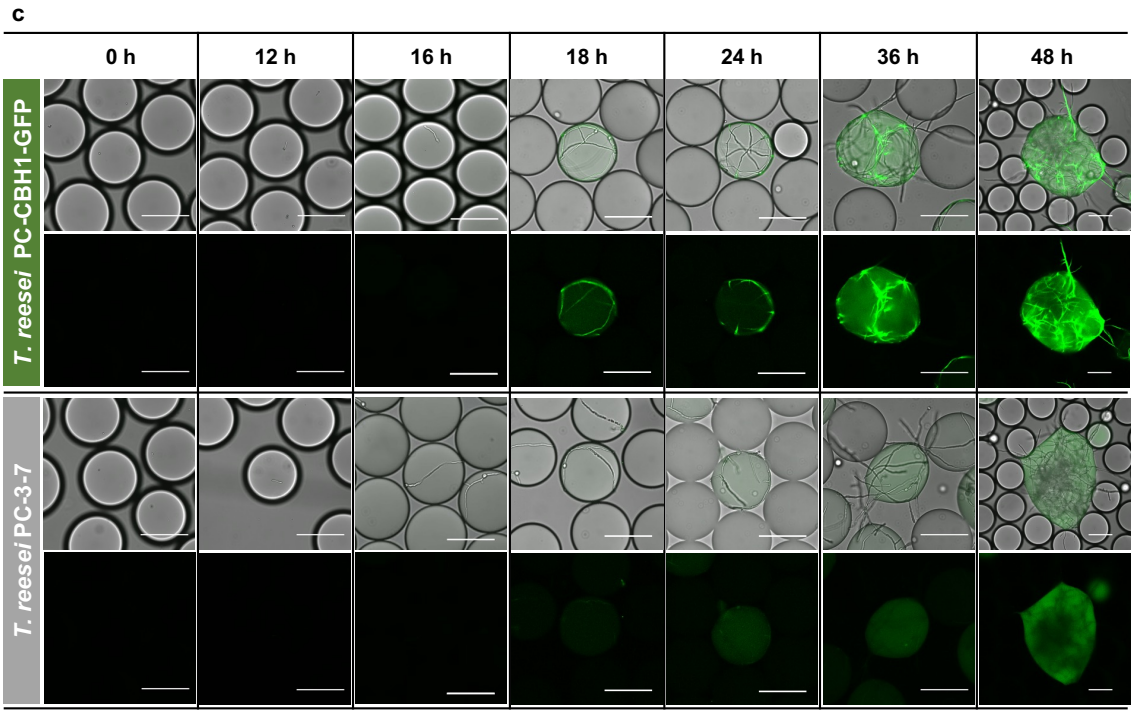

Figure 2-2. Cultivation of the filamentous fungus *T. reesei* in WODLs. (a) Droplet culture of *T. reesei* PC-CBHI-GFP and its parental strain *T. reesei* PC-3-7 in selected carbon sources. Single spores were encapsulated in droplets, incubated at 28 °C for 24 h, and then observed with a fluorescence microscope. (b) Forward scatter (FSC) histograms illustrating droplet size distributions. The FSC values were analyzed by the FADS system. *T. reesei* spores were encapsulated in droplets containing different carbon sources, incubated for 24 h, and then injected into the sorting chips for the FSC analysis. The empty droplets served as controls. Approximately 3,000 droplets were used in each assay. (c) Micrographs of spore germination, growth, and GFP expression of *T. reesei* PC-CBHI-GFP in droplets containing sophorose-induction medium (40× and 20× magnification). The scale bars depict 100 μm.

2.3.2 Droplet-based microfluidic screening for GFP-expressing fungi from an artificial spore library

Early GFP detection in droplets allows droplet screening to isolate GFP-expressing fungi, so the possibility was investigated of using FADS to separate the GFP-expressing fungi from an artificial spore mixture (**Figure 2-3a**). The *T. reesei* PC-CBHI-GFP spores were mixed with its parental PC-3-7 spores at a 1 to 4 ratio. Single spores were then compartmentalized in the droplets containing the sophorose-induction medium. The average droplet spore number was 0.21 spores per droplet ($\lambda \sim 0.21$), with 3.54% of droplets harbouring *T. reesei* PC-CBHI-GFP, 15.10% of droplets containing *T. reesei* PC-3-7, 0.66% of droplets containing both strains, and 80.70% empty droplets. Also, WODL culturing of the parental strain was used as a negative control. During the incubation periods from 18 h to 24 h, droplets were analyzed for the intensity of green fluorescence via the FADS system. Based on the fluorescence assessment of the negative control, a sorting gate was established, in which positive droplets indicating the GFP-expressing fungi could be distinguished from the rest of the droplet population (**Figures 2-3b and c**)

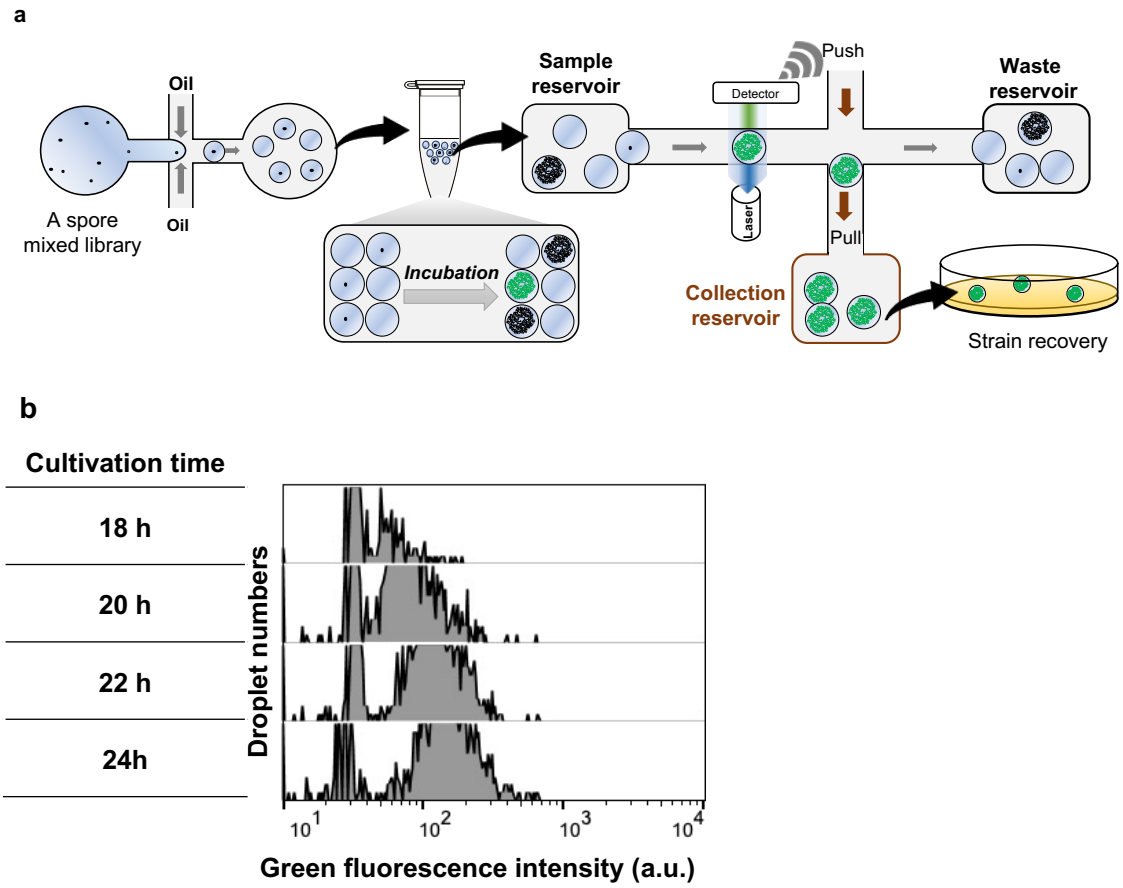

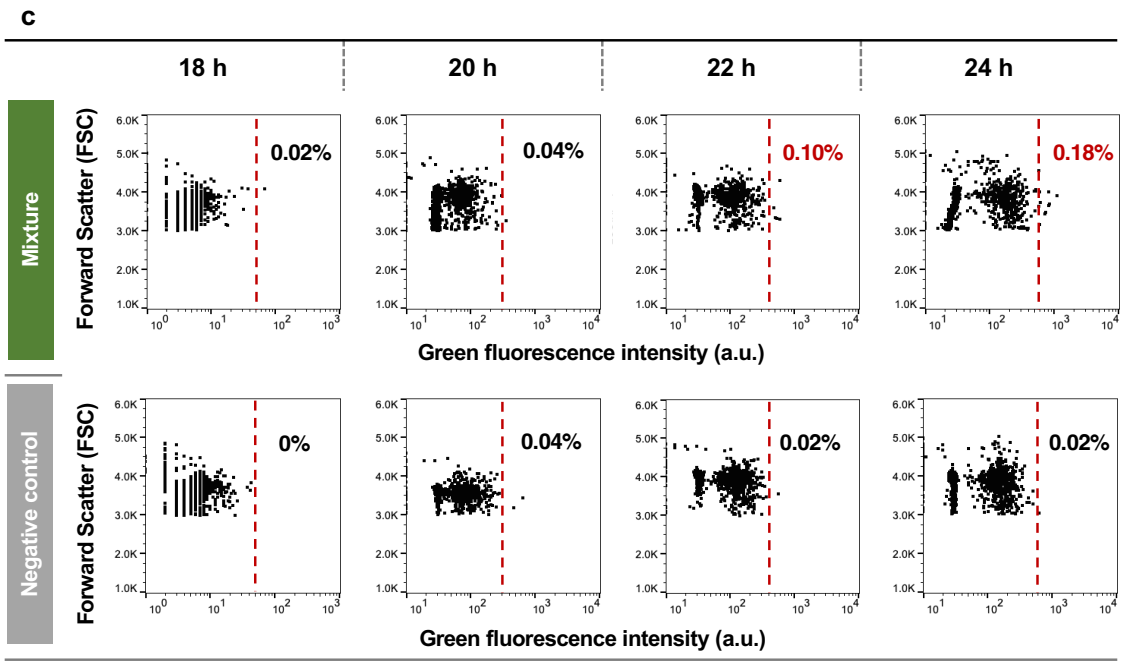

Supplementary Figure 2-3. Rapid analysis of droplet populations from 18 h to 24 h incubation and PCR identification of sorted candidates. (a) Schematic diagram of droplet screening based on fluorescent gene expression. Before droplet culture and screening, spores of *T. reesei* PC-CBHI-GFP were mixed with spores of its parental strain, PC-3-7, at a 1 to 4 ratio and then encapsulated in the droplets supporting fungal growth and gene expression. After droplet cultivation, the droplet population was screened, and a high throughput process separated the positive droplets containing GFP-expressing fungi. The sorted droplets were subsequently plated for fungal recovery. (b) The FSC and green fluorescence analysis of droplet populations after droplet cultivation. Based on the fluorescence assignment of the negative control, a sorting gate was devised in which a positive droplet population with higher fluorescence intensity could be discriminated against from the rest of the droplet population. These data represent the proportions of positive droplet numbers in the droplet population. Approximately 5,000 droplets were analyzed during each round of analysis. (c) Histograms represent the green fluorescence levels of the negative control after culture periods of 18, 20, 22, and 24 h.

The FADS analysis did not detect high levels of green fluorescence from droplet cultures incubated for 18-h to 20-h (**Figure 2-3c**). During the 22-h incubation, a small proportion of droplets containing GFP-expressing fungi were distinguishable from the rest of the droplet population. By 24-h of culturing, the value increased to 0.19±0.07% of

the droplet population (**Figure 2-4a)**. As a result, the screening process with a screening speed of up to 8,000 droplets·min^{-1} was then carried out to isolate the targeted fungi based on their GFP expression. After incubating for 24 h, 860 droplets were separated from the population of over 7.0×10^5 droplets (containing approx. 8.6×10^4 fungal spores) for nearly 2 h (**Figure 2-4b**). The separated droplets were then streaked onto plates for strain recovery with 100 droplets per plate and were identified by colony polymerase chain reaction (PCR). In the PCR identification, 52±18 of *T. reesei* PC-CBHI-GFP colonies out of 103±16 recovered fungal colonies (50.2%) showed a *gfp-cbh1* integration band (**Figure 2-4c**). This achievement suggested that a droplet-based microfluidic platform could employ the reporter gene *gfp* as a selectable marker for screening genetically engineered *T. reesei*.

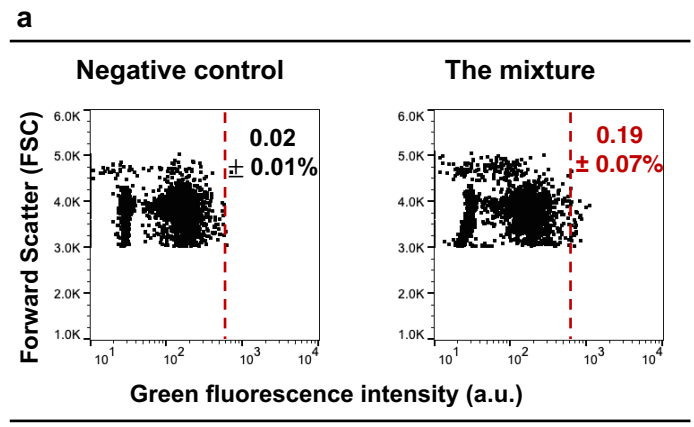

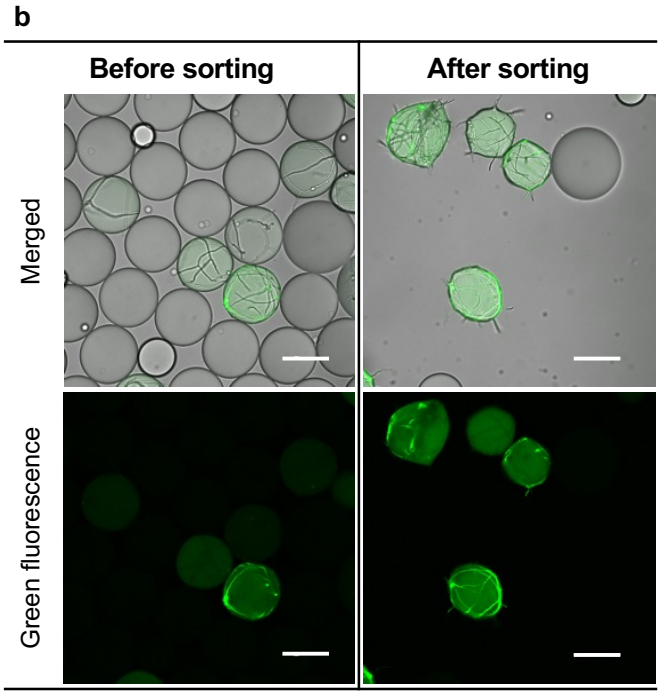

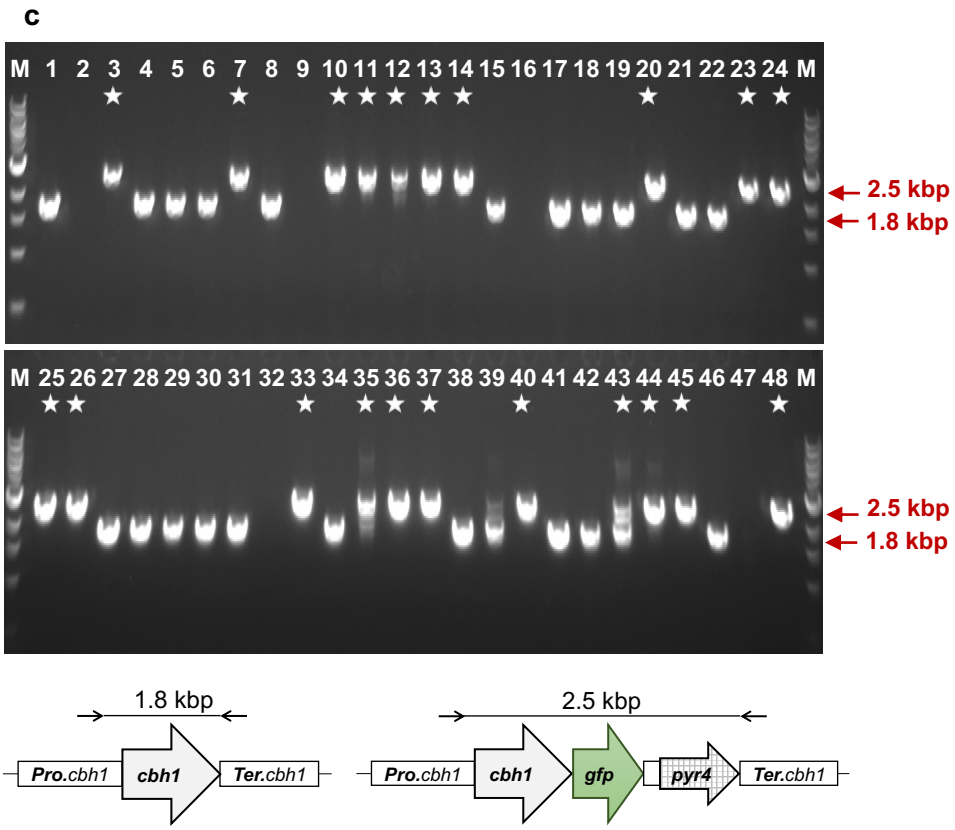

Figure 2-4. Rapid isolation of *T. reesei* based on GFP expression from an artificial spore library. (a) The FSC and green fluorescence analysis of droplet populations after a 24-h incubation. Based on the fluorescence assignment of the negative control, a sorting gate was set up in which a positive droplet population with higher fluorescence intensity could be discriminated against from the rest of the droplet population. The data represent an average proportion of the positive droplet number in the droplet population (mean±standard deviations) from three independent experiments. For each analytical round, 5,000 droplets were analyzed. (b) Micrographs of droplets before and after the high-throughput screening. The scale bars depict 100 μm. (c) Colony PCR identification of 48 selected recovery fungi using primer pair Seq.cbh1_Fw and Seq.cbh1_Rv. The expected length of the *T. reesei* PC-CBHI-GFP fragment was 2.5 kb and that of its parental strain was 1.8 kb. The star symbol indicates the *T. reesei* PC-CBHI-GFP strain.

2.3.3 Regeneration of fungal protoplasts in droplets compared to those on bilayer-agar plates

After proving the applicability of a droplet-based microfluidic platform for the cultivation, detection, and isolation of growing beneficial fungi based on GFP expression, the study proposed to employ the platform to accelerate the genetic transformation of filamentous fungi. Due to the lack of information about fungal protoplast regeneration in droplets, whether the WODL culture would be feasible for fungal regeneration was investigated. The study also compared the droplet cultivation method with the traditional bilayer-agar plate cultivation method (**Figure 2-5a**). Before being capsulated in the droplets, *T. reesei* QM9414 protoplasts were subjected to the polyethylene glycol (PEG) treatment without exogenous DNA. The average number of protoplasts per droplet was set to 0.05 ($\lambda \sim 0.05$), ensuring a strict single protoplast encapsulation. To estimate the frequency of fungal protoplasts regenerated within droplets, about 3,000 droplets were generated based on the generation time in the droplet generator (**Figure 2-1**), then incubated off-chip for 1 to 3 d, and eventually transferred to PDA-X plates for colony number estimation. For the plate culture, 100 fungal protoplasts were mixed with molten top agar, plated, and incubated until regenerating fungal colonies appeared.

Microscopic observations indicate that *T. reesei* protoplasts regenerated and developed quickly in the droplets (**Figure 2-5b**). On the first day of droplet cultivation, fungal protoplasts could reform their cell walls and germinate inside the droplets (**Figure 2-5c**). The following day, regenerating fungal cells were still confined within the droplets. With a longer incubation time, however, the hyphal tips of the regenerating fungi extended beyond the boundaries of individual droplets (**Figure 2-5b**). In contrast to the results of droplet cultivation, there were no regenerating fungal colonies on the bilayer-agar plates during the same 3-incubation period (**Figure 2-5d**). The frequency of *T. reesei* protoplast regeneration in droplets was significantly higher than that of the plates (**Figure 2-5e**). Between 1-d and 2-d of droplet culture, the proportion of fungal protoplasts regenerated within droplets rose from 7.09±0.53% to 23.83±1.59% of total encapsulated protoplasts. This ratio could reach 31.62±6.09% on the third day of droplet culture in which the regenerating fungal hyphae grew outside the droplets. By contrast, only 1.56±0.01% of total plated fungal protoplasts regenerated on the double-agar plates after 7-d incubation. The following three days observed a slight increase to 3.65±0.74% in the proportion of the plated protoplasts recovering and forming colonies. The data indicated

that the WODL culture could accelerate the regeneration process of filamentous fungi with a faster generation time and higher regeneration ratio.

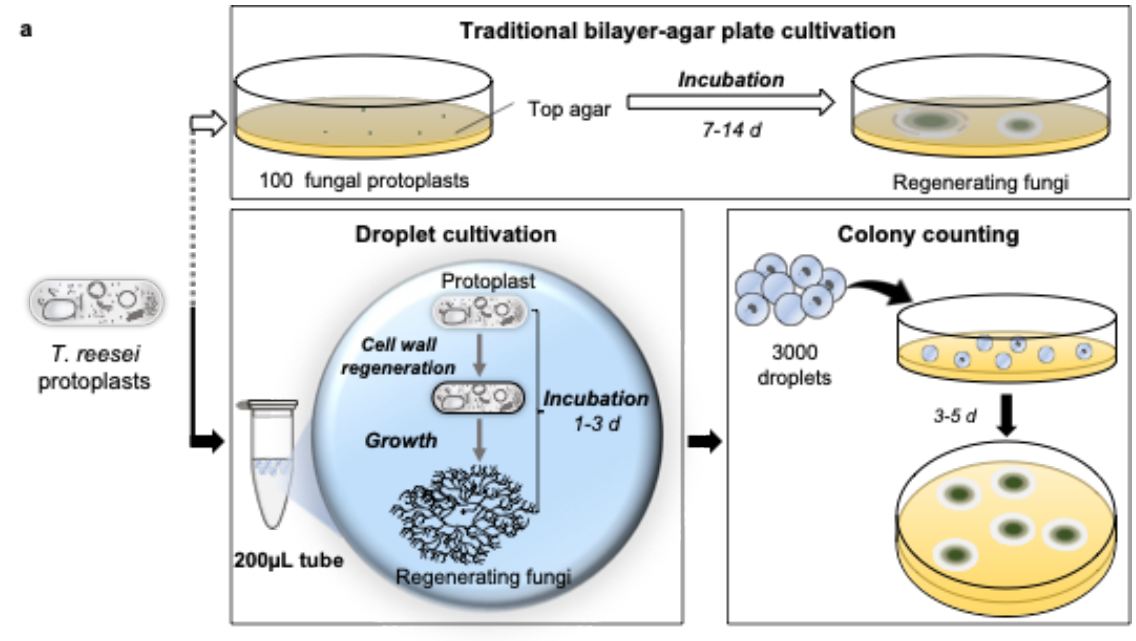

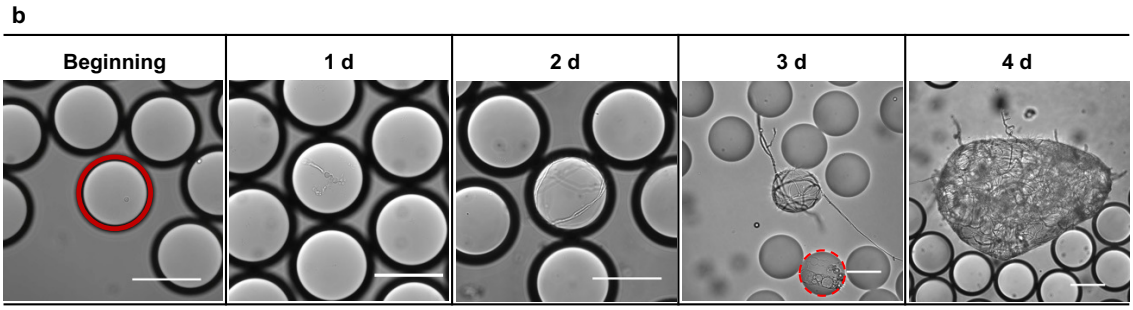

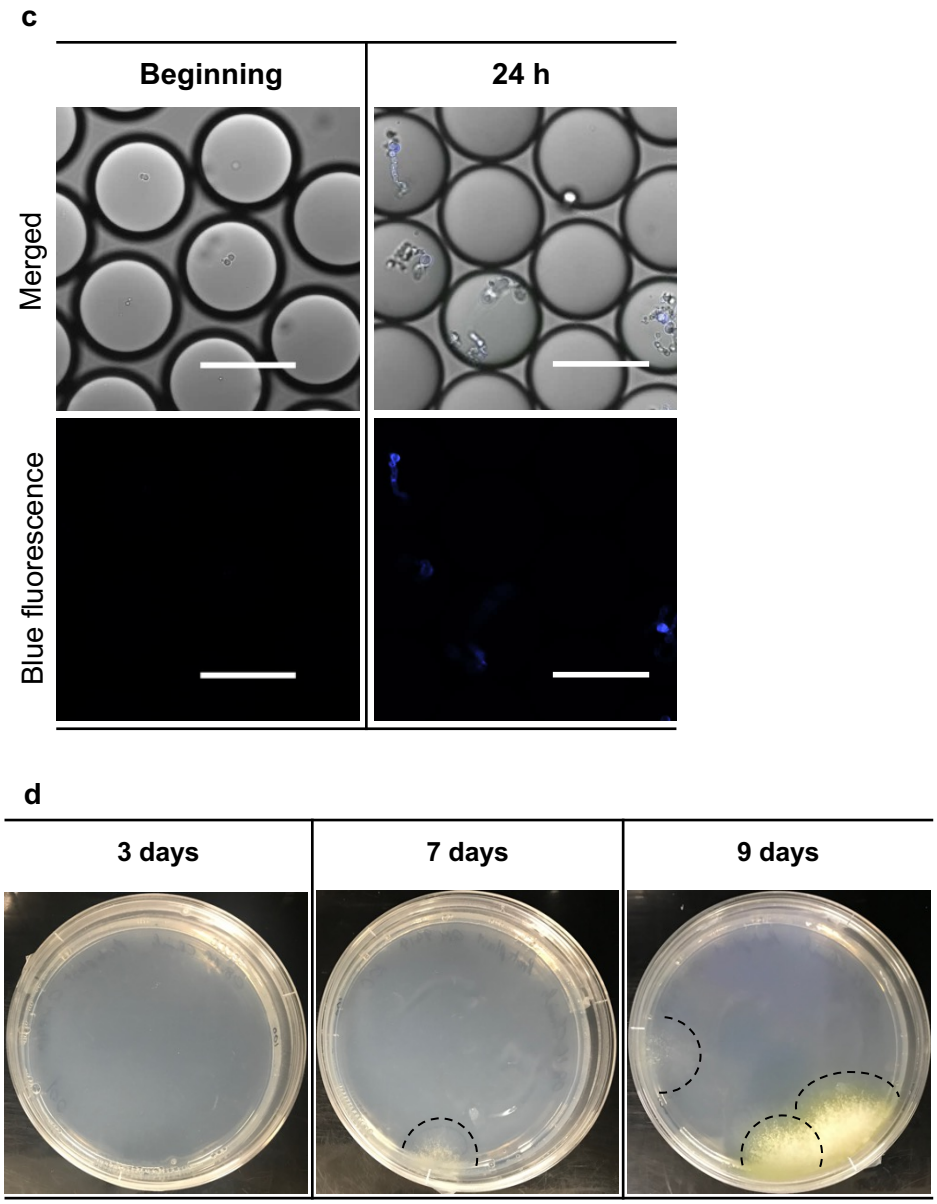
c
Beginning
24 h
Merged
Blue fluorescence
d
3 days
7 days
9 days
e
Droplet cultivation
Plate cultivation
Regeneration frequency (%)
Culture period (days)
0
10
20
30
40
1 2 3 4 5 6 7 8 9 10
0
2
4
6
8

Figure 2-5. Regeneration of *T. reesei* protoplasts in the WODLs. (a) Micrographs of fungal protoplasts in the droplets within 4-d cultivation. Solid red circles highlight the single protoplast encapsulated in the droplets. The dashed red circle highlights a non-regenerating protoplast. The scale bars are 100 μm. (b) Schematic for estimating the *T. reesei* protoplast regeneration frequencies in the conventional bilayer-agar plate cultivation and the WODL culture. For the droplet culture, about 3000 droplets (approx. 100 fungal protoplasts) were formed, incubated for 1 to 3 d, and then streaked onto PDA-X plates for the formation of regenerating fungal colonies. For the plate culture, 100 fungal protoplasts were spread on bilayer-agar plates and incubated until fungal colonies appeared. (c) Micrographs of fungal protoplasts in the droplets after protoplast compartmentalization in the WODLs and after a 1-day droplet culture. The droplets contained minimal medium plus 0.1 $\mu g \cdot mL^{-1}$ of Calcofluor White, a fluorescent cell-wall dye. The scale bar represents 100 μm. (d) Fungal regeneration on traditional bilayer-agar plates. After the PEG treatment during transformation, 100 fungal protoplasts were plated and incubated until colony formation. Dashed black semi-circles highlight fungal colonies derived from 100 plated protoplasts. (e) The regeneration frequency of fungal protoplasts in the droplet culture compared to that of the plate culture. These data represent an average of three independent experiments. Error bars indicate standard deviations.

2.3.4 Establishment of high-throughput analysis and screening for fungal transformants based on the GFP expression

Since WODLs cultures could be employed for *T. reesei* protoplast regeneration, a novel droplet-based workflow for the fungal transformation was proposed (**Figure 2-6a**). The fluorescence marker gene *gfp* driven by the inducible *cbh1* promoter was selected as a single selection marker. After the transformation process, the transformed protoplasts were encapsulated in 10^6 droplets with an average number of fungal protoplasts at 0.64 protoplasts per droplet ($\lambda \sim 0.64$). Also, the droplet compartmentalization of non-transformed protoplasts served as a negative control and was used to set the sorting gate.

Before the screening process, the study evaluated the effects of inducer concentrations and culture time on gene expression detection during the early phase of protoplast regeneration within droplets. Like *T. reesei* PC-CBHI-GFP spores, transformed *T. reesei* protoplasts were encapsulated and cultured in droplets with 1% sophorose. During a 48-h incubation, no detectable GFP expression occurred, but an increased level of the fluorescent signal was detected in some droplets (**Figure 2-6b**). Autofluorescence is the cause of the false-positive droplets and would be an obstacle to the screening process. It was predicted that a higher inducer concentration in the droplet culture could enhance marker gene expression (**Figures 2-6c**). The FADS analysis indicated that the positive droplets could be distinguished from the droplet library in 24-h droplet cultures. For longer cultivation times, the ratio of false-positive droplets increased significantly (**Figure 2-6d**). These results suggested the optimal culture conditions for the *gfp*-transformed protoplasts would be 2% sophorose-supplemented media in 24-h droplet cultures before the rapid screening.

Next, the high throughput sorting of fungal transformants with the highest levels of GFP expression was carried out (**Figures 2-6e**). From a population of 4×10^5 droplets (containing approximately 2.02×10^5 *T. reesei* protoplasts), 247 droplets were sorted within 94 min. The sorted droplets were then streaked on plates and incubated for strain recovery. After incubation, the recovered fungal colonies were selected, and *gfp* integration was confirmed by colony PCR analysis. Consequently, 28 out of 29 (96.6%) sorted fungal candidates displayed a GFP integration band in addition to a wild-type *cbh1* band (**Figure 2-6f**). Furthermore, single spores were isolated from sorted candidates and analyzed gene recombination again. The PCR verification of 48 randomly selected

isolated colonies showed that 6 colonies (12.5%) were non-homologous recombinants, and the rest were the wild-type (**Figure S2-6g**). These results indicated that the droplet culture and screening scheme could successfully isolate the desired fungal transformants from a transformed protoplast library.

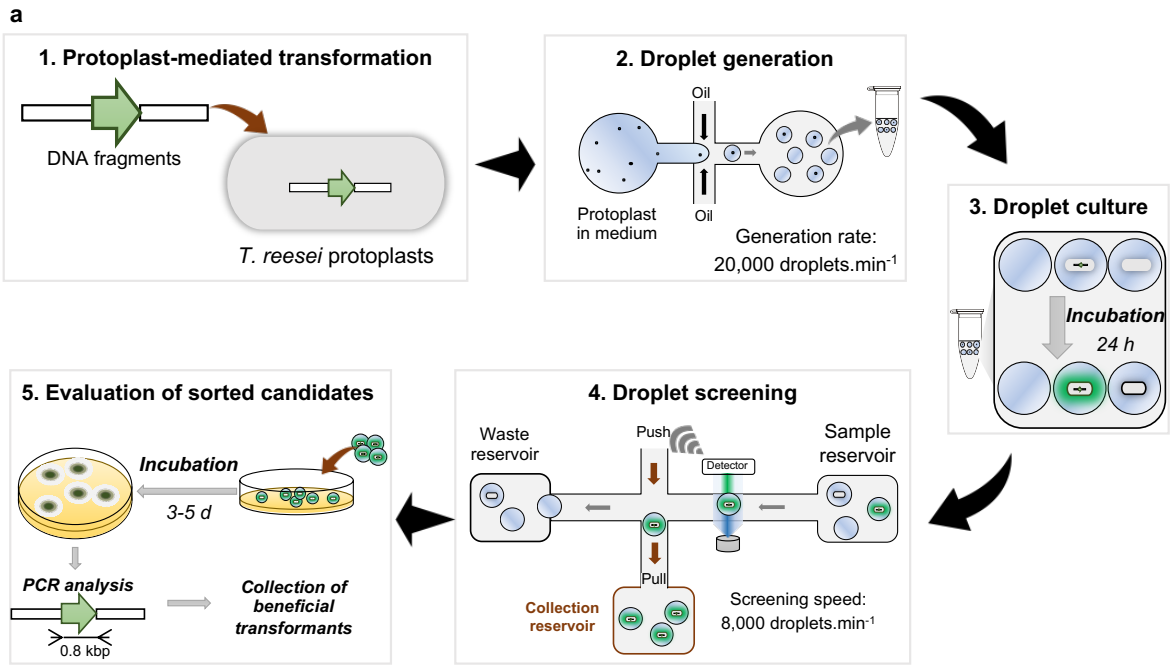

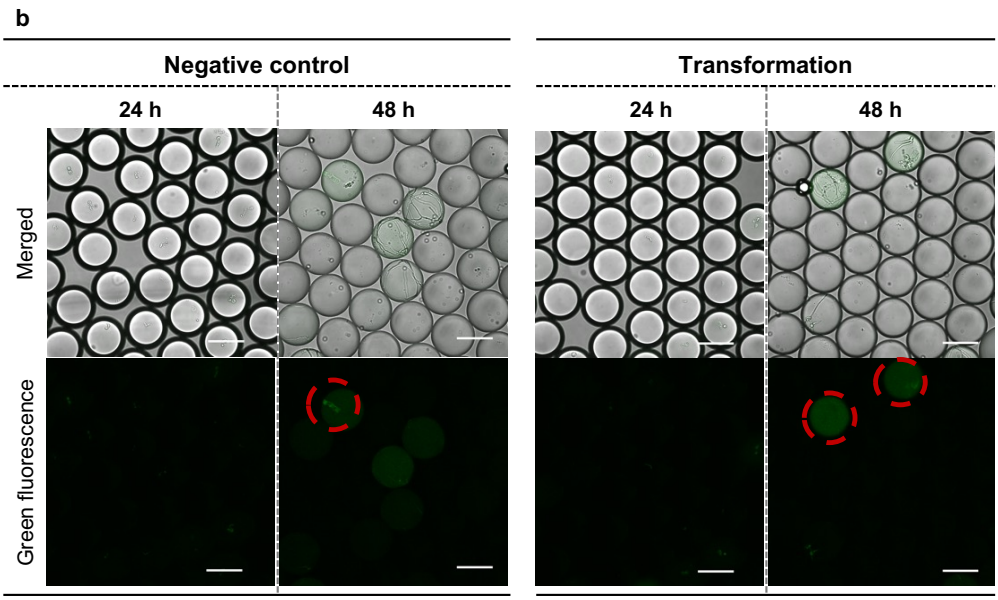
b
Negative control
Transformation
24 h
48 h
24 h
48 h
Merged
Green fluorescence

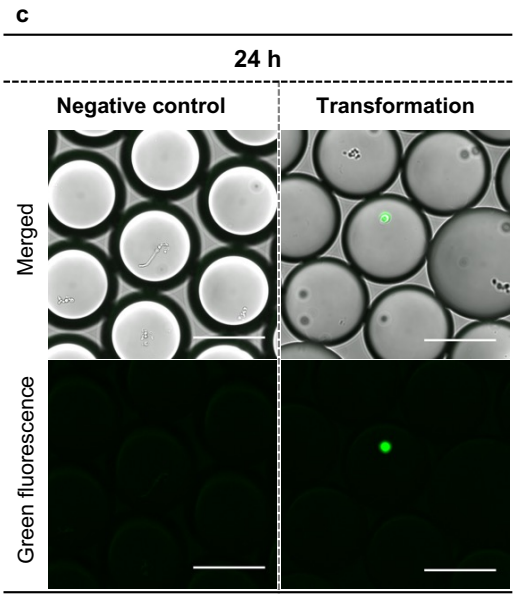
c
24 h
Negative control
Transformation
Merged
Green fluorescence

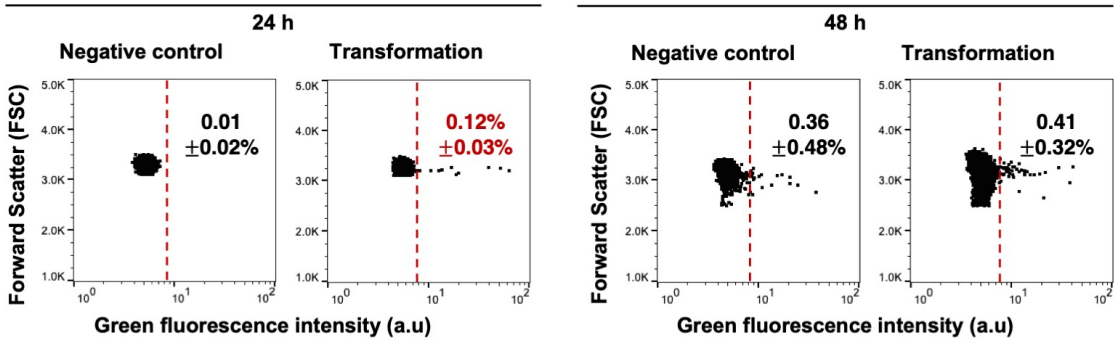
d
24 h
48 h
Negative control
Transformation
Negative control
Transformation
Forward Scatter (FSC)
0.01
±0.02%
0.12%
±0.03%
0.36
±0.48%
0.41
±0.32%
Green fluorescence intensity (a.u)
Green fluorescence intensity (a.u)

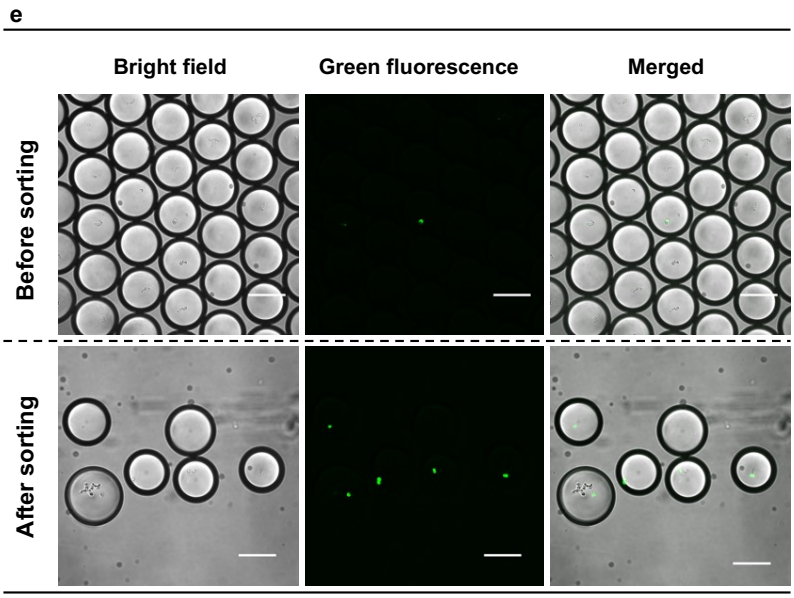
e
Bright field
Green fluorescence
Merged
Before sorting
After sorting

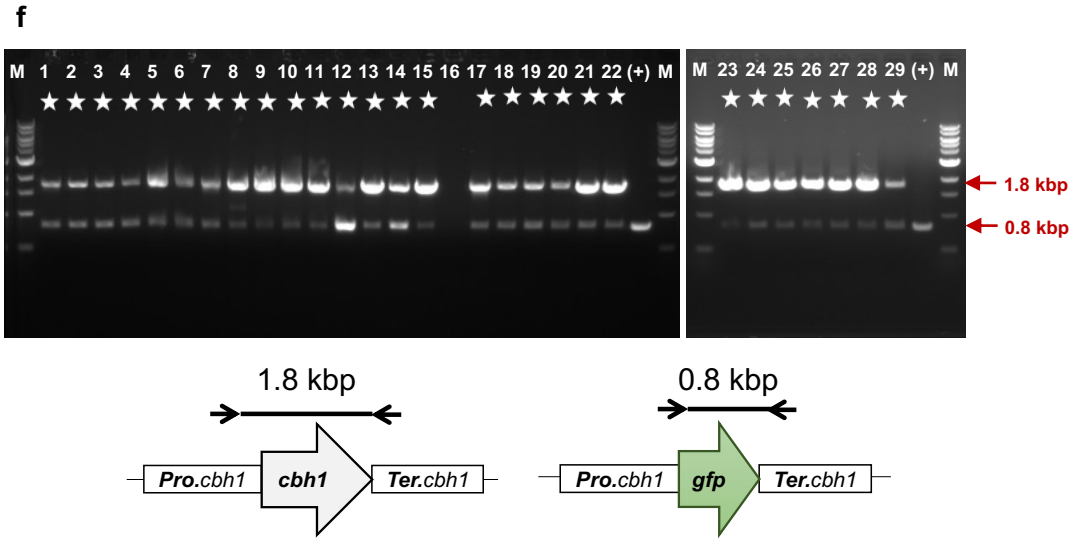
f
M 1 2 3 4 5 6 7 8 9 10 11 12 13 14 15 16 17 18 19 20 21 22 (+) M
M 23 24 25 26 27 28 29 (+) M
1.8 kbp
0.8 kbp
1.8 kbp
Pro.cbh1
cbh1
Ter.cbh1
0.8 kbp
Pro.cbh1
gfp
Ter.cbh1

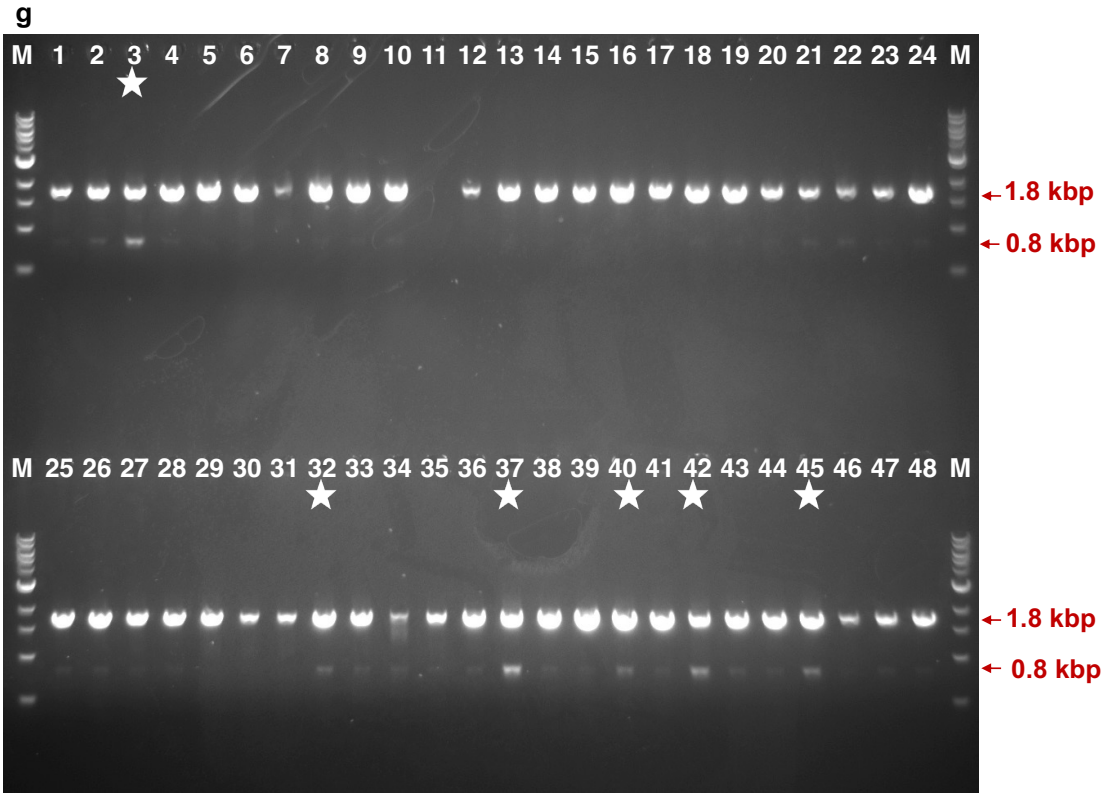

Figure 2-6. High-throughput analysis and screening of *T. reesei* transformants based on their GFP expression. (a) Schematic diagram of the high-throughput workflow for the genetic transformation of *T. reesei* employing the droplet-based microfluidic platform. (b) Microscopic imaging of droplet cultures grown in 1% sophorose induction medium and incubated for 24- and 48-h. Although the transformed protoplasts regenerated in the droplets, no GFP expression was detected. An increase in autofluorescence levels was observed in droplets containing the generating fungi and droplets containing non-regenerating fungi during the 48-h culture period. Dashed red circles highlight the autofluorescence. The scale bar represents 100 µm. (c) Micrograph of 24-h incubated droplets grown in 2% sophorose induction medium. The GFP-expressing transformant was observed in droplets. The scale bar represents 100 µm. (d) The FSC intensity and green fluorescence analysis of droplet populations containing the 2% sophorose medium after 24-h and 48-h incubation. Droplets harboring non-transformed *T. reesei* protoplasts served as a negative control to set the sorting gate (Dashed red lines). Numbers indicate the proportion of positive droplets among the entire droplet population. For each analytical round, 10,000 droplets were analyzed. (e) Microscopic images of droplets before and after sorting. The scale bars are 100 µm. (f) The PCR analysis of sorted fungi. The expected length of the amplified DNA from the transformant was 0.8 kbp, whereas

that of the wild-type strain was 1.8 kbp. The colony PCR products of sorted fungi with the Seq.cbh1 primers included Seq.cbh1_Fw and Seq.cbh1_Rv. Plasmid pUpro.cbh1-gfp was used as a positive control (+) for PCR (rightmost lane). The star symbols indicate *gfp*-transformed fungal strains. (g) PCR analysis of 48 randomly selected fungal colonies after a round of single spore isolation. The star symbol indicates transformants displaying *gfp* integration band.

2.4 Discussion

Droplet microfluidic technology has opened new avenues for microbiological research with numerous unique advantages, such as the possibility of high-throughput generation and manipulation of micro-volume bioreactors [1,27]. This versatile and powerful platform has contributed significantly to studies on bacteriophages, bacteria, yeasts, and algae, but negligibly to fungal research [2,3]. Furthermore, the genetic modification techniques for filamentous fungi, particularly *T. reesei*, are generally time-consuming and effort-intensive due to the long time and low rates for regenerating fungal protoplasts as well as poor performance selections. Here, a droplet platform has been employed to develop a novel high-throughput genetic transformation workflow for the filamentous fungus *T. reesei*.

Droplet culture allowed filamentous fungus *T. reesei* PC-CBHI-GFP strains to express the fluorescent marker GFP during the early stages of fungal growth. Different from droplet cultivation of bacteria, yeasts, or algae, the cultivation of filamentous fungi is much more challenging. The main obstacle to culturing these fungi in droplets is the rapid expansion of branched fungal mycelia beyond the boundaries of individual droplets [2]. To overcome this obstacle, this study used GFP, a selectable fluorescent marker, to rapidly detect growing *T. reesei* before its expanding mycelial network led to droplet coalescences. For this reason, the feasibility of using droplet culture for the *T. reesei* PC-CBHI-GFP strain carrying a *gfp* gene under the control of the strong and inducible *cbh1* promoter was investigated. Due to the *cbh1* promoter being controllable, several cellulase-inducing carbon sources were used to promote intracellular GFP expression during the early stages of fungal growth within the droplets. Sophorose has the greatest potential as an inducer for GFP expression, but its application in classical cultivation methods, such as flasks or plates, was hindered by the high cost [12,28]. With the advantage of volume miniaturization, the droplet culture enabled us to use this costly inducer for fungal cultivation. After a 24-h incubation, GFP expression was observed in the presence of sophorose but not in the presence of other inducers **(Figure 2-2a).** The tracking of GFP expression in droplets containing the sophorose medium showed that *T. reesei* PC-CBHI-GFP grew and began expressing visible fluorescence at 18 h of incubation. Up to 24-h cultivation, the fungal hyphae were generally still confined within the droplets, and about 98% of the droplet population remained stable (**Figure 2-2b**). For longer cultivation time, despite the increasing levels of green fluorescence, the fungal

hyphal network expanded outside the droplets and led to the merging of surrounding droplets. Hyphal expansion is a problem because the formation of large clumps can block the microfluidic sorting channels during the screening process. In addition, the study observed autofluorescence in droplets harbouring the growing non-GFP-expressing fungi that could lead to the detection and isolation of false-positive droplets (**Figure 2-2c**). The autofluorescence could be attributed to biological fluorophores: fungal cell-wall components (chitin and sporopollenin), coenzymes (flavins), pigments (lipofuscin and melanin), and secondary metabolites (alkaloids, phenolics, and terpenoids) [29]. Thus, the study succeeded in culturing *T. reesei* in droplets and inducing the expression of a fluorescent marker gene during the early growth phase after spore germination.

Droplet culture also permitted the high-throughput evaluation and screening of GFP-expressing fungi from an artificial spore library (**Figure 2-3 and 2-4**). Based on the evaluation of nearly 30,000 droplets, 860 positive droplets (i.e. containing approx. 860 growing fungi) were isolated from a 700,000-droplet population within 2 h (Figures 2b, c). Most of the isolated fungi were recovered and formed colonies on the plates, with about 50% of the colonies being the *T. rees*ei PC-CBHI-GFP strain (Supplementary Fig. S3c). Autofluorescence limited the enrichment of GFP-expressing fungi in droplets. False-positive droplets were visualized in the isolated droplet population and an increasing level of autofluorescence was detected from 18 h to 24 h incubation in the negative control. During *T. reesei* spore germination, previously reported higher autofluorescence resulted from fungal growth [30]. Despite the problem of false-positive droplet collection, the droplet-based microfluidic screening displayed high potential in isolating massive numbers of targeted fungi within a few hours. For screening based on GFP fusion, the fluorescence-activated cell sorting (FACS) system is also a powerful tool for germinated spores, but not for actively growing fungi [20]. This is the first report of a rapid isolation method for growing filamentous fungi based only on GFP expression. In addition to the FACS platform, this study has provided a versatile and novel tool for fungal research and cultivation.

The regeneration of *T. reesei* protoplasts within droplets was much faster and in higher numbers than on bilayer-agar plates used in the classic protoplast-mediated transformation method (**Figure 2-5**). Before establishing the high-throughput approach for the genetic transformation of filamentous fungi, the study investigated the applicability of droplet cultures in fungal protoplast regeneration. The results indicated

that within only 1-2 d of droplet cultivation, the encapsulated fungal protoplasts recover their cell walls and initiate hyphal grown within the droplets. In contrast, on plates, the incubation time required for the appearance of visible fungal colonies is at least a week, a duration that was also reported previously for the regeneration of *T. reesei* ATCC66589 [31]. Moreover, the findings indicated that the regeneration frequency of *T. reesei* protoplasts within droplets was 8-fold higher than on bilayer-agar plates. This result is supported by a previous study on the regeneration of protoplasts from the fungus *Antrodia cinnamomea* in solid and liquid culture environments [32]. The quicker regeneration time and higher regeneration rate of fungal protoplasts in droplet cultures, as opposed to plate cultures, are attributed to the protection from a high-temperature medium, the constant supply of oxygen, and the stochastic confinement of single fungal protoplasts in droplets. In the encapsulation process, the fungal protoplasts are mixed with the medium at room temperature before being confined within droplets. In the plating process, protoplasts are often added to a molten agar medium at a temperature range of 42-60 °C before being plated [33–35]. The lack of cell-wall protection renders the fungal protoplasts sensitive to the high temperatures of the molten medium. As reported by Díaz et al., a molten medium at over 45 °C inhibited the regeneration of the filamentous fungus *Pseudogymnoascus verrucosus* protoplasts, but the medium at temperatures below 42 °C allowed for fungal protoplast regeneration. Another explanation lies in the use of the oil phase HFE-7500 in the vicinity of droplets, a step that ensures a constant oxygen supply for the growth of filamentous fungi located inside the droplets. The solubility of oxygen in HEF-7500 oil, over 100 mL of oxygen·L^{-1} at 1 bar of air, is much higher than that of water (approx. 4.8 mL of oxygen·L^{-1}) [36,37]. As stated by Sklodowska and Jakiela, the culture medium with the addition of HEF-7500 oil induced a 1.4-fold increase in the growth rate of *E. coli* over the control medium without oil [36]. Furthermore, single protoplast encapsulation eliminates nutrient competition between fungal transformants and non-transformants. Indeed, a report by Chengcheng Li showed that the protein and cellulase production of a recombinant *T. reesei* strain expressing red fluorescence protein controlled by a *cbh1* promoter was slightly lower than that of the wild-type after a 5-d cultivation period [38]. The separate compartmentalization of transformed fungal protoplasts in droplets enables the isolation of slow-regenerating transformants from their fast-regenerating competitors. This method has been successfully applied to separate

slow-growing bacteria from a mixed library in which the fast-growing species were often dominant [39,40].

As a proof-of-concept, a high-throughput workflow to accelerate the genetic transformation of filamentous fungi has been established (**Fig 2-6**). In the fungal transformation process, in addition to the low recovery rate and prolonged recovery time, the isolation of fungal transformants with high expression levels required repeated rounds of plate cultures and evaluations, resulting in time-consuming and labour-intensive processes [22]. To tackle those limitations, the study used droplet cultures to induce marker gene expression in *T. reesei* transformants, followed by droplet screening for the rapid detection and isolation of candidates with high levels of GFP expression. Before the screening process, culture conditions for marker gene expression were optimized. The results indicated that GFP expression is detectable in the presence of 2% sophorose after droplet cultivation for 24 h. The inducer concentration for the *T. reesei* QM-GFP transformants was double that for strain *T. reesei* PC-CBHI-GFP. The higher induction dosage could be due to the effect of carbon catabolite repression on the *cbh1* promoter of the parental strain *T. reesei* QM9414, but not that of strain PC-3-7 [41]. More extended cultivation of fungal protoplasts will cause increasing numbers of false-positive droplets like the droplet culture of *T. reesei* spores. Based on the FADS analysis, sorting gates were set up and sorted positive droplets harbouring GFP-expressing transformants from a population of over 400,000 droplets for nearly 1.5 h. Most sorted and recovering fungi were heterokaryons that displayed *gfp* integration along with the wild-type band in the PCR analysis due to the multi-genomic nature of fungal cells [42]. Despite the limitation, the screenings from such heterokaryotic transformants with high gene expression levels increased the probability of finding beneficial transformants [43]. This study is the pioneer report on combining the droplet-based culture and droplet-assisted screening for transformed protoplasts of filamentous fungi based on a marker gene.

In addition to the usage of a visual marker gene to select fungal transformants in droplets rapidly, the screening could be based on regenerating and growing transformant protoplasts under selection pressures. In such cases, identifying regenerating fungal protoplasts plays a critical role. A possible method for this kind of direct detection will rely on the capability of fungal transformants to secrete extracellular enzymes. Two previous studies have reported selecting enzyme-hyper-producing fungal strains in droplets [7,12]. By encapsulating transformed fungal protoplasts in droplets containing a

selection medium plus a fluorescent enzyme substrate, the regenerating transformants with high levels of enzyme secretion are easily separated. The viable fungal transformants may be directly assessed by the use of other fluorescent compounds, such as co-staining with propidium iodide and SYTO 9 [44], Calcofluor White [44], resazurin [45], or salicylic acid [46]. The fluorescence-based assessment of cell viability in droplets is likely to be challenged by leakages of fluorescent molecules from positive droplets to neighbouring negative ones [47]. The challenge, however, can be tackled by adding supplements to the droplets [48] or modifying the fluorescent substrates [49]. Furthermore, the autofluorescence resulting from fungal growth could be considered a tool for droplet screening of viable transformants.

Overall, the novel approach presents outstanding benefits over traditional methods regarding the timing and frequency of fungal regeneration and the rapid isolation of targeted fungal transformants. The total time cost for this approach is about 1-2 weeks, with a round of droplet cultivation and preliminary screening, two rounds of genomic PCR evaluation, and a round of single-spore separation. This workflow is expected to open up many opportunities for accelerating the genetic modification of filamentous fungi in research and practical applications. In this field of research, studies on the molecular mechanisms involved in gene function and expression should become incredibly rapid and insightful. Thanks to this novel method, industrial fungal strains can be generated in a short period and used to produce bioactive compounds, hydrolytic enzymes, and recombinant proteins.

2.5 References

[1] Kaminski TS, Scheler O, Garstecki P. Droplet microfluidics for microbiology: techniques, applications and challenges. Lab Chip 2016;16:2168–87. https://doi.org/10.1039/c6lc00367b.

[2] Beneyton T, Wijaya IPM, Postros P, Najah M, Pascal L, Couvent A, et al. High-throughput screening of filamentous fungi using nanoliter-range droplet-based microfluidics. Sci Rep 2016;6:27223. https://doi.org/10.1038/srep27223.

[3] Neun S, Zurek PJ, Kaminski TS, Hollfelder F. Ultrahigh throughput screening for enzyme function in droplets. Methods Enzymol 2020;643:317-43. https://doi.org/10.1016/bs.mie.2020.06.002.

[4] Autour A, Ryckelynck M. Ultrahigh-throughput improvement and discovery of enzymes using droplet-based microfluidic screening. Micromachines 2017;8(4):128. https://doi.org/10.3390/mi8040128.

[5] Ma F, Chung MT, Yao Y, Nidetz R, Lee LM, Liu AP, et al. Efficient molecular evolution to generate enantioselective enzymes using a dual-channel microfluidic droplet screening platform. Nat Commun 2018;9:1030. https://doi.org/10.1038/s41467-018-03492-6.

[6] Nakamura A, Honma N, Tanaka Y, Suzuki Y, Shida Y, Tsuda Y, et al. 7-Aminocoumarin-4-acetic acid as a fluorescent probe for detecting bacterial dipeptidyl peptidase activities in water-in-oil droplets and in bulk. Anal Chem 2022;94(5):2416–24. https://doi.org/10.1021/acs.analchem.1c04108.

[7] Beneyton T, Thomas S, Griffiths AD, Nicaud JM, Drevelle A, Rossignol T. Droplet-based microfluidic high-throughput screening of heterologous enzymes secreted by the yeast *Yarrowia lipolytica*. Microb Cell Fact 2017;16:18. https://doi.org/10.1186/s12934-017-0629-5.

[8] Abatemarco J, Sarhan MF, Wagner JM, Lin JL, Liu L, Hassouneh W, et al. RNA-aptamers-in-droplets (RAPID) high-throughput screening for secretory phenotypes. Nat Commun 2017;8:332. https://doi.org/10.1038/s41467-017-00425-7.

[9] Best RJ, Lyczakowski JJ, Abalde-Cela S, Yu Z, Abell C, Smith AG. Label-free analysis and sorting of microalgae and cyanobacteria in microdroplets by intrinsic chlorophyll fluorescence for the identification of fast growing strains. Anal Chem 2016;88(21):10445–51. https://doi.org/10.1021/acs.analchem.6b02364.

[10] Sung YJ, Kim JYH, Choi H Il, Kwak HS, Sim SJ. Magnetophoretic sorting of microdroplets with different microalgal cell densities for rapid isolation of fast growing strains. Sci Rep 2017;7:10390. https://doi.org/10.1038/s41598-017-10764-6.

[11] Tatenhove-Pel RJ van, Hernandez-Valdes JA, Teusink B, Kuipers OP, Fischlechner M, Bachmann H. Microdroplet screening and selection for improved microbial production of extracellular compounds. Curr Opin Biotechnol 2020;61:72–81. https://doi.org/10.1016/j.copbio.2019.10.007.

[12] He R, Ding R, Heyman JA, Zhang D, Tu R. Ultra-high-throughput picoliter-droplet microfluidics screening of the industrial cellulase-producing filamentous fungus *Trichoderma reesei*. J Ind Microbiol Biotechnol 2019;46(11):1603–10. https://doi.org/10.1007/s10295-019-02221-2.

[13] Li D, Tang Y, Lin J, Cai W. Methods for genetic transformation of filamentous fungi. Microb Cell Fact 2017;16:168. https://doi.org/10.1186/s12934-017-0785-7.

[14] Alberti F, Foster GD, Bailey AM. Natural products from filamentous fungi and production by heterologous expression. Appl Microbiol Biotechnol 2017;101:493–500. https://doi.org/10.1007/s00253-016-8034-2.

[15] Olmedo-Monfil V, Cortés-Penagos C, Herrera-Estrella A. Three decades of fungal transformation. In: Balbás, P., Lorence, A. editors. Recombinant Gene Expression, Methods in Molecular Biology, Totowa, NJ: Humana Press; 2004, p. 297–313.

[16] Zou G, Shi S, Jiang Y, van den Brink J, de Vries RP, Chen L, et al. Construction of a cellulase hyper-expression system in *Trichoderma reesei* by promoter and enzyme engineering. Microb Cell Fact 2012;11:21. https://doi.org/10.1186/1475-2859-11-21.

[17] Sugano SS, Suzuki H, Shimokita E, Chiba H, Noji S, Osakabe Y, et al. Genome editing in the mushroom-forming basidiomycete *Coprinopsis cinerea*, optimized by a high-throughput transformation system. Sci Rep 2017;7:1260. https://doi.org/10.1038/s41598-017-00883-5.

[18] Singh A, Taylor LE, Vander Wall TA, Linger J, Himmel ME, Podkaminer K, et al. Heterologous protein expression in *Hypocrea jecorina*: A historical perspective and new developments. Biotechnol Adv 2015;33(1):142–54. https://doi.org/10.1016/j.biotechadv.2014.11.009.

[19] Throndset W, Kim S, Bower B, Lantz S, Kelemen B, Pepsin M, et al. Flow cytometric sorting of the filamentous fungus *Trichoderma reesei* for improved strains.

Enzyme Microb Technol 2010;47(7):335–41. https://doi.org/10.1016/j.enzmictec.2010.09.003.

[20] Bleichrodt RJ, Read ND. Flow cytometry and FACS applied to filamentous fungi. Fungal Biol Rev 2019;33(1):1–15. https://doi.org/10.1016/j.fbr.2018.06.001

[21] Gao F, Hao Z, Sun X, Qin L, Zhao T, Liu W, et al. A versatile system for fast screening and isolation of *Trichoderma reesei* cellulase hyperproducers based on DsRed and fluorescence-assisted cell sorting. Biotechnol Biofuels 2018;11:261. https://doi.org/10.1186/s13068-018-1264-z.

[22] Wang G, Jia W, Chen N, Zhang K, Wang L, Lv P, et al. A GFP-fusion coupling FACS platform for advancing the metabolic engineering of filamentous fungi. Biotechnol Biofuels 2018;11:232. https://doi.org/10.1186/s13068-018-1223-8.

[23] Shida Y, Yamaguchi K, Nitta M, Nakamura A, Takahashi M, Kidokoro SI, et al. The impact of a single-nucleotide mutation of *bgl2* on cellulase induction in a *Trichoderma reesei* mutant. Biotechnol Biofuels 2015;8:230. https://doi.org/10.1186/s13068-015-0420-y.

[24] Daranagama ND, Suzuki Y, Shida Y, Ogasawara W. Involvement of Xyr1 and Are1 for trichodermapepsin gene expression in response to cellulose and galactose in *Trichoderma reesei*. Curr Microbiol 2020;77:1506-17. https://doi.org/10.1007/s00284-020-01955-y.

[25] Penttilä M, Nevalainen H, Rättö M, Salminen E, Knowles J. A versatile transformation system for the cellulolytic filamentous fungus *Trichoderma reesei*. Gene 1987;61(2):155–64. https://doi.org/10.1016/0378-1119(87)90110-7.

[26] Watanabe M, Serizawa M, Sawada T, Takeda K, Takahashi T, Yamamoto N, et al. A novel flow cytometry-based cell capture platform for the detection, capture and molecular characterization of rare tumor cells in blood. J Transl Med 2014;12:143. https://doi.org/10.1186/1479-5876-12-143.

[27] He Z, Wu H, Yan X, Liu W. Recent advances in droplet microfluidics for microbiology. Chinese Chem Lett 2022;33(4):1729-42. https://doi.org/10.1016/j.cclet.2021.08.059.

[28] Fitz E, Wanka F, Seiboth B. The promoter toolbox for recombinant gene expression in *Trichoderma reesei*. Front Bioeng Biotechnol 2018;6:135. https://doi.org/10.3389/fbioe.2018.00135.

[29] Pöhlker C, Huffman JA, Pöschl U. Autofluorescence of atmospheric bioaerosols - fluorescent biomolecules and potential interferences. Atmos Meas Tech 2012;5:37–71. https://doi.org/10.5194/amt-5-37-2012.

[30] Mathis H, Margeot A, Bouix M. Optimization of flow cytometry parameters for high-throughput screening of spores of the filamentous fungus *Trichoderma reesei*. J Biotechnol 2020;321:78–86. https://doi.org/10.1016/j.jbiotec.2020.05.015.

[31] Iwakuma H, Koyama Y, Miyachi A, Nasukawa M, Matsumoto H, Yano S, et al. Generation of a glucose de-repressed mutant of *Trichoderma reesei* using disparity mutagenesis. Biosci Biotechnol Biochem 2016;80(3):486–92. https://doi.org/10.1080/09168451.2015.1104236.

[32] Wu J De, Chou JC. Optimization of protoplast preparation and regeneration of a medicinal fungus *Antrodia cinnamomea*. Mycobiology 2019;47(4):483–93. https://doi.org/10.1080/12298093.2019.1687252.

[33] Díaz A, Villanueva P, Oliva V, Gil-Durán C, Fierro F, Chávez R, et al. Genetic transformation of the filamentous fungus *Pseudogymnoascus verrucosus* of antarctic origin. Front Microbiol 2019;10:2675. https://doi.org/10.3389/fmicb.2019.02675.

[34] Liu Z, Friesen TL. Polyethylene glycol (PEG)-mediated transformation in filamentous fungal pathogens. In: Melvin D. Bolton, Bart P.H.J. Thomma editors. Plant Fungal Pathogens, Methods in Molecular Biology, Totowa, NJ: Humana Press; 2012, p. 365-375.

[35] Turgeon BG, Condon B, Liu J, Zhang N. Protoplast transformation of filamentous fungi. In: Amir Sharon editors. Molecular and Cell Biology Methods for Fungi, Methods in Molecular Biology, Totowa, NJ: Humana Press; 2010, p. 3-19.

[36] Sklodowska K, Jakiela S. Enhancement of bacterial growth with the help of immiscible oxygenated oils. RSC Adv 2017;7:40990–5. https://doi.org/10.1039/c7ra07095k.

[37] Battino R, Rettich TR, Tominaga T. The solubility of oxygen and ozone in liquids. J Phys Chem Ref Data 1983;12:163. https://doi.org/10.1063/1.555680.

[38] Li C, Pang AP, Yang H, Lv R, Zhou Z, Wu FG, et al. Tracking localization and secretion of cellulase spatiotemporally and directly in living *Trichoderma reesei*. Biotechnol Biofuels 2019;12:200. https://doi.org/10.1186/s13068-019-1538-0.

[39] Bachmann H, Fischlechner M, Rabbers I, Barfa N, Dos Santos FB, Molenaar D, et al. Availability of public goods shapes the evolution of competing metabolic strategies. PNAS 2013;110(35):14302–7. https://doi.org/10.1073/pnas.1308523110.

[40] Liu W, Kim HJ, Lucchetta EM, Du W, Ismagilov RF. Isolation, incubation, and parallel functional testing and identification by FISH of rare microbial single-copy cells from multi-species mixtures using the combination of chemistrode and stochastic confinement. Lab Chip 2009;9:2153–62. https://doi.org/10.1039/b904958d.

[41] De Oliveira Porciuncula J, Furukawa T, Mori K, Shida Y, Hirakawa H, Tashiro K, et al. Single nucleotide polymorphism analysis of a *Trichoderma reesei* hyper-cellulolytic mutant developed in japan. Biosci Biotechnol Biochem 2013;77(3):534–43. https://doi.org/10.1271/bbb.120794.

[42] Kilaru S, Schuster M, Murray R, Steinberg G. Optimal timing for Agrobacterium-mediated DNA transformation of *Trichoderma reesei* conidia revealed by live cell imaging. Fungal Genet Biol 2020;142:103448. https://doi.org/10.1016/j.fgb.2020.103448.

[43] Liu Q, Zhang Y, Li F, Li J, Sun W, Tian C. Upgrading of efficient and scalable CRISPR-Cas-mediated technology for genetic engineering in thermophilic fungus *Myceliophthora thermophila*. Biotechnol Biofuels 2019;12:293. https://doi.org/10.1186/s13068-019-1637-y.

[44] Ingham CJ, Schneeberger PM. Microcolony imaging of *Aspergillus fumigatus* treated with echinocandins reveals both fungistatic and fungicidal activities. PLoS One 2012;7(4):e35478. https://doi.org/10.1371/journal.pone.0035478.

[45] Barua P, You MP, Bayliss K, Lanoiselet V, Barbetti MJ. A rapid and miniaturized system using Alamar blue to assess fungal spore viability: implications for biosecurity. Eur J Plant Pathol 2017;148:139–50. https://doi.org/10.1007/s10658-016-1077-5.

[46] Kort R, Nocker A, de Kat Angelino-Bart A, van Veen S, Verheij H, Schuren F, et al. Real-time detection of viable microorganisms by intracellular phototautomerism. BMC Biotechnol 2010;10:45. https://doi.org/10.1186/1472-6750-10-45.

[47] Gruner P, Riechers B, Semin B, Lim J, Johnston A, Short K, et al. Controlling molecular transport in minimal emulsions. Nat Commun 2016;7:10392. https://doi.org/10.1038/ncomms10392.

[48] Sandoz PA, Chung AJ, Weaver WM, Di Carlo D. Sugar additives improve signal fidelity for implementing two-phase resorufin-based enzyme immunoassays. Langmuir 2014;30(23):6637–43. https://doi.org/10.1021/la5004484.

[49] Fenneteau J, Chauvin D, Griffiths AD, Nizak C, Cossy J. Synthesis of new hydrophilic rhodamine based enzymatic substrates compatible with droplet-based microfluidic assays. Chem Commun 2017;53:5437–40. https://doi.org/10.1039/c7cc01506b.

Chapter 3: Ultra-high-throughput screening of *Trichoderma reesei* strains capable of carbon catabolite repression release and cellulase hyper-production using a microfluidic droplet platform

3.1 Introduction

The filamentous fungus *Trichoderma reesei* is the most well-known cellulolytic fungus, being able to produce high yields of extracellular protein and to synthesize eukaryotic proteins. In industrial fermentation, the strain could secrete over 100 g of protein per liter [1], with around 80% of the secreted protein comprising cellulase and hemicellulase [2]. These enzymes play an indispensable role in the saccharification of lignocellulose to fermentable sugars used in biorefining, as well as being widely used in other industries: food, animal feed, textiles, pulp and paper, grain alcohol fermentation, starch processing, pharmaceuticals, malting, and brewing [2]. The industrial production of *T. reesei* cellulase is often high-cost because of the use of insoluble cellulosic materials for fungal culture [3]. Sophorose, cellobiose, and lactose are soluble carbon sources that can be used instead of insoluble types to induce the secretion of major cellulase [3,4], but the inducing effects of these carbon sources can be repressed by carbon catabolite repression (CCR) in the presence of glucose [5,6]. In the presence of easily metabolized carbon sources such as glucose, CCR prevents *T. reesei* from wasting energy and material in the secretion of main cellulases that degrade large and complex compounds outside the cells [7]. For the development of industrial fungal strains, it is necessary to construct cellulase-overproducing *T. reesei* strains with CCR released. Random mutagenesis has been widely used as an effective method of improving cellulase productivity in *T. reesei* [8]. However, the low-throughput screening process is time-consuming and labor-intensive, yielding only a tiny population of isolated beneficial mutants [8,9]. Fluorescence-activated cell sorting (FACS) can rapidly select germinated fungal mutants using fluorescent markers [8,10,11] but cannot isolate fungi based on secreted enzymes [12].

The droplet-based microfluidic platform is a versatile and robust tool for directed evolution and metagenomic screening of enzymes. It has numerous advantages, the first

being the scaled-down reaction volumes [13]. Compared to regular 96-well plates, carrying out enzyme assay reactions in water-in-oil droplets (WODLs) brings a reduction in excess of 10^7-fold in reaction volumes [14]. The compartmentalization of microorganisms in small-volume WODLs enables them to secrete metabolites earlier than in a bulk culture of 96-well plates or flasks [15]. Moreover, volume miniaturization makes the use of expensive substances more affordable and improves the detection sensitivity [9,16]. Secondly, the separate confinement of enzymatic reactions is a significant advantage of the droplet platform. In the enzyme engineering process, variants with different genotypes can secrete various metabolic products, so bulk culture methods are not ideal for culturing individual mutants. By contrast, droplet microfluidics can generate large numbers of WODLs for culturing microbes at the single-cell level. A previous report showed that the droplet system eliminated nutrient competition between slower-growing and faster-growing *Lactococcus lactis* variants, enabling the separation of slower-growing mutants with improved metabolic efficiency [17]. Another essential feature of the technology is the ability to analyze and screen large numbers of individual droplets in ultra-high-throughput (uHTP) conditions. uHTP screening can accelerate the engineering process and increase the likelihood of finding beneficial candidates, with remarkable reductions in time and labor costs [13,18]. The current state-of-the-art technology can screen a droplet population 1000 times faster than automated microtiter plate-based systems [19]. Droplet-based microfluidic systems can culture and screen for *T. reesei* after 16 hours of incubation in 1 nL droplets [20] and for *Aspergillus niger* after 24 hours of incubation in 10 nL droplets [13]. Despite these benefits, the applications of this technology in the culturing and screening of filamentous fungi based on secreted products remain limited due to the fast growth of fungal hyphae [9,13,18], leading to droplet breakages.

In this study, to generate cellulase-hyperproducing *T. reesei* strains with release from CCR, an uHTP workflow using a microfluidic droplet platform was applied to culture and rapidly isolate desired mutants from a randomly mutagenized library. The findings indicate that the use of the microfluidic platform could be a robust method of culturing and screening a million variants based on their secreted cellulase within a period of a few hours. Several mutants potentially able to secrete protein and produce cellulase in the presence of glucose have been successfully enriched and evaluated. The molecular mechanisms behind cellulase production in these mutants have also been analyzed.

Applying WODL culture and screening will accelerate the construction of industrial fungal strains, contributing to cost-effective and efficient lignocellulosic biorefining.

3.2 Materials and methods

3.2.1 Filamentous fungal strains and culture conditions

T. reesei QM9414 (ATCC26921) was used in this study [9,21]. The *cre1* disruptant QMΔ*cre1* was obtained from the laboratory stock [22]. The strain was grown on potato dextrose agar (PDA; BD, NJ, USA) plates, and its conidia were obtained and stored at −80 °C until use. PDA plus 0.1% Triton X-100 (PDA-X) plates were used for the recovery of isolated fungal mutants.

For the droplet culture, a minimal medium consisting of a carbon source, 50% $(NH_4)_2SO_4$, 1.50% KH_2PO_4, 0.06% $MgSO_4$, 0.06% $CaCl_2$, and a 0.10% trace element solution [5 g L^{-1} $FeSO_4 \cdot 7H_2O$, 2 g L^{-1} $CoCl_2$, 1.6 g L^{-1} $MgSO_4 \cdot H_2O$, and 1.2 g L^{-1} $ZnSO_4 \cdot 7H_2O$] was used. Fluorescein di-β-D-cellobioside (FCB, AAT Bioquest), a cellulase fluorescent substrate, was supplemented to the medium with a final dose of 40 μM for detecting and monitoring cellulase activity in droplets. Cellulase cleaves the β-1,4-D-glycosidic bonds of the fluorogenic substrate and releases fluorescein with a green fluorescence [23]. Fluorescein has an excitation peak of 498 nm and an emission peak of 517 nm, and its intensity can be measured by fluorescence-activated droplet sorting (FADS).

For flask cultivation, 1×10^6 spores were inoculated in 50 mL of culture medium containing a carbon source, 0.05% Bacto yeast extract, 0.10% Bacto peptone, 0.14% $(NH_4)_2SO_4$, 0.20% KH_2PO_4, 0.03% $CaCl_2 \cdot 2H_2O$, 0.03% $MgSO_4 \cdot 7H_2O$, and a 0.10% trace element solution [5 g L^{-1} $FeSO_4$, 2 g L^{-1} $MnSO_4 \cdot H_2O$, 1 g L^{-1} $CuSO_4 \cdot 5H_2O$, 2 g L^{-1} $ZnSO_4 \cdot 7H_2O$, 1 g L^{-1} $(NH_4)_6Mo_7O_{24} \cdot 4H_2O$, 2 g L^{-1} $CoCl_2 \cdot 6H_2O$, and 1 g L^{-1} $NiCl_2 \cdot 6H_2O$] in 50 mM Na-tartrate buffer (pH 4.0). Flasks were incubated at 28 °C with shaking at 220 rpm in an incubator (Bioshaker GBR-300, Taitec Corporation, Saitama, Japan).

3.2.2 Ultraviolet (UV)-induced mutations

A spore suspension of *T. reesei* QM9414 with a density of 10^7 spores mL^{-1} on a 90 mm Petri plate was exposed to UV light using a CL-1000, UV Crosslinker, 254 nm, 100 V, 8 W (Ultra-Violet Products Ltd., Upland, CA, USA). Irradiation was performed at a UV light intensity of 160 × 100 μJ cm^{-2}, in which the survival ratio was approximately 4% (**Figure 3-1**). The irradiated spores were cultured and screened in 1 nL WODLs.

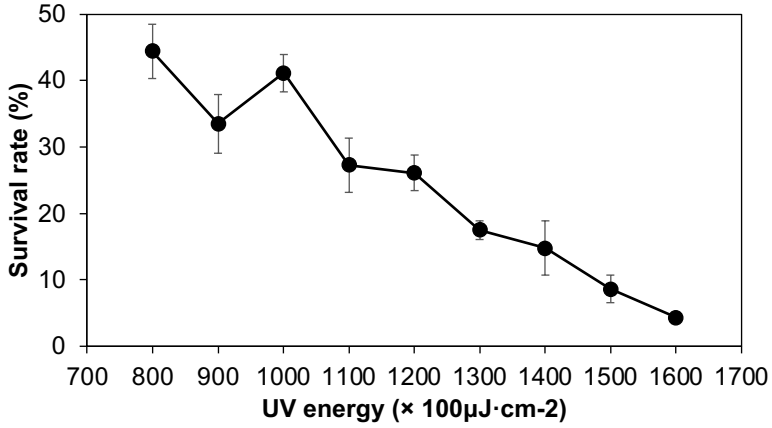

Supplementary Figure 3-1. The survival rate of *T. reesei* spores after UV irradiation at different UV energies.

3.2.3 Droplet generation and microscopic observations

Droplet generation chips (Bio-Rad Laboratories, Inc., Hercules, CA, USA) and a droplet generator (On-chip Biotechnologies, Tokyo, Japan) were used to confine fungal spores in WODLs, as previously described [9]. About 20,000 WODLs with a polydispersity of less than 1.0% in droplet volumes were generated, transferred into 2 mL tubes, and incubated for fungal growth.

For microscopic visualizations, 40 μL of HFE-7500 oil with 0.1% (w/w) FluoroSurfactant 008 (On-chip Biotechnologies) and a 4 μL droplet sample were injected into a micro-Slide VI flat (IBIDI, Martinsried, Germany) to observe WODL samples under a confocal laser microscope (Eclipse Ti2, Nikon, Tokyo, Japan) operated with Nis-element Ar software (Nikon, Tokyo, Japan).

3.2.4 High-throughput analysis and sorting for beneficial fungal mutants

Rapid analyzing and sorting of the WODLs were performed by an FADS system (On-chip Biotechnologies), following the manufacturer's instructions [24]. Each WODL sample was loaded onto a sorting chip and inserted into the sorter to measure forward scatter (FSC) intensity and green fluorescence intensity (488 nm excitation and 543 ± 22 nm detection) and to screen droplets with a throughput of up to 8000 droplets min^{-1}. The sorted droplets were collected in a collection reservoir. Data output was analyzed by FlowJo v10.8.1 (Tree Star, Inc, Ashland, OR, USA).

3.2.5 Biochemical analyses

Carboxymethyl-cellulase (CMCase) activities of culture supernatants were determined using 1.0% carboxymethylcellulose (CMC; Sigma-Aldrich, MO, USA) as a substrate in 50 mM sodium acetate buffer (pH 5.0) at 50 °C for 15 min. The DNS method Field [25] for CMCase measured the reducing sugars produced during the enzyme reaction. One unit of enzyme activity was defined as the amount of enzyme that produced 1 μmol of reducing sugars per minute in glucose equivalents. Secreted protein concentration was measured by the Bradford method [25], using bovine gamma globulin as the standard.

3.2.6 Real-time quantitative reverse transcription PCR (qRT-PCR)

Total RNA was extracted from frozen mycelia using the hot-phenol method and Trizol LS Reagent (Invitrogen, Carlsbad, CA, USA). The extracted RNA was purified using an Illustra RNAspin Mini RNA Isolation kit (GE Health Care, USA). cDNA synthesis from total RNA was done using a transcriptor first-strand cDNA synthesis kit (Roche Applied Science, Bavaria, Germany). qRT-PCR was performed using the QuantStudio 3 system (Thermo Fisher Scientific Inc., Waltham, MA, USA). Amplification reactions were conducted in 20 μL of reaction mixture with 0.5 μM forward primer, 0.5 μM reverse primer, and 2 μL of 100-fold diluted cDNA. Expression levels were calculated relative to the value of the *act1* gene encoding actin [26]. Each sample was examined in triplicate. All PCR primers used for the expression analysis are listed in **Table 3-1**.

Supplementary Table 3-1. Primers used in this study.

Gene name	Primer sequence (5' → 3')	
Glycosyl hydrolase genes	**Fw**	**Rv**
cbh1	CTTGGCAACGAGTTCTCTT	TGTTGGTGGGATACTTGCT
cbh2	CGTCAAATTGTCGTGGAA	ACTGAGCATTGGCACACTT
egl1	CGGCTACAAAAGCTACTACG	CTGGTACTTGCGGGTGAT
bgl1	AGTGACAGCTTCAGCGAG	GGAGAGGCGTGAGTAGTTG
bgl2	CGTGCTCTTCACCAACAA	TCTTGCTGATCCACACCA

Transcription factor genes	Fw	Rv
xyr1	TGCGAGACCATTGTTAGG	CTGCTGCTCAGCTAAATCTT
ace3	GACATTTTCCCCGAAGGAGA	GTTGGAGTGGAAGTAGCGAATG
bglr	TGGATAGCTACTACCAGGGC	CAGACTAAGGGGACGTTGT
ace1	GAGGTTGATGAAGGCTTTG	CACTTGGCATATCGGTAAAC
cre1	TCTACGGCTCCTTCTTCTC	ACAGGTTTCTCAGACTCGG
Housekeeping gene	**Fw**	**Rv**
act1	TCCATCATGAAGTGCGAC	GTAGAAGGAGCAAGAGCAGTG

3.2.7 Genomic DNA sequencing and analysis

Chromosomal DNA of QM9414 and its mutants were extracted from the mycelia in liquid nitrogen using a combination of phenol-chloroform extraction and ethanol precipitation. The genomes were sequenced by Illumina MiSeq platform served as a reference for comparative genomic analysis. The genome sequence of wild-type strain QM6a (https://mycocosm.jgi.doe.gov/Trire2/Trire2.home.html) served as a reference for comparative genomic analysis.

3.3 Results

3.3.1 Growth and cellulase secretion of UV-irradiated *T. reesei* in water-in-oil droplets (WODLs)

To apply droplet-based microfluidic platforms on uHTP screening for cellulase hyper-producing *T. reesei* mutants, the ability to culture fungal mutants in WODL for an extended period is essential. However, the long cultivation time would lead to the rapid expansion of branched fungal mycelia beyond droplets, resulting in microfluidic channel blockages in the screening process. To overcome this obstacle, the study used a minimal medium for the WODL culture of *T. reesei* mutants derived from the parent strain QM9414, a high cellulase-producing strain. After the UV light mutagenesis, the non-irradiated and irradiated spores were cultured in droplets containing different carbon sources and a cellulase fluorescent substrate FCB.

Microscopic observations indicated that the growth of mutants was significantly slower than that of their parent strain in droplets, regardless of the carbon source (**Figure 3-2a**). Further, the WODL culture enabled the mutants to grow for extended cultivation periods of up to 72 hours (**Figure 3-2b and c**). During cultivation, the levels of green fluorescence signals increased concurrently with fungal growth in the droplets. In contrast, when fungi without UV irradiation were cultured for 72 hours in WODLs, high levels of fluorescent signals were observed, and the leakages of fluorescent compounds were visualized in the surrounding droplets after 48 hours of incubation. In addition to the droplet leakages, their mycelia extended beyond droplets and formed fungal clumps (**Figure 3-2d)**.

Droplets carrying UV-irradiated spores were used as the sample for cellulase detection via FADS analysis, while those harboring non-irradiated spores served as the negative control. FADS analysis of droplets harboring fungal spores and the glucose-sophorose medium within 72 hours of incubation indicated that with a similar sorting gate, the proportion of droplets with the highest fluorescence signals in the negative control was more significant than in the sample (**Figure 3-2e**). These findings suggested that the WODL culture of the QM9414 parental strain was unsuitable as a negative control when setting a sorting threshold of the uHTP screening process due to the differences in fungal developments and enzyme secretions. As a result, the sorting threshold must be adjusted to separate the droplets with the strongest fluorescent signals from the rest of the droplet population.

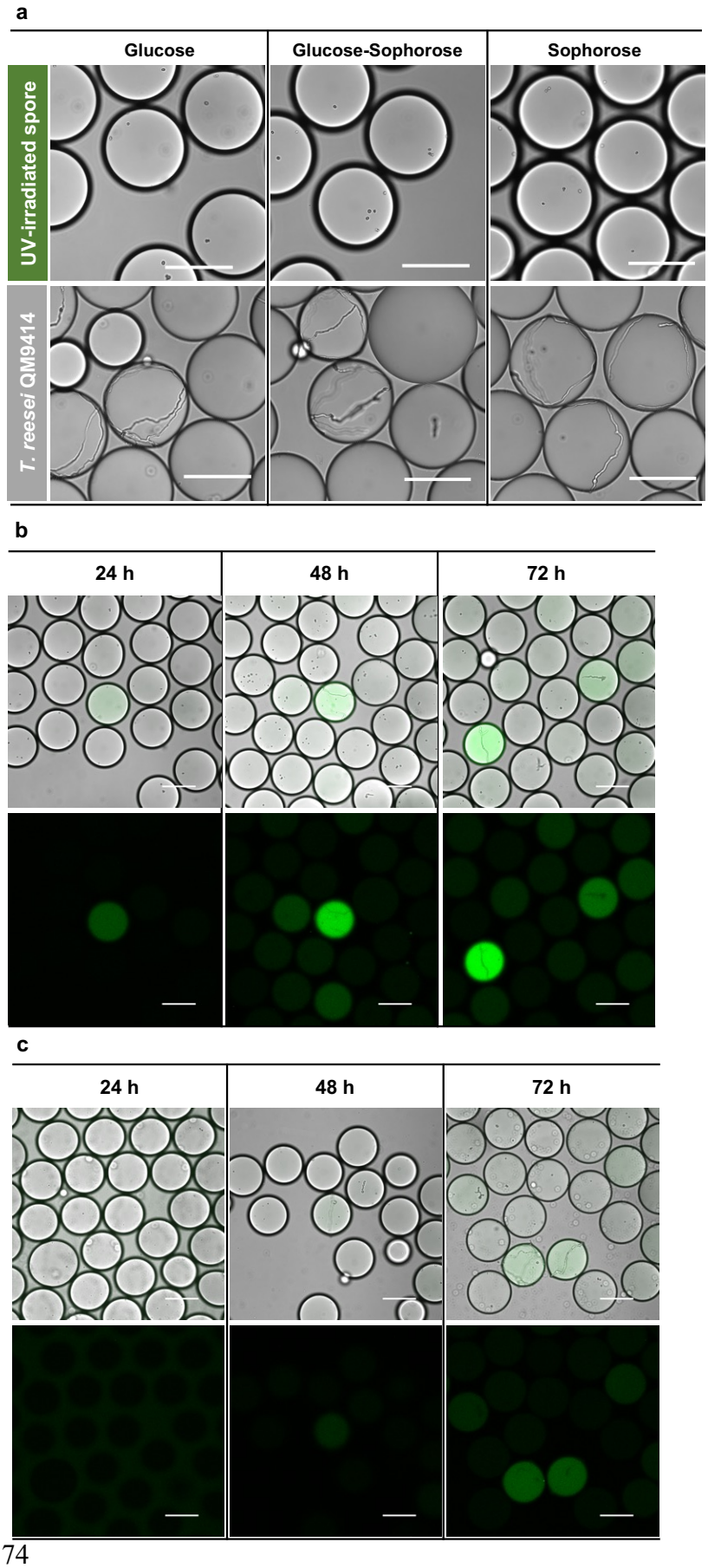
a
Glucose
Glucose-Sophorose
Sophorose
UV-irradiated spore
T. reesei QM9414
b
24 h
48 h
72 h
c
24 h
48 h
72 h

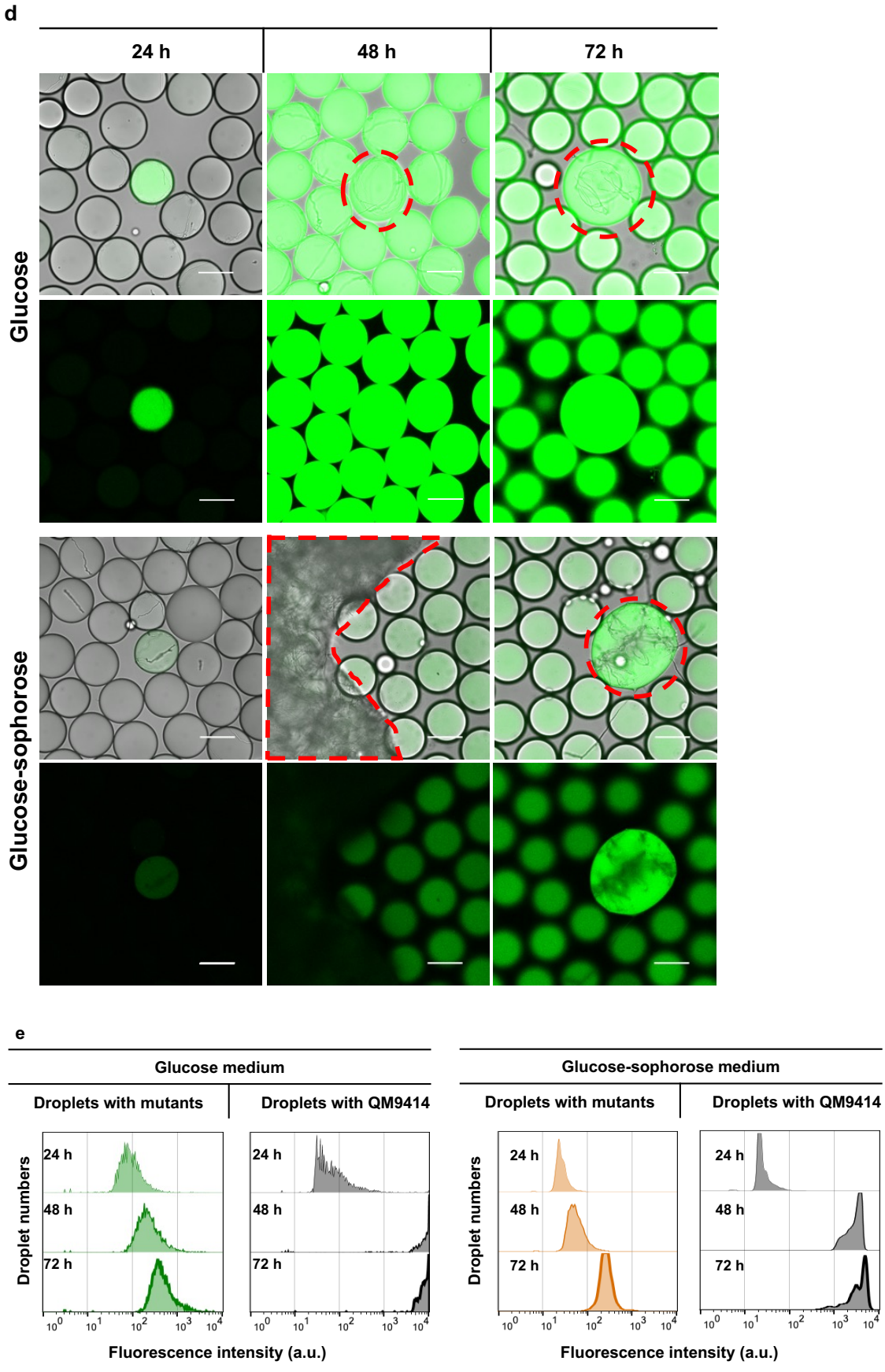
d
24 h
48 h
72 h
Glucose
Glucose-sophorose
e
Glucose medium
Glucose-sophorose medium
Droplets with mutants
Droplets with QM9414
Droplet numbers
24 h
48 h
72 h
Fluorescence intensity (a.u.)

Figure 3.2 Cultivation of *Trichoderma reesei* QM9414 and mutants in WODLs. (a) Droplet culture of UV-irradiated fungi and their parental strain in various media. Droplets with fungal spores were incubated at 28 °C for 24 hours and then observed under a fluorescence microscope. The scale bars depict 100 μm. (b) Micrographs of the growth of UV-irradiated spores in droplets containing 2.0% (w/v) glucose. The scale bars depict 100 μm. (c) Micrographs of the growth of UV-irradiated spores in droplets containing 1.0% (w/v) glucose and 1.0% (w/v) sophorose. The scale bars depict 100 μm. (d) Single spores of *T. reesei* QM9414 were encapsulated in 2.0% (w/v) glucose and in a mixture of 1.0% (w/v) glucose and 1.0% (w/v) sophorose. Droplets were then incubated at 28 °C and observed under a fluorescence microscope at various times. The dashed red circle highlights the formation of fungal clumps due to the fast growth of QM9414 in droplets. The scale bars depict 100 μm. (e) Green fluorescence analysis of droplets carrying UV-irradiated spores and those harboring *T. reesei* QM9414 spores in different carbon sources. In each analytical round, 5,000 droplets were analyzed.

3.3.2 Droplet-based screening workflow for CCR-releasing *T. reesei* mutants from an extensive mutant library

WODL cultures were used successfully in the growth and cellulase secretion of *T. reesei* mutants, so the possibility of using FADS to isolate beneficial strains from a sizeable mutation library was investigated (**Figure 3-3a**). After UV exposure, approximately 2.5×10^5 viable mutant spores were encapsulated in a population of 10^6 glucose-containing droplets and incubated for 24–72 hours. The average numbers of growing and non-growing spores in droplets were set to 0.25 per droplet ($\lambda_1 \sim 0.25$) and 5.64 per droplet ($\lambda_2 \sim 5.64$), respectively. From the Poisson distribution, it was estimated that roughly 76% of droplets carried non-growing spores, 19.5% of droplets harbored a growing spore and a non-growing spore, and 2.4% of droplets had two growing spores and non-growing spores. Before uHTP screening, FADS analysis showed that an increasing proportion of droplets with high fluorescence levels could be detected within 72 hours of cultivation (**Figure 3-3b**).

To collect CCR-releasing mutants, screening of the first mutation generation was carried out after 24 hours of WODL culture. This was because cellulase production by glucose starvation might occur in the late stage of culture when glucose is depleted. The sorting gates were set to enable separation from the droplet population of the top 0.5% of droplets having the highest green fluorescent signals, from which the greatest number of potential mutants among the mutation library could be obtained (**Figure 3-3c**). During uHTP screening, 2,118 droplets with the highest levels of green fluorescence were separated from a population of over 5.41×10^5 droplets within about 1.7 hours (**Figure 3-3d**). The sorted droplets were then streaked onto PDA-X for strain recovery, and 26 fungal candidates were recovered on the plates (**Figures 3-3e)**. Some of those 26 sorted and recovering candidates grew and formed spores poorly. Only the fast-growing fungal candidates (21 mutants) were screened in flasks so as to collect the most beneficial ones with CCR release and cellulase hyperproduction abilities. The fast-growing mutants were inoculated for 48 hours in flasks containing 1% (w/v) glucose (**Figure 3-3f**). The data showed that five of the 21 sorted candidates (MG-9, MG-13, MG-20, MG-23, and MG-25) showed higher protein production levels and enzyme activities than those of QM9414. One mutant (MG-26) displayed higher protein production but lower enzyme activities. Two mutants (MG-4 and MG-5) showed lower protein production but higher enzyme activities than QM9414. MG-9, with cellulase activities nearly 2.1-fold higher than

QM9414, was selected for further examination. These data indicated that the droplet culture and screening scheme could be successfully employed to rapidly isolate the desired fungal mutants from an extensive mutation library.

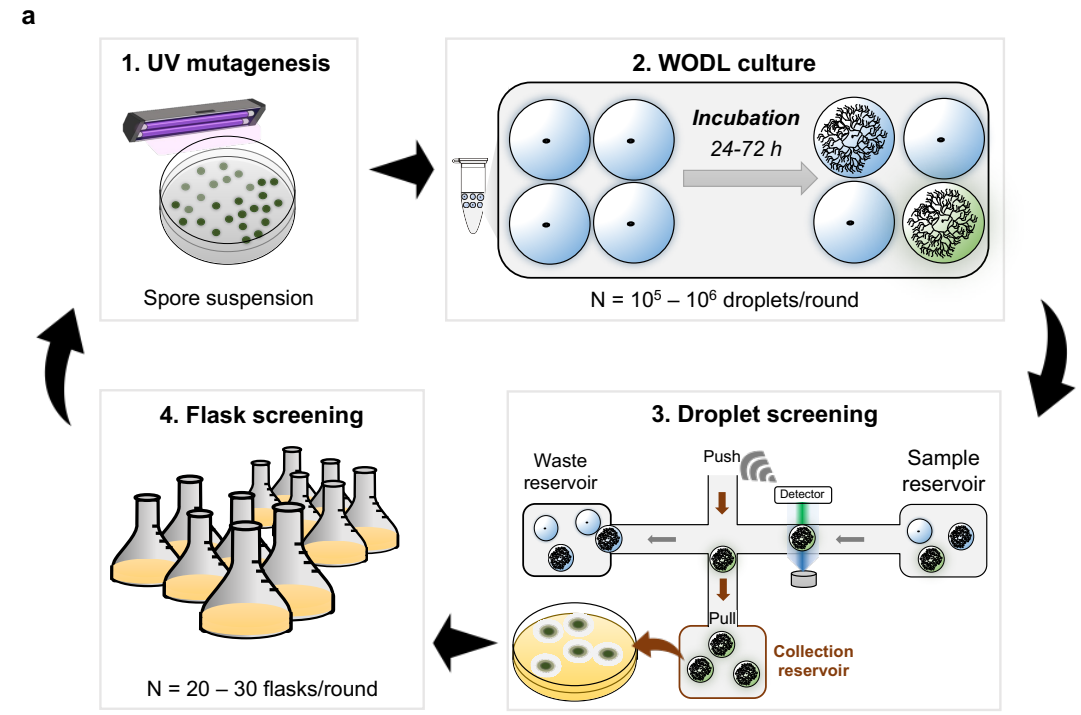

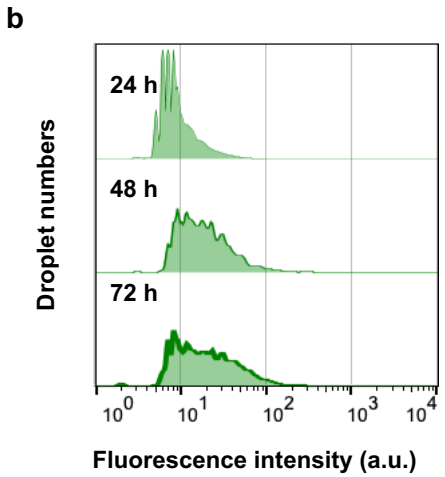

c

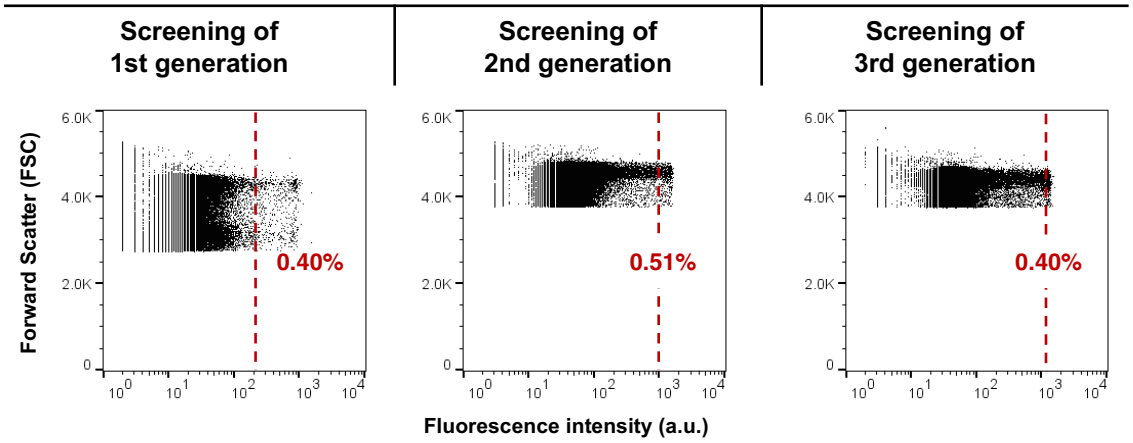
Screening of
1st generation
Screening of
2nd generation
Screening of
3rd generation
Forward Scatter (FSC)
6.0K
4.0K
2.0K
0
0.40%
0.51%
0.40%
Fluorescence intensity (a.u.)

d

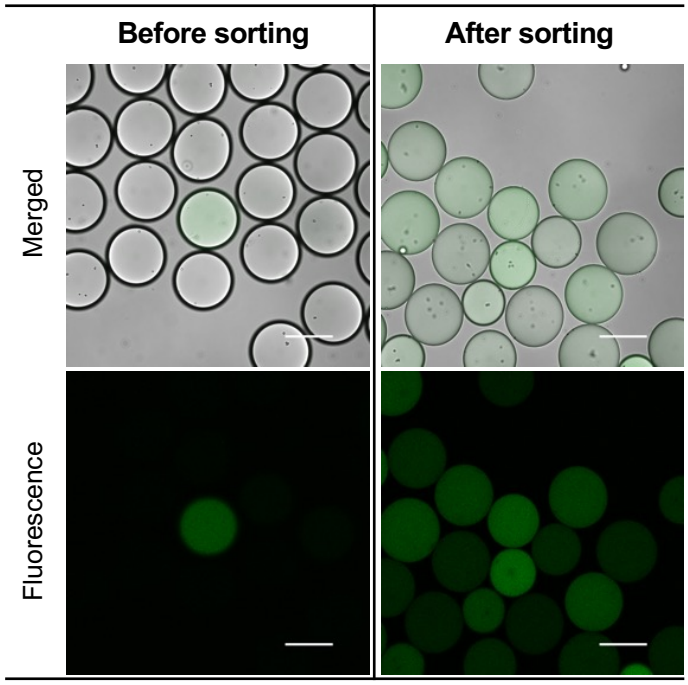
Before sorting
After sorting
Merged
Fluorescence

e

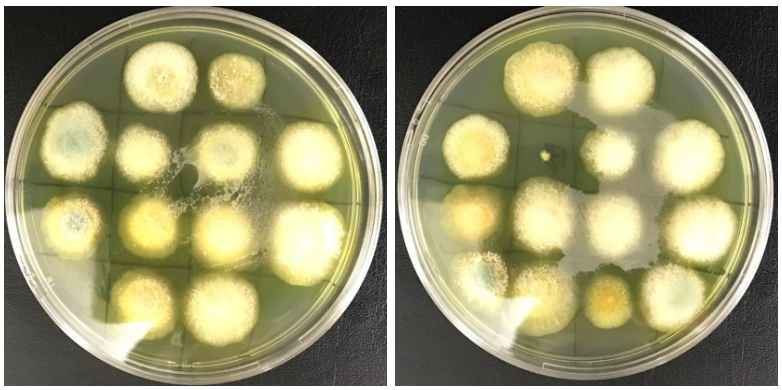

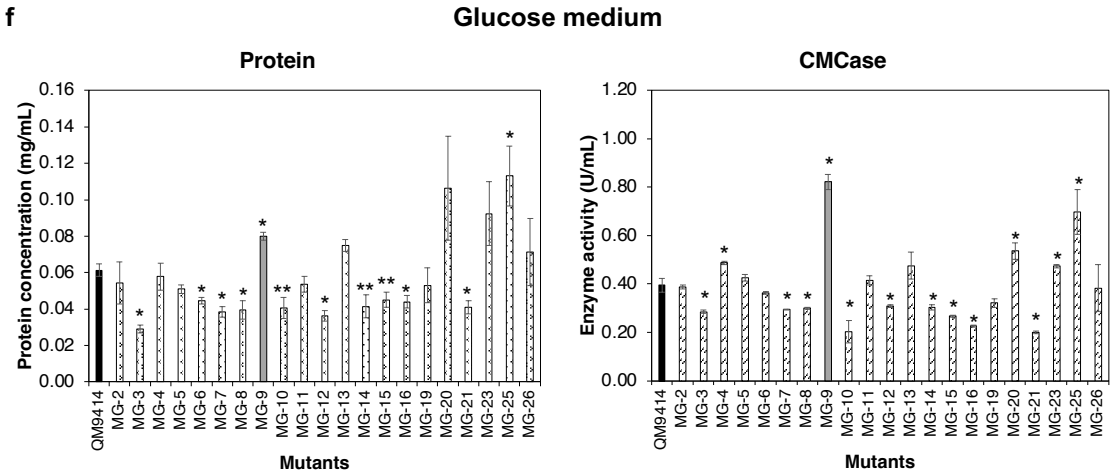

Figure 3-2. A high-throughput mutagenesis workflow for strain improvements of filamentous fungus *T. reesei* based on cellulase activity, using a cellulase fluorescent substrate FCB. (a) Schematic diagram of the workflow for screening CCR-releasing mutants with the ability to overproduce cellulase. An extensive library of *T. reesei* mutants was generated using UV light mutagenesis. The UV-induced mutants were encapsulated and cultured in WODLs for 24–72 hours. After the WODL culture, FADS rapidly sorted the droplets with the top 0.5% strongest fluorescent signals, and they were streaked on PDA-X plates for strain recovery. The recovering fungal mutants were screened for protein and cellulase production in flask fermentations. The process could be repeated for several mutagenesis rounds. (b) The fluorescence analysis of droplets carrying UV-irradiated spores using FADS. The minimal medium in a droplet consisted of 2.0% (w/v) glucose. In each analytical round, 5,000 droplets were analyzed. (c) Droplet-based screening of CCR-releasing fungal mutants from an extensive variant library. The sorting gate (dashed red lines) was set such that the top 0.5% of droplets with the highest green fluorescence signal could be separated from the rest of the population. The data represent an average proportion of the sorted droplet number in the population. (d) Micrographs of droplets carrying fungal mutants on glucose before and after uHTP screening after 24 hours of droplet culture. The scale bars depict 100 μm. (e) Twenty-six mutants of the first mutation generation were recovered on PDA-X plates. After uHTP screening, the sorted droplets were streaked onto PDA-X plates and incubated until colony formation. The recovering fungal mutants were then transferred to new PDA-X plates for storage and further investigation. (f) Secretory protein production and CMCase activities in the culture supernatant of fungal mutants cultivated in medium with 1.0%

(w/v) glucose for 48 hours. Data represent the average of three independent experiments. Error bars indicate standard deviations. Student's t-test was used to identify statistically significant differences between QM9414 and mutants (* $P \leq 0.05$; ** $P \leq 0.1$).

3.3.3 Repeated mutagenesis and evaluations of CCR-releasing *T. reesei* mutants

The *T. reesei* mutant MG-9 was identified as a potential CCR-released candidate having better protein and cellulase production than QM9414 on glucose, but its ability to secrete cellulase and extracellular protein required improvement to make it suitable for industrial applications. To generate second-generation mutants with significantly improved cellulase secretion under the repression condition, MG-9 was used as a parent strain. A similar mutagenesis workflow was conducted up to the third mutation generation (**Figure 3-3a**). For the second round of strain improvements, after UV mutation and 24-hour droplet culture, 2,086 droplets were sorted from a 4.23 × 10^5 droplet population within roughly 1.2 hours (**Figure 3-3c**), and 20 mutants were recovered on the plates. Among the second-generation mutants, MG-9-3 displayed the most improved protein production and enzyme activities, with 1.5-fold greater protein production and 1.3-fold higher cellulase activity than the MG-9 parental strains (**Figures 3-4a**). At the third mutagenesis, using MG-9-3 as the parental strain, 30 recovery mutants were collected after uHTP screening of 5.46 × 10^5 droplets within 1.5 hours (**Figure 3-3c**). Subsequent flask screening of recovery candidates revealed that only the MG-9-3-30 mutant showed remaining enzyme activity, compared to the MG-9-3 parent strain, while reduced enzyme activities were observed in the others (**Figure 3-4b**).

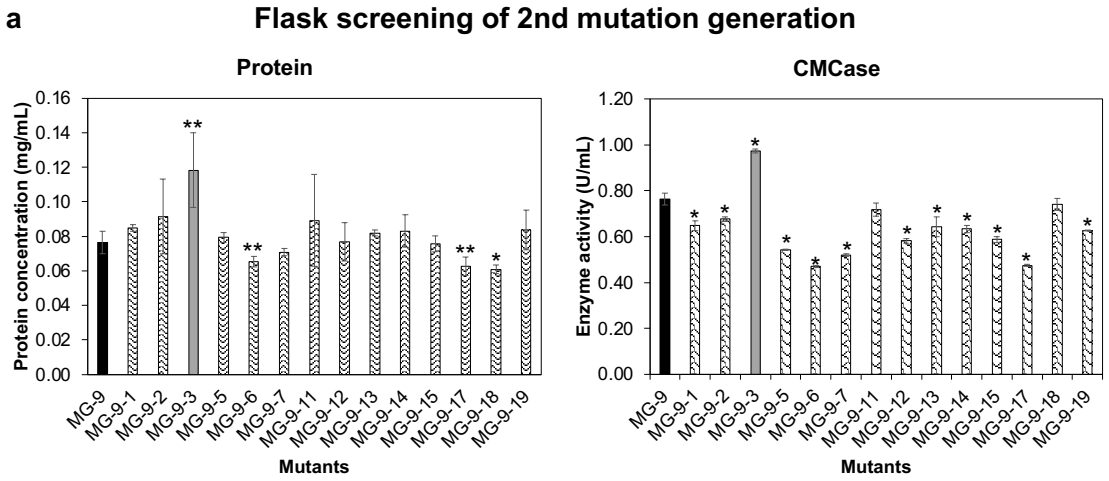

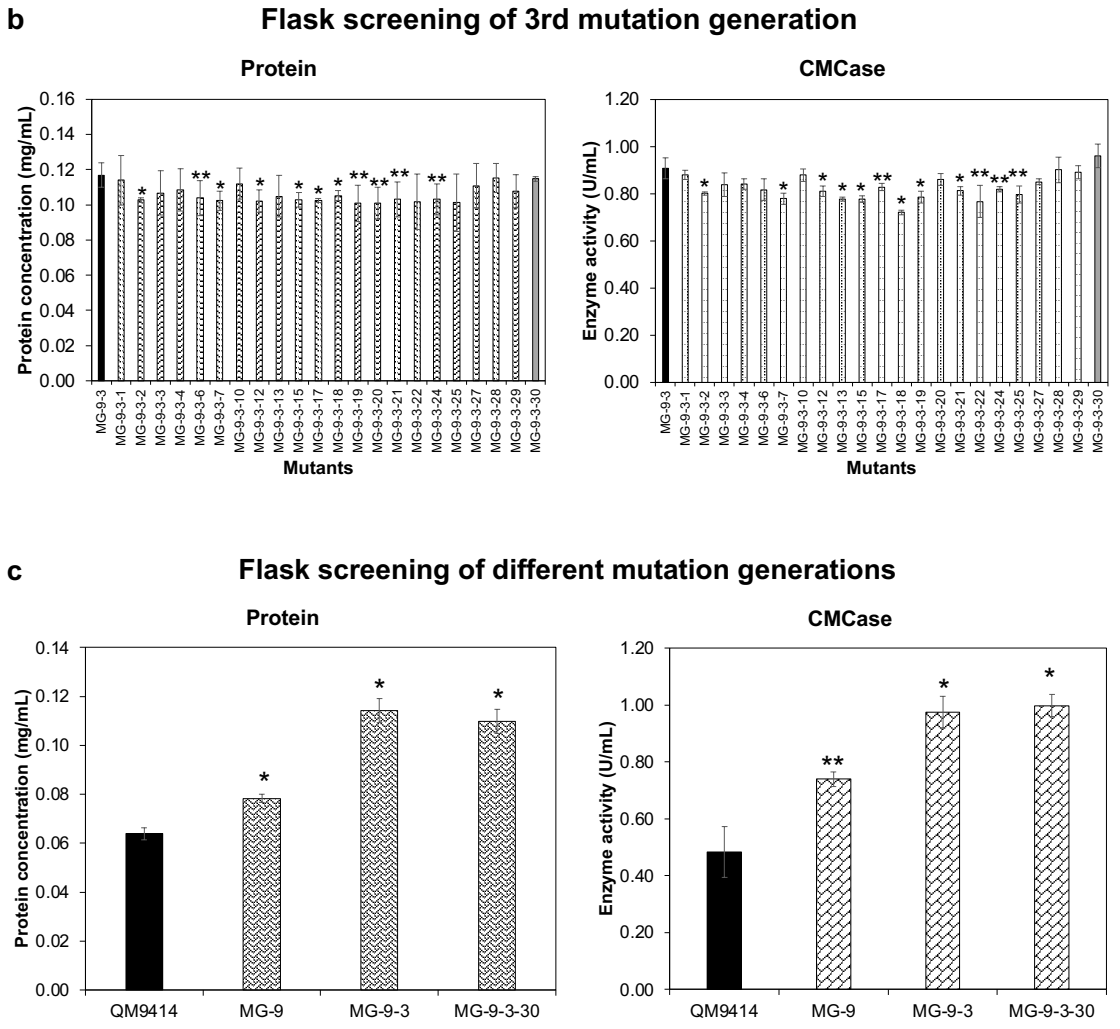

Figure 3-4. Flask fermentations of CCR-releasing *T. reesei* mutants compared to the MG-9 parent strain (black bars). Secretory protein production and CMCase activities in the culture supernatant of second-generation mutants (a) and third-generation mutants (b) when cultivated in a medium with 1.0% (w/v) glucose for 48 hours. (c) Secretory protein production and CMCase activities in the culture supernatant of three generations of mutants and the parental strain QM9414 (black bars) on glucose after 48-hour flask culture. Data represent the average of three independent experiments. Error bars indicate standard deviations. Student's t-test was used to identify statistically significant differences between QM9414 and mutants (* $P \leq 0.05$; ** $P \leq 0.1$).

Next, mutants MG-9-3, MG-9-3-30, and their parental strain QM9414 were grown on different carbon sources in shake-flask fermentation (**Figure 3-5**). When grown on glucose as the sole carbon source (**Figure 3-5a**), the productions of protein and

cellulase by MG-9-3 were doubled, compared to those by QM9414, and those by MG-9-3-30 were 1.7 to 1.8-fold greater after 24 hours of cultivation. After 72 hours of flask culture, the protein synthesis by the two mutants fell to under 0.1 mg protein mL^{-1} and 1 U CMCase·mL^{-1}, while those by QM9414 rose to 0.11 ± 0.01 mg $mL^{-1,}$ and enzyme activity rose to 1.24 ± 0.03 1 U CMCase mL^{-1}. The measurement of sugar residue in media showed that the glucose consumption rate of mutants was slower than that of QM9414 (**Figure 3-5b**). The increase in cellulase production by the parent strain during the 48–72-hour cultivation period indicated the possibility of the response toward glucose starvation when the glucose in the media was depleted. In the glucose–cellulose medium (**Figure 3-5c**), there were no increases in protein production and cellulase activities by the two mutant strains after 96 hours of flask cultivation. In contrast, steady increases in protein and cellulase secretions could be observed in QM9414. After 168 hours, the two mutants' secretory protein and cellulase secretions and the parent strain had risen remarkably, while those of QM9414 had gradually increased. At the end of flask fermentation, the protein productions of MG-9-3 and MG-9-3-30 were roughly 1.5-fold that of QM9414, while the CMCase activities were 1.9-fold and 1.7-fold higher than that of QM9414, respectively (**Figure 3-5c**). By contrast, using cellulose as the sole carbon source, the two mutants displayed lower protein production and cellulase secretion than the parent strain (**Figure 3-5d**). The enzyme activities of the mutants on cellulose were similar to those on the glucose and cellulose mixture.

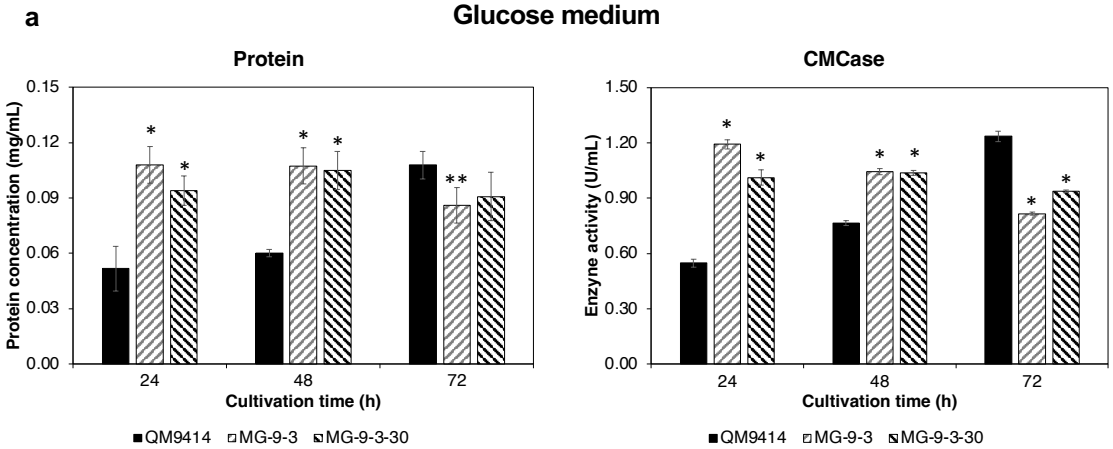

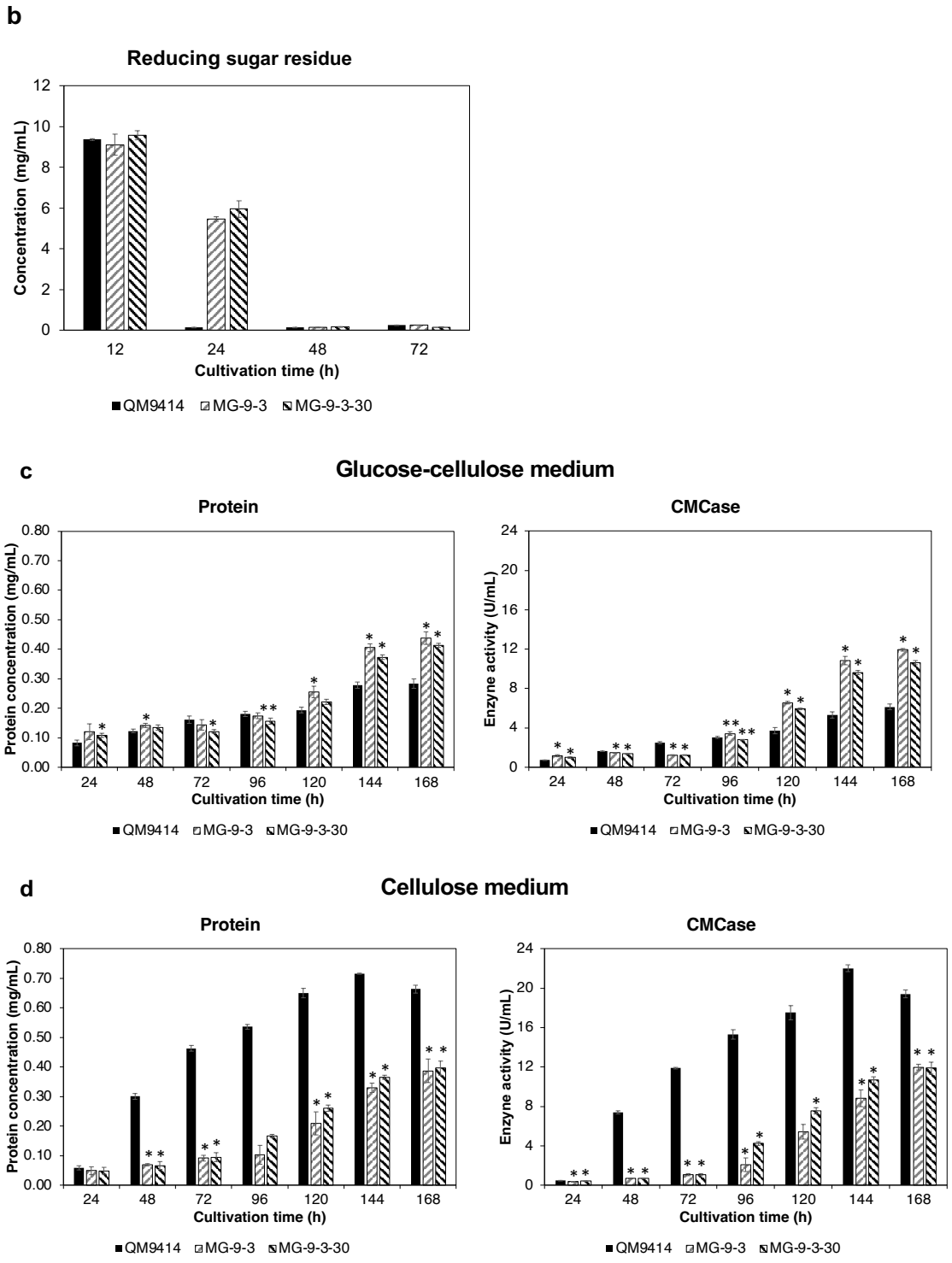

Figure 3-5. Protein and cellulase production by second- and third-generation mutants, compared to the parent strain (black bars) in different carbon sources. (a) Time course of the amount of secretory protein production and CMCase activities in the culture supernatant of the mutants in the 2.0% (w/v) glucose medium for 72 hours. (b) Reducing sugar in media was measured at 12, 24, 48, and 72 hours of cultivation of the

mutants and QM9414 on glucose. Time course of the amount of secretory protein production and CMCase activities in the culture supernatant of the mutants in a mixed medium of 1.0% (w/v) microcrystalline cellulose and 1.0% (w/v) glucose for 168 hours (c), and in 1.0% (w/v) cellulose medium for 168 hours (d). Reducing sugar in media was measured at 12, 24, 48, and 72 hours of cultivation of the mutants and QM9414 on glucose. Data are expressed as mean ± standard deviations of three biological replicates. Error bars indicate standard deviations. Student's t-test was used to identify statistically significant differences between QM9414 and mutants (* $P \leq 0.05$; ** $P \leq 0.1$).

3.3.4 Rapid isolation and flask fermentation of cellulase hyper-producing *T. reesei* mutants

The uHTP screening for *T. reesei* mutants on glucose resulted in isolating mutants with cellulase hyper-production in the presence of glucose at the early cultivation stage but with lower production on cellulose as a sole carbon source (**Figures 3-4 and 3-5**). This phenomenon could be attributed to the absence of cellulase induction during the droplet culture, so the study investigated the fungal mutant culture in droplets containing glucose and sophorose, a strong soluble cellulase inducer. FADS analysis of incubated droplets during a 72-hour incubation indicated a significantly increased level of fluorescent signals (**Figure 3-6a**). Based on the secreted enzyme, the screening of 4.35×10^5 droplets after 72 hours of WODL culture resulted in the separation of 1,439 droplets within about 1.2 hours (**Figure 3-6b**) and the recovery of 30 fungal colonies. To evaluate their protein and enzyme production abilities, the fastest-growing candidates were inoculated into flasks containing a mixture of 1.0% (w/v) glucose and 1.0 % (w/v) cellulose. After 120 hours of fermentation, 18 (64.3%) of 28 selected candidates displayed higher protein productions than the QM9414 parent strain, while the rest showed similar or lower productions (**Figure 3-6c**). Enzymatic analysis indicated that 16 (54.1%) of 28 screened candidates showed higher enzyme activity levels than the QM9414 parent strain (**Figure 3-6d**). Five mutants with the most improved protein production and enzyme activities, including M-5, M-6, M-10, M-11, and M-15, were subjected to further detailed investigations of cellulase enhancements on different carbon sources for 168 hours.

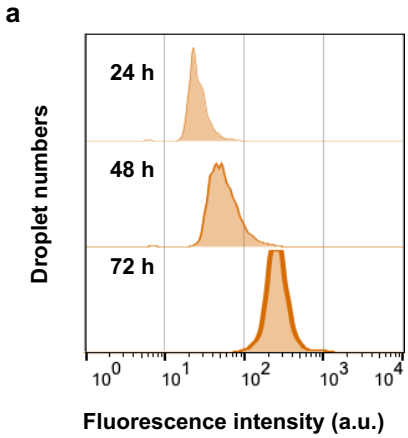
a
24 h
48 h
72 h
Droplet numbers
10^0
10^1
10^2
10^3
10^4
Fluorescence intensity (a.u.)

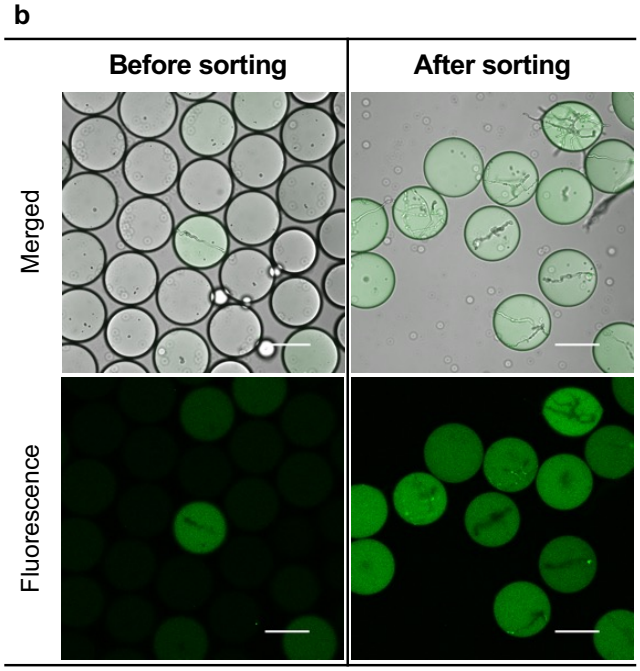
b
Before sorting
After sorting
Merged
Fluorescence

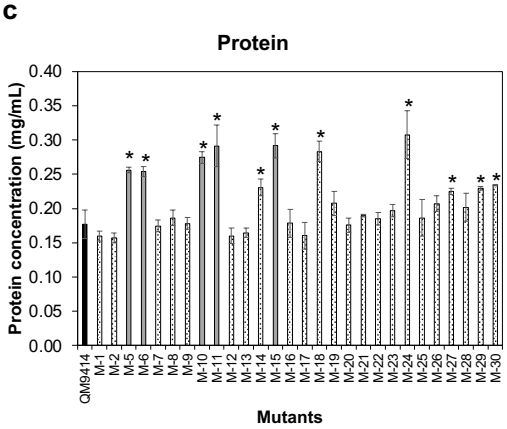
c
Protein
Protein concentration (mg/mL)
0.00
0.05
0.10
0.15
0.20
0.25
0.30
0.35
0.40
QM9414
M-1
M-2
M-5
M-6
M-7
M-8
M-9
M-10
M-11
M-12
M-13
M-14
M-15
M-16
M-17
M-18
M-19
M-20
M-21
M-22
M-23
M-24
M-25
M-26
M-27
M-28
M-29
M-30
Mutants

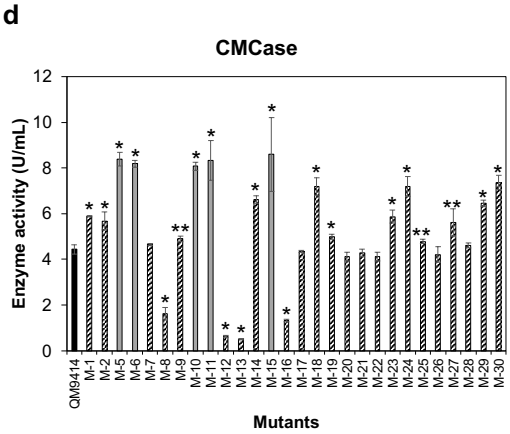
d
CMCase
Enzyme activity (U/mL)
0
2
4
6
8
10
12
QM9414
M-1
M-2
M-5
M-6
M-7
M-8
M-9
M-10
M-11
M-12
M-13
M-14
M-15
M-16
M-17
M-18
M-19
M-20
M-21
M-22
M-23
M-24
M-25
M-26
M-27
M-28
M-29
M-30
Mutants

Figure 3-6. Droplet sorting and flask screening for cellulase hyper-producing fungal strains. (a) The fluorescence analysis of glucose–sophorose medium droplets after incubation for 24, 48, and 72 hours. For each analytical round, 5,000 droplets were analyzed. (b) Micrographs of 72-hour incubated droplets carrying T. reesei mutants in glucose–sophorose medium before and after uHTP sorting. The sorting threshold was set such that the top 0.3% of droplets with the highest fluorescence levels could be collected from among the droplet population. The scale bars depict 100 μm. (c) Secretory protein production and (d) CMCase activities in the culture supernatant of sorted fungal mutants when cultivated in a medium containing 1.0% (w/v) glucose and 1.0 % (w/v) microcrystalline cellulose for 120 hours. Data represent the average of three independent experiments. Error bars indicate standard deviations. Student's t-test was used to identify statistically significant differences between QM9414 and mutants (* $P \leq 0.05$; ** $P \leq 0.1$).

On cellulose as a sole carbon source, and with 48–168 hours of flask culture, all five selected candidates generally exhibited higher protein production over *T. reesei* QM9414, with the highest level being achieved by the M-10 mutant (**Figure 3-7a**). M-10 displayed 1.3-fold and 1.4-fold improvements in protein production and CMCase activities over QM9414, on average. When cultured in a mixed medium of cellulose and glucose, six mutants showed greater protein production and cellulase secretion than the parent strain. Among them, M-5 exhibited the highest production of protein and cellulase: 1.6-fold and 2.2-fold higher than those of QM9414 during 120–168 hours of cultivation (**Figure 3-7b**). By contrast, when glucose was used as a sole carbon source, the selected mutants showed no significant changes in cellulase production compared to QM9414 at 24 hours of incubation and rather lower values at later stages of incubation (**Figure 3-7c**). The cellulase production pattern of the mutant on different carbon sources was similar to the *cre1* disruption strain (**Figure 3-8**). These findings suggest that the addition of a cellulase inducer in the WODL culture of *T. reesei* mutants allowed for the rapid collection of CCR-releasing *T. reesei* mutants.

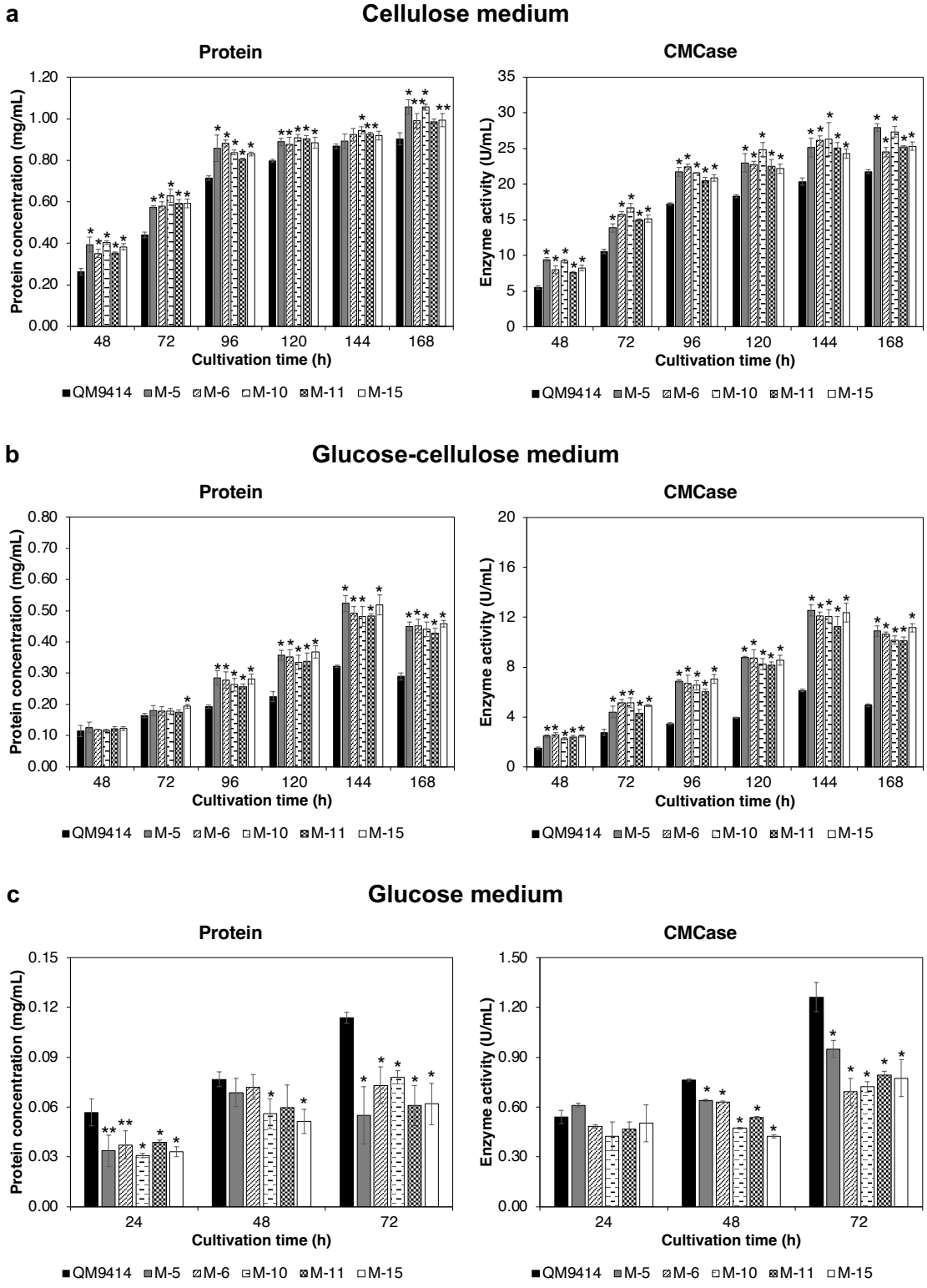

Figure 3-7. Flask evaluation of five improved fungal mutants and the parent strain QM9414 (black bars) in various carbon sources. Time course of the amount of secretory protein production and CMCase activities in the culture supernatant of the mutants cultured on 1.0% (w/v) cellulose (a), on a mixture of 1.0% (w/v) glucose and

1.0% (w/v) cellulose (b), and on 1.0% (w/v) glucose (c). Data represent the average of three independent experiments. Error bars indicate standard deviations. Student's t-test was used to identify statistically significant differences between QM9414 and mutants (* $P \leq 0.05$; ** $P \leq 0.1$).

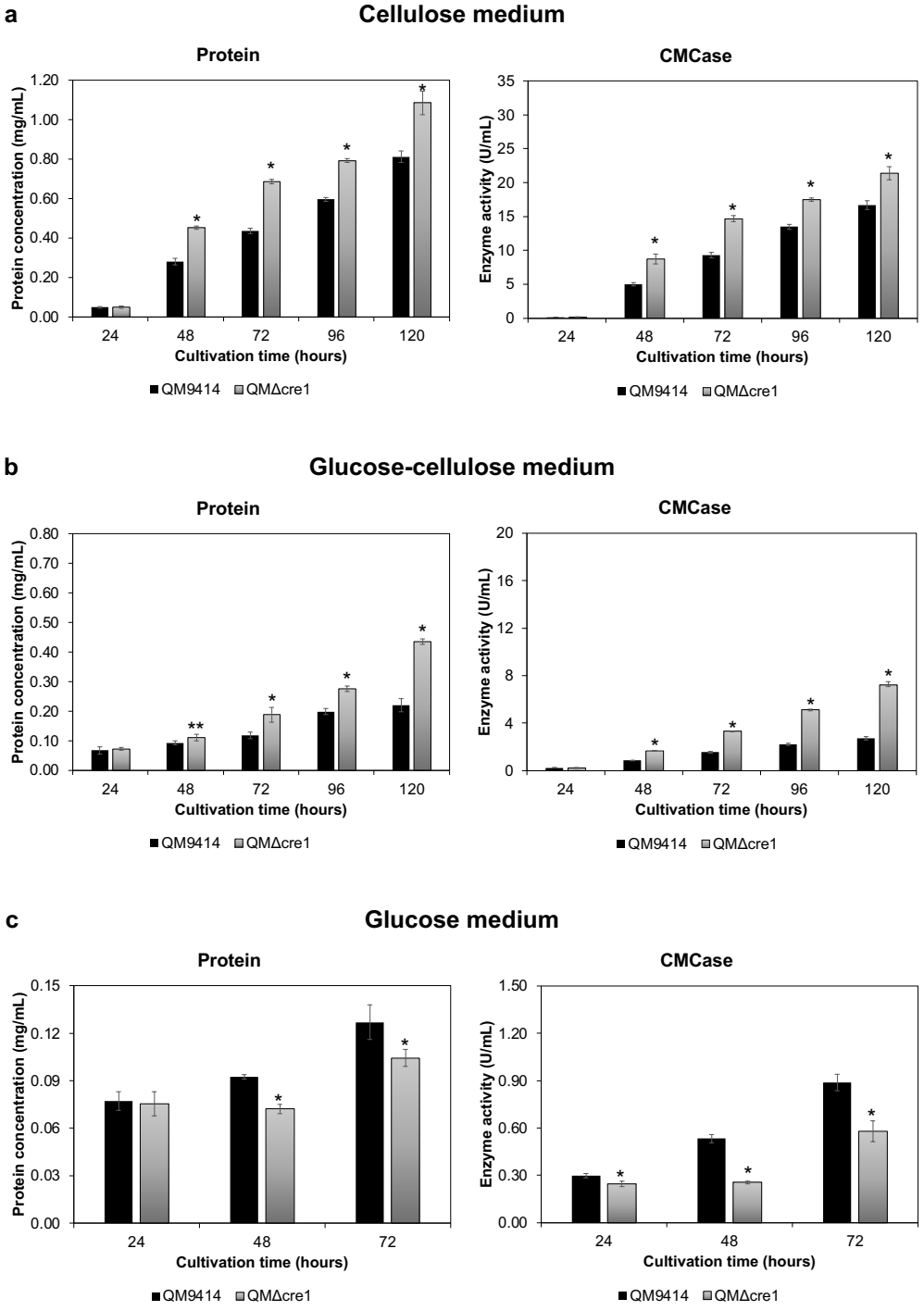

Supplementary Figure 3-8. Flask evaluation of five improved fungal mutants compared to the parent strain QM9414 (black bars) and the *cre1* deletants QMΔ*cre1*. Time course of the amount of secretory protein production and CMCase activities in the culture supernatant of the mutants cultured on 1.0% (w/v) cellulose (a), on a mixture of 1.0% (w/v) glucose and 1.0% (w/v) cellulose (b), and on 1.0% (w/v) glucose (c). Data represent the average of three independent experiments. Error bars indicate standard deviations. Student's t-test was used to identify statistically significant differences between QM9414 and mutants (* $P \leq 0.05$; ** $P \leq 0.1$).

3.3.5 Hyphal morphology of sorted *T. reesei* mutants

Morphological features may be linked to the ability to produce enzymes, so the study sought to identify potential distinct morphological characteristics of the selected mutants MG-9-3, MG-9-3-30, and M-5 and compare them to the QM9414 parental strain (**Figures 3-9**). After cultivation on glucose, fungal hyphae were collected, stained with the blue fluorescence dye Calcofluor White, and observed under confocal microscopy. The analysis indicated that the hyphal surface was covered by fibrous materials, with the most significant amounts belonging to MG-9-3 at 24 hours and MG-9-3-30 at 48 hours. The observations suggested a correlation between cellulase production and the amount of fibrous material produced by cellulase hyper-producers MG-9-3 and MG-9-3-30. Furthermore, these two mutants produced hyphae that were swollen and extensively branched with adventitious septa in comparison to the QM9414. Notably, MG-9-3-30 formed swelling at the hyphal tips (**Figure 3-7**). Conversely, the hyphae of QM9414 and M-5 grew longer without swelling or branching.

a

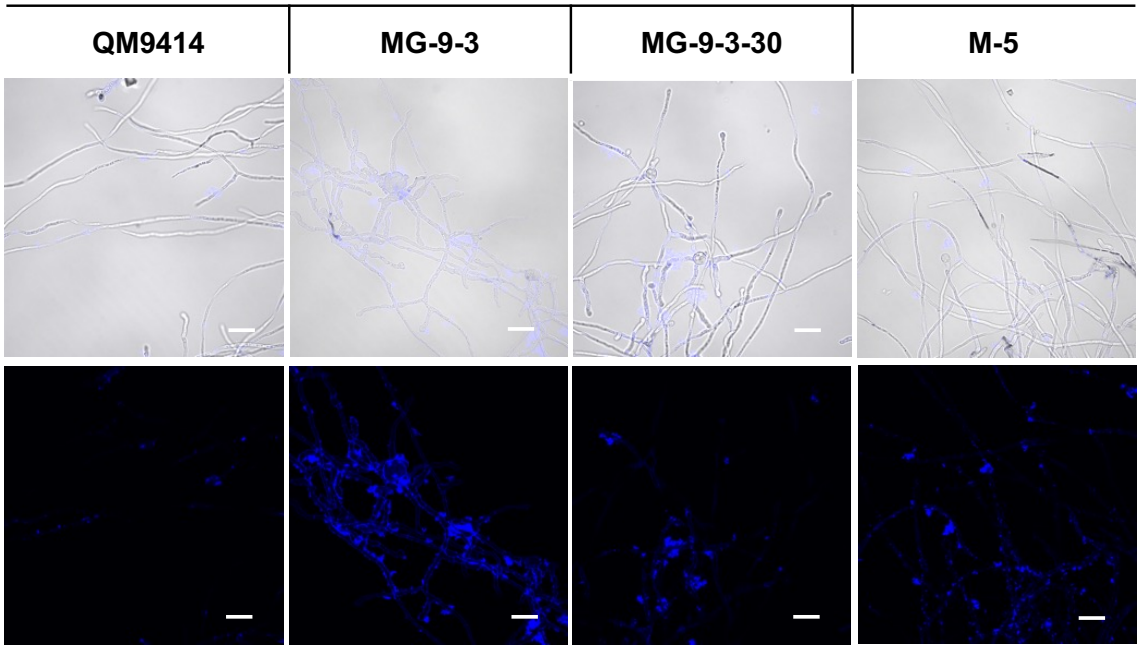

b

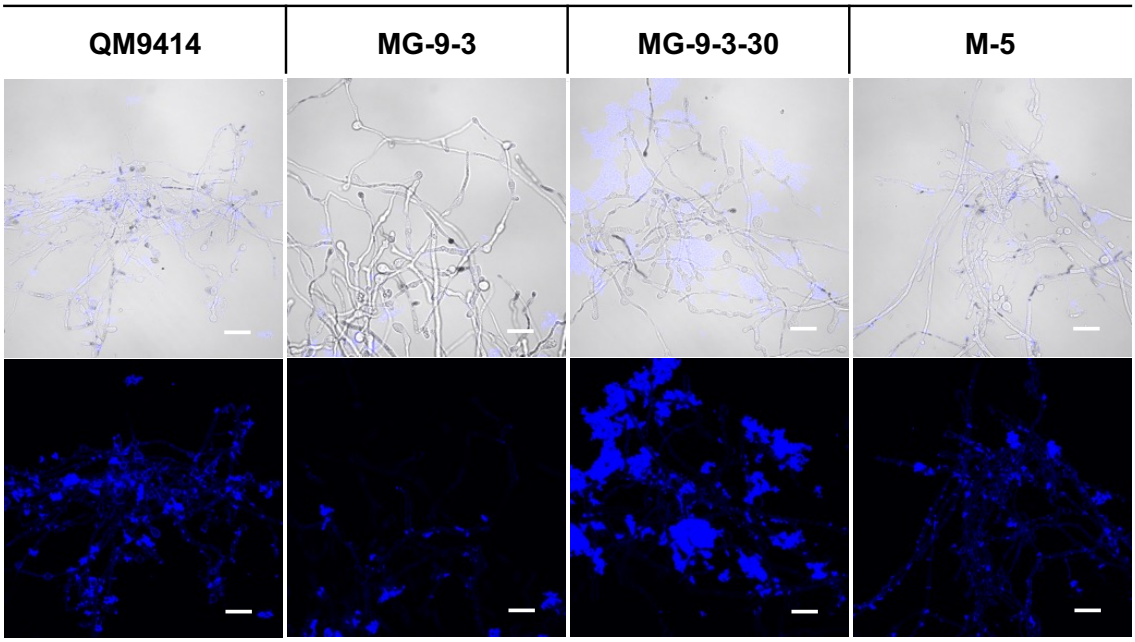

Figure 3-9. Micrographs of the MG-9-3, MG-9-3-30, M-5 mutants and the QM9414 parental strain. The hyphae were cultivated in flasks containing 1% glucose medium for 24 hours (a) and 48 hours (b) before microscopic observation. Calcofluor White was used to stain fungal cell walls. The scale bar represents 20 μm.

3.3.6 Cellulase and transcription factor gene expressions of selected *T. reesei* mutants

To gain a deeper understanding of the mechanisms responsible for CCR release and cellulase overproduction in mutants, gene transcription analyses were conducted. qRT-PCR was performed using total cDNA from mycelia grown on glucose as templates. The expression levels of *cbh1*, *cbh2*, *egl1*, *bgl1*, and *bgl2* as cellulase genes; *xyr1*, *ace3*, *bglr*, *cre1*, and *ace1* as regulatory protein-encoding genes; and *trasp* as a protease gene, were measured by qRT-PCR.

When cultivated on glucose as a sole carbon source, the cellulase gene expression amounts of mutants were greater than those of the parent strain (**Figure 3-10a),** although higher expression levels of cellulase repressors were observed in the mutants (**Figure 3-10b**). In particular, the CCR-releasing mutant MG-9-3, the second-generation mutant derived from QM9414, displayed significantly higher expression amounts of *cbh1*, *cbh2*, *egl1* and *bgl1*, respectively, over those in QM9414. As for the transcription factors in this mutant, the expression of the cellulase activator *xyr1* was the most remarkable rise, followed by increases of the activators *ace3* and *bglr*. Meanwhile, increases in expression levels of the repressors *cre1* and *ace1* were observed in MG-9-3, compared to QM9414. The third-generation mutant MG-9-3-30 exhibited higher *cbh1*, *cbh2*, and *bgl2* expressions than in QM9414. Higher expression levels of cellulase activators *xyr1, ace3,* and *bglr* were observed in this strain. The expression level of *cre1* in MG-9-3-30 was half of QM9414, while that of *ace1* was greater. Unlike the two CCR release strains, mutant M-5 exhibited improved expression patterns of *cbh1*, *cbh2,* and *bgl2* than QM9414, respectively. The expression levels of cellulase activators *xyr1*, *ace3,* and *bglr* were increased in M-5, but those of repressors *cre1* and *ace1* were more significant than in the parent strain. In other words, the expression levels of cellulase repressors in M-5 were higher than those of the activators on glucose as a sole carbon source. By contrast, when using the mixture of cellulose and glucose, the *cre1* expression level was lower in M-5 than in the parent strain (**Figure 3-10c)**. Additionally, the protease Trichodermapepsin (TrAsP) expression levels rose in all selected mutants, with the highest upregulation observed in M-5 (**Figure 3-10d**).

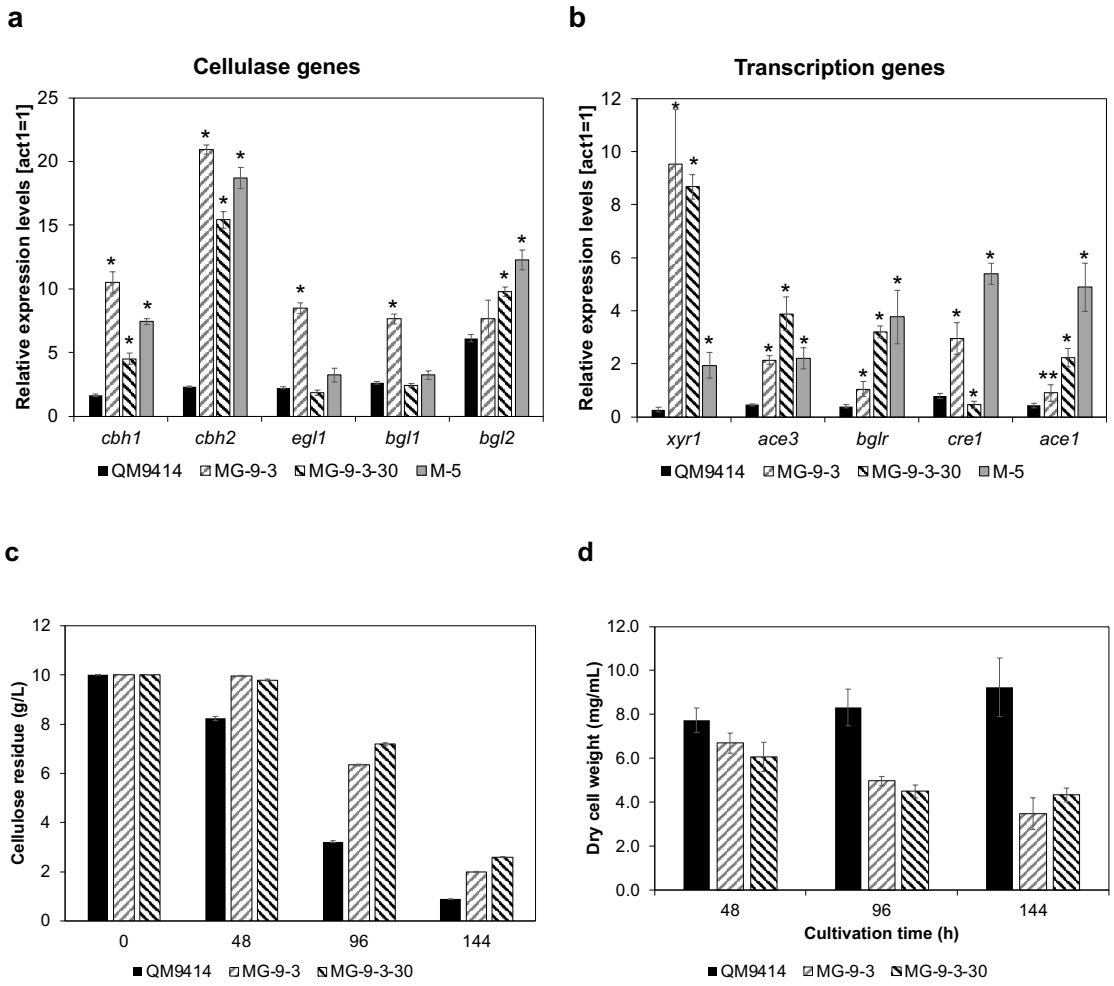

Figure 3-10. Expression profile of *T. reesei* glycosyl hydrolase genes (a) and transcription factor genes (b) of *T. reesei* mutants MG-9-3, MG-9-3-30, and M-5, and parent strain QM9414, cultivated on glucose for 48 hours. Transcriptional analysis of cellulase genes *cbh1*, *cbh2*, *egl1*, *bgl1*, and *bgl2*, and transcription factor genes *xyr1*, *ace3*, *bglr*, *cre1*, and *ace1* was performed by qRT-PCR. The expressions of the cellulase repressor CRE1 after 48 and 72 hours of cultivation on the glucose-cellulose medium (c) and of a main protease Trichodermapepsin (TrAsP) in *T. reesei* mutants MG-9-3, MG-9-3-30, and M-5, and parent strain QM9414 after 48 hours of cultivation on glucose (d). All values were normalized to the β-actin (*act1*) expression. Data represent the average of three independent experiments. Error bars indicate standard deviations. Student's t-test was used to identify statistically significant differences between QM9414 and mutants (* $P \leq 0.05$; ** $P \leq 0.1$).

3.3.7 Genome analysis of QM9414 and its mutants

To identify the mutations which play vital roles in glucose uptake retardation of the MG linage and in CCR release of the M linage, genome sequencing of QM9414 and the mutants was performed. The genome analysis illustrated that 158 single nucleotide variations (SNVs) were detected in glucose uptake retarded mutant MG-9, 317 SNVs in MG-9-3, and 600 SNVs in MG-9-3-30 (**Figure 3-11**). Meanwhile, 37 mutations were identified in CCR-releasing mutant M-5. Among the SNVs, 24, 43, and 67 SNVs with high impacts (nonsense mutations) and moderate impacts (missense mutation) were determined at the first, second, and third mutation generation of the MG linage. Also, M-5 with 5 moderate/high-impacted SNVs was noticed (**Table 3-2**). Up/downstream mutations and insertion–deletion mutations (indel) were also noticed in the mutants.

Table 3-2 shows SNVs of mutants with moderate to high impact. In the MG linage, these SNVs were found in coding regions, specifically in tr69557 encoding GH3 or BGLII and tr75568 encoding Thioredoxin - an enzymatic detoxifier, across all three generations of the M lineage. Compared to the parent strain, there were single-nucleotide differences at position 352 of tr69557 where Isoleucine was substituted by Asparagine, and at position 207 of tr75568 where Lysin was replaced by Glutamic. The mutation of I352N could result in a change in the activity of BGLII, while the K207E mutation might change the function of the enzymatic detoxifier Thioredoxin. From the second generation, the S199F mutation was found in the tr47055, encoding a small GTPase RAC1, and a nonsense mutation was found in tr70021, encoding an Esterase. Meanwhile, in the M linage, tr122284 encoding VEA protein was mutated at the 447 position where Serine was substituted by Phenylalanine. This protein plays a crucial role in the VELVET protein complex, which controls the growth and secondary metabolism in *T. reesei*.

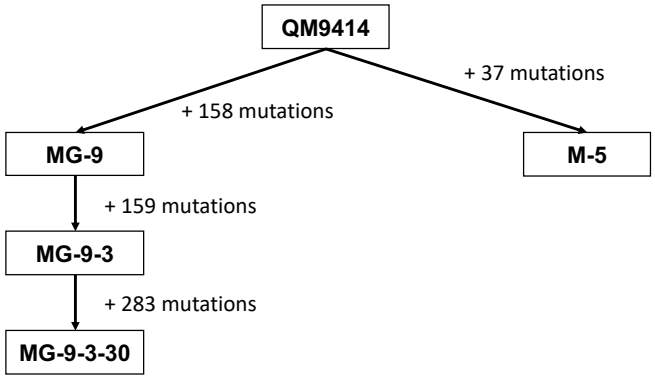

Figure 3-11: The lineages of *T. reesei* mutants developed in this study.

Table 3-2. List of SNVs identified between strains QM9414 and mutants.

	MG-9-3-30			M-5
	MG-9-3			
	MG-9			
Total mutation number	158	317	600	37
High-impacted mutations	1	2	4	0
Moderate-impacted mutations	23	41	65	5
Substitution mutations	31	60	111	7
Up/downstream mutations	121	246	452	25
Indel mutations	7	13	42	5

Table 3-2. List of SNVs identified between strains QM9414 and MG-9 (a); MG-9-3 (b); MG-9-3-30 (c) and M-5 (d).

a

Protein ID	Mutation	Elements	Amino acid change	Annotation/function
120153	C>T	Stop codon		26S proteasome regulatory subunit
69557	T>A	Exon	I352N	GH3
75568	A>G	Exon	K207E	Thioredoxin
76451	G>A	Exon	G1137D	C6 transcription factor
58952	T>G	Exon	I1077M	Calcium-transporting ATPase
46421	C>T	Exon	P230L	α-1,2 mannosyltransferase
60664	G>A	Exon	G811E	pH domain-containing protein
81576	A>T	Exon	Y976F	α subunit of assimilatory sulfite reductase
121486	C>T	Exon	P116S	Transmembrane amino acid transporter
5871	C>T	Exon	S885L	Nuclear protein
35556	T>C	Exon	F951S	AAA domain-containing protein
55055	A>T	Exon	N451I	Methylenetetrahydrofolate reductase
119989	C>T	Exon	A73V	Hydrophobin-2
79153	A>G	Exon	E46G	5-Oxoprolinase
79124	T>C	Exon	F238L	Kinesin-domain-containing protein

109835	G>A	Exon	V37M	Thaumatin family protein
103350	A>T	Exon	K139M	MRP-S28 domain-containing protein
42449	C>T; C>T	Exon	S117F; L118F	Acetyltransferase
111863	G>A	Exon	R110Q	Unknown
78966	C>T	Exon	L332F	NAD dependent epimerase/dehydratase
102461	T>C	Exon	F1002S	ATP-dependent DNA helicase
1925	C>T	Exon	T5M	Ceramide very long chain fatty acid hydroxylase
69648	C>T	Exon	60987	Cytochrome P450
75568	A>G	Exon	K207E	Thioredoxin
21641	T>A	Exon	Y601N	Carboxypeptidase Y receptor

b

Protein ID	Mutation	Elements	Amino acid change	Annotation/function
69557	T>A	Exon	I352N	GH3
75568	A>G	Exon	K207E	Thioredoxin
47055	C>T	Exon	S199F	Ras small GTPase RAC1
70021	A>G	Stop codon		Esterase
120153	C>T	Stop codon		26S proteasome regulatory subunit
76451	G>A	Exon	G1137D	C6 transcription factor
58952	T>G	Exon	I1077M	Calcium-transporting ATPase
46421	C>T	Exon	P230L	α-1,2 mannosyltransferase
60664	G>A	Exon	G811E	pH domain-containing protein
81576	A>T	Exon	Y976F	α subunit of assimilatory sulfite reductase
121486	C>T	Exon	P116S	Transmembrane amino acid transporter
5871	C>T	Exon	S885L	Nuclear protein
35556	T>C	Exon	F951S	AAA domain-containing protein
55055	A>T	Exon	N451I	Methylenetetrahydrofolate reductase
119989	C>T	Exon	A73V	Hydrophobin-2
79153	A>G	Exon	E46G	5-Oxoprolinase
79124	T>C	Exon	F238L	Kinesin-domain-containing protein
109835	G>A	Exon	V37M	Thaumatin family protein

103350	A>T	Exon	K139M	MRP-S28 domain-containing protein
42449	C>T; C>T	Exon	S117F; L118F	Acetyltransferase
111863	G>A	Exon	R110Q	Unknown
78966	C>T	Exon	L332F	NAD dependent epimerase/dehydratase
102461	T>C	Exon	F1002S	ATP-dependent DNA helicase
1925	C>T	Exon	T5M	Ceramide very long chain fatty acid hydroxylase
69648	C>T	Exon	S351L	Cytochrome P450
21641	T>A	Exon	Y601N	Carboxypeptidase Y receptor
57600	C>T	Exon	P142L	FACT complex protein
60508	G>A	Exon	R487K	SET domain protein
77167	C>T	Exon	P303Ser	Ankyrin repeat protein
62556	G>A	Exon	E179K	Chitinase
61066	C>A	Exon	Q263K	Choline dehydrogenase
112222	A>G	Exon	Q256R	NACHT and TPR domain protein
66517	T>A	Exon	F205I	Homoserine O-acetyltransferase
80277	G>A	Exon	D554N	RHO1 guanine nucleotide exchange factor 1
26019	C>T	Exon	R337W	Chromosome segregation ATPase
82208	C>T	Exon	S30L	Conidial pigment polyketide synthase PKSP/ALB1
123934	T>C	Exon	Y474H	Dynamin GTPase
102673	A>G	Exon	R56Gly	Zinc finger protein
64898	A>T	Exon	L133P	Polynucleotide phosphorylase/polyadenylase
109415	T>C	Exon	P316S	DNA mismatch repair protein MUTS
103920	C>T	Exon	Y8D	HSP33 protein
110853	T>G	Exon	S20I	Glutathione S-transferase

c

Protein ID	Mutation	Elements	Amino acid change	Annotation/function
69557	T>A	Exon	I352N	GH3
75568	A>G	Exon	K207E	Thioredoxin
47055	C>T	Exon	S199F	Ras small GTPase RAC1
70021	A>G	Stop codon		Esterase

36543	C>T	Exon	A215V	STE12-like transcription factor
120153	C>T	Stop codon		26S proteasome regulatory subunit
76451	G>A	Exon	G1137D	C6 transcription factor
58952	T>G	Exon	I1077M	Calcium-transporting ATPase
46421	C>T	Exon	P230L	α-1,2 mannosyltransferase
60664	G>A	Exon	G811E	pH domain-containing protein
81576	A>T	Exon	Y976F	α subunit of assimilatory sulfite reductase
121486	C>T	Exon	P116S	Transmembrane amino acid transporter
5871	C>T	Exon	S885L	Nuclear protein
35556	T>C	Exon	F951S	AAA domain-containing protein
55055	A>T	Exon	N451I	Methylenetetrahydrofolate reductase
119989	C>T	Exon	A73V	Hydrophobin-2
79153	A>G	Exon	E46G	5-Oxoprolinase
79124	T>C	Exon	F238L	Kinesin-domain-containing protein
109835	G>A	Exon	V37M	Thaumatin family protein
103350	A>T	Exon	K139M	MRP-S28 domain-containing protein
42449	C>T C>T	Exon	S117F L118F	Acetyltransferase
111863	G>A	Exon	R110Q	Unknown
78966	C>T	Exon	L332F	NAD dependent epimerase/dehydratase
102461	T>C	Exon	F1002S	ATP-dependent DNA helicase
1925	C>T	Exon	T5M	Ceramide very long chain fatty acid hydroxylase
69648	C>T	Exon	60987	Cytochrome P450
21641	T>A	Exon	Y601N	Carboxypeptidase Y receptor
70021	A>G	Stop codon		Esterase
57600	C>T	Exon	P142L	FACT complex protein
60508	G>A	Exon	R487K	SET domain protein
77167	C>T	Exon	P303Ser	Ankyrin repeat protein
62556	G>A	Exon	E179K	Chitinase
61066	C>A	Exon	Q263K	Choline dehydrogenase
112222	A>G	Exon	Q256R	NACHT and TPR domain protein
47055	C>T	Exon	Q68H	Ras small GTPase RAC1

66517	T>A	Exon	S199F	Homoserine O-acetyltransferase
80277	G>A	Exon	F205I	RHO1 guanine nucleotide exchange factor 1
26019	C>T	Exon	D554N	Chromosome segregation ATPase
82208	C>T	Exon	R337W	Conidial pigment polyketide synthase PKSP/ALB1
123934	T>C	Exon	S30L	Dynamin GTPase
102673	A>G	Exon	Y474H	Zinc finger protein
64898	A>T	Exon	R56Gly	Polynucleotide phosphorylase/polyadenylase
109415	T>C	Exon	L133P	DNA mismatch repair protein MUTS
103920	C>T	Exon	P316S	HSP33 protein
110853	T>G	Exon	Y8D	Glutathione S-transferase
65380	T>A	Stop codon		α-1,2-Mannosidase
21758	G>A	Exon	E206K	2-Methylisocitrate lyase, mitochondrial
105315	C>T	Exon	P131S	Sorting nexin MVP1
123710	G>A	Exon	S526N	Zn(2)-C6 fungal-type domain-containing protein
107900	C>T	Exon	S161L	Gln/Pro-rich protein
107779	T>A	Exon	I235K	α/β superfamily hydrolase
61222	G>A	Exon	E207K	Unknown
106960	T>A	Exon	H107Q	Unknown
60346	C>T	Exon	P86L	Para-aminobenzoate synthase PABAA
57671	G>A	Exon	D149N	Glycerophosphocholine phosphodiesterase
62912	A>C	Exon	K85Q	Unknown
60557	C>T	Exon	S279F	Unknown
22633	A>T	Exon	K354M	S-glutathione dehydrogenase
109760	C>T	Exon	H282Y	Transcription factor HBP-1A
109903	T>A	Exon	F1667L	DNA repair protein MUS7
122584	G>A	Exon	D331N	RNA cytidine acetyltransferase
63869	T>C	Exon	L232P	DNA repair family protein
123164	G>A	Exon	G477E	Signal recognition particle subunit SRP72
123185	G>A	Exon	M522I	Adenylate kinase isoenzyme 6 homolog
81884	A>T	Exon	Y98F	Signal sequence receptor subunit alpha
43680	G>A	Exon	G74D	RRM domain-containing protein
49979	C>T	Exon	P39L	Oligopeptide transporter

2050	A>T	Exon	N484I	MIF4G domain-containing protein

d

Protein ID	Mutation	Elements	Amino acid change	Annotation/function
122284	C > T	Exon	S447F	VEA protein
81473	C > T	Exon	P137S	Caffeine-induced death protein
21425	C > T	Exon	A83V	ATP-dependent RNA helicase
62057	C > T	Exon	S286F	Transcription-coupled repair protein
52267	C > T	Exon	P363L	Mannitol-1-phosphate dehydrogenase

3.4 Discussion

Droplet microfluidic technology has recently emerged as an attractive novel tool for enzyme engineering [27]. Bacteria [28,29], yeasts [16,30], and algae [31,32] are preferred screening hosts for this purpose. Filamentous fungi are rarely used due to the fast growth of their branched hyphae. The filamentous fungus *T. reesei* is a well-studied cellulolytic microorganism and a potential cellulase producer and is an essential source for biodegradation of lignocelluloses during fermentation [6]. Therefore, the generation of potential cellulase hyper-producing *T. reesei* strains with released CCR is important for the effective utilization of this fungus for industrial purposes. Random mutagenesis methods are widely employed to generate cellulase hyper-producing stains suitable for industrial applications [4] but require considerable time and effort to screen desired mutants from a large pool of variants. In this study, a droplet-assisted platform can be used to facilitate the screening process for *T. reesei* mutants with CCR release and cellulase hyperproduction abilities from an extensive UV-irradiated mutant library.

Droplet culture has several outstanding advantages for rapidly detecting desired *T. reesei* mutants (**Figures 3-2**). The first is that it provides separate confinements of single variants, which ensures a strong link between genotype and phenotype, the foundation for screening based on enzyme activity [18]. *T. reesei* could be successfully cultivated in droplets but noticed differences in growth between the parental strain and mutants. UV irradiation can damage molecules and compromise cell semi-permeability through its capacity to initiate photochemical and uncontrolled free radical reactions [33,34]. Mutants with slight damage can survive through cellular repair systems, such as photoreactivation, excision repair, and post-replication repair, while others with excessive damage cannot survive [35]. Apart from non-UV-derived spores in droplets, UV-derived mutants must repair their damage before growth and enzyme biosynthesis. This probably explains why mutants that survived UV irradiation had reduced growth in WODLs compared to their QM9414 parental strain. The detection of cellulase activity in the WODL culture of the QM9414 parental strain on glucose could be attributed to the expression of some low-abundance glycoside hydrolases (GHs) that cleave the fluorescent substrate FCB or to de-repression of cellulase gene expression by glucose depletion. A previous study illustrated that the overall transcription of GH-encoding genes in *T. reesei* QM9414 was low in the presence of glucose, but the gene expressions of several GHs, such as endoglucanase (CEL5B), β-1,4-glucanase (GH5), and β-1,3-

glucanosyltransferase (GH72), were upregulated even in the repressed condition [36]. Secondly, the WODL culture permitted the use of the costly inducer for culturing and screening *T. reesei*. Sophorose is the most potential inducer for cellulase production of *T. reesei*, but its high cost reduces its suitability in traditional cultivating and screening methods [20]. With scaled-down culture volumes in droplets, this carbon source could be used as a source for *T. reesei* growth and as an inducer for cellulase production. Finally, cellulase secretion from filamentous fungal mutants in droplets was detectable at the extended cultivation period of up to 72 hours. It generally takes approximately 24 hours for *T. reesei* spores to germinate and begin secreting enzymes, and the peak enzyme activity is typically achieved after a few days of incubation [37]. Unlike when culturing other microbes in droplets, culturing fungi in droplets without time control will lead to droplet breakage, fungal clump formation, and microfluidic channel blockages because of the quick expansion of fungal mycelia [12,16,20]. A previous report on the screening of *T. reesei* mutants from an atmospheric and room-temperature plasma mutagenesis library showed that the use of a rich cultural medium permitted the rapid detection and isolation of cellulase secretion within 12 hours of incubation [20]. To tackle the obstacle, a minimal medium was used for culturing UV-irradiated *T. reesei* mutants for long cultivation periods of 24, 48, and 72 hours in droplets.

In this study, droplet-based screening can facilitate faster and more efficient generation of novel *T. reesei* mutants with abilities of CCR release and cellulase hyper-production through repeated random mutagenesis compared to traditional screening methods (**Figures 3-3 and 3-4**). Using the microfluidic droplet tool for mutagenesis by UV light will enable the screening of hundreds of thousands of variants within a period of a few hours while significantly reducing the amounts of medium and costly substrates compared to classical mutation methods. With three mutagenesis rounds, a total of 1.51×10^6 droplets（containing approximately 3.8×10^5 viable UV-induced *T. reesei* spores) were screened within 4.4 hours; 6.20×10^3 were sorted, and 76 *T. reesei* mutant colonies were recovered on the plates. In classical random mutagenesis methods, agar plate screening efficiently and commonly isolates the desired mutants from mutagenized pools [4,38]. For this screening strategy, a previous report showed that approximately 2.0×10^4 mutants could be evaluated in each round [4], which requires considerable culture medium, time, and labor. Besides, it often takes roughly 72–120 hours for *T. reesei* mutants to form clear halo zones or develop positive colors on plates before the selection.

Based on CCR release and high cellulase production capacities, two *T. reesei* mutants, MG-9-3 and MG-9-3-30 were obtained at the second and third mutation generations, respectively, from the QM9414 background strain (**Figures 3-4 and 3-5**). In *T. reesei*, CCR is triggered by glucose and represses the cellulase genes, causing a low cellulase production [6,39]. Despite many efforts to generate CCR-released *T. reesei* strains, cellulase production improved only when a low glucose concentration (below 0.2% (w/v) of glucose) was supplemented to the cellulose medium [3,40]. The results indicated that the two sorted mutants outperformed QM9414 in cellulase production in the presence of 1% (w/v) glucose, with a 1.8-fold improvement in CMCase activities in the glucose medium and 1.5-fold in glucose–cellulose medium (**Figure 3-5)**. The findings suggested that CCR inhibition in cellulase transcription could be released. This is the first report of *T. reesei* strains that could grow and secrete high yields of cellulase with the high-dosage glucose supplement. For industrial cellulase production, the supplemented glucose in a cellulose medium would allow *T. reesei* to use the easily metabolizable carbon for mycelium development in the early stages and then switch to cellulose as a cellulase inducer, resulting in an improved cellulase production [3]. In the mutants, a decreased glucose consumption rate on glucose, compared to QM9414 was observed (**Figure 3-5b**). Thus, it is hypothesized that the glucose transporter system in these mutants could be impaired or damaged after irradiation, reducing glucose repression and promoting release from CCR. Another possibility is that the mutants might be released from CCR because of some mutations in CCR-related genes. Despite the potential capability, the two mutants displayed low protein production levels and cellulase activities on cellulose as a sole carbon source (**Figure 3-5d**). The reduced cellulase production on cellulose alone might indicate that cellulose inducibility in MG-9-3 and MG-9-3-30 had been partly impaired. To obtain cellulase-overproducing *T. reesei* strains on cellulose and on the cellulose–glucose mixture, it is speculated that adding a cellulase inducer into the WODL culture was necessary [41] because the glucose–sophorose mixture induced *T. reesei* cellulase secretion stronger than cellobiose and lactose [42,43]. As expected, the study could isolate several high-yielding *T. reesei* strains (M-5, M-6, M-10, M-11, and M-15) from the UV mutagenized library (**Figure 3-6**). Despite no notable increase in cellulase production when glucose was used as the only carbon source, the collected strains exhibited were better able to produce cellulase than QM9414 in the glucose–cellulose medium. (**Figure 3-7**). This cellulase production pattern was similar to

the *cre1* disruptant (**Figure 3-8**). Disruption of *cre1* in *T. reesei* results in CCR release, but a slight improvement in cellulase productivity is observed when glucose is used as the sole carbon source (Nakari-Setälä *et al.*, 2009). In the cellulase hyper-producing strain Rut-C30 that possesses a truncation in the *cre1* gene, cellulase gene expression is only partial; cultivation of this mutant on glucose results in only low cellulase levels (Kubicek *et al.*, 2009). This implies that both CCR release and transcription activation are necessary to fully activate cellulase gene expression. Therefore, it is possible that mutants screened on glucose-sophorose have mutations in the CRE1-mediated CCR mechanism. Among the isolated candidates, M-5 displayed a 2.2-fold improvement in cellulase activity than QM9414 in the mixed medium. This is significant because the presence of high glucose dosage in the cellulose-containing medium led to a considerable decrease in cellulase biosynthesis, even in a recombinant strain SEU-7 based on *cre1* deficient strain Rut-C30 [3].

The enzyme-producing capabilities of selected mutants may be linked to changes in their morphological phenotypes. The first morphology is associated with the hyphal surface structure. The findings indicate that the hyphal surface of mutants was partially covered with fibrous material (**Figures 3-9**). This layer may be composed of exopolysaccharides, which have a role in capturing secreted enzymes near the cell wall for efficient cellulose degradation [6]. When cultivated on glucose, MG-9-3 and MG-9-3-30 displayed more extensively branched and swollen hyphae and adventitious septa formation than QM9414. A previous study showed that the extensively branched hyphae of *T. reesei* DES-15 improved cellulase production [45]. The morphological analyses also suggest a correlation between cellulase production and morphology in *T. reesei*.

Gene transcription analyses revealed the molecular mechanisms behind CCR release and cellulase overproduction in mutants MG-9-3, MG-9-3-30, and M-5 (**Figure 3-10**). The findings indicate that when high-concentration glucose is present, the cellulase gene expressions in these mutants are upregulated in comparison to the parent strain. This is because there are remarkable enhancements in the transcriptional activators such as *xyr1*, *ace2,* and *bglr* in the mutants [7]. Notably, the XYR1-encoding gene expression levels in MG-9-3, MG-9-3-30, and M-5 were 35.3-fold, 32.1, and 7.2-fold more significant than in QM9414 on glucose. Studies on XYR1 overexpression in QM9414 and RUT-C30 revealed improvements in cellulase production [46,47]. The ACE3 regulator has been reported to mediate cellulase production directly and indirectly by

binding to promoters of cellulase genes, the *xyr1*-encoding gene, and the cellulose response transporter gene *crt1* [48]. The significantly increased degree of the BglR-encoding gene, which upregulates genes encoding β-glucosidases including *bgl2*, *cel1b*, *cel3b,* and *cel3c* [49], was highlighted in the transcriptional analyses of MG-9-3-30 and M-5. BGLII is able to generate transglycosylation products from glucose, stimulating cellulose biosynthesis in *T. reesei* [37]. The reduced influence of repressors could be another reason for the cellulose overproduction in the sorted mutants. Previous studies identified several CRE1- and ACE1-binding sites in promoter regions of cellulase and activator genes, which controlled the gene expression [50,51]. Thus, the decrease could result from mutations in repressor proteins or their binding sites in cellulase or transcription factor genes. In M-5, the abundance of cellulase-negative regulators over positive ones could explain its low cellulase production on glucose as the sole carbon source. Another plausible explanation is the considerably increased gene expression of Trichodermapepsin, which may have caused modifications or degradation of cellulase in the media [52]. A thorough comparative genomic analysis of QM9414 and selected mutants is necessary in order to comprehend mutations linked to enhanced cellulase production in high-concentration glucose.

Multiple mutations were discovered after sequencing and analyzing the genome of mutants related to QM9414 (**Figure 3-11 and Table 3-2**). Significantly, the I352N mutation in the *bgl2* was predicted to impact the activity of BGLII in the MG lineage. This finding is consistent with a prior study that observed an increase in cellulase expression on cellobiose due to a single-nucleotide mutation in the cellulase gene [37]. Besides, the change in the Thioredoxin-encoding gene could play a partial role in the cellulase synthesis in the M lineage. This hypothesis agrees with a previous report that compared the genomes of *T. reesei* RUT-C30 and its hyper-cellulolytic mutant SS-II [53]. From the 2nd generation, mutation of the small GTPase RAC1 could lead to changes in hyphae morphology (**Figure 3-8**). A hyperbranching phenotype and enhancements in cellulase activity on lactose were observed when the *rac1* was disrupted [53]. Furthermore, a nonsense mutation in the acetyl xylan esterase tr70021, which is involved in cell-matrix adhesion, may have caused the formation of fibrous materials around the fungal hyphae. For the glucose uptake, the glucose transporter SPT1 (tr50618) was mutated at the promoter region from the 2nd mutation generation, and the maltose permease (69957) was mutated at the exon region. Finally, the S447F mutation of the

VEA was identified in the M-5 mutant. The overexpression of *vel1* transcript levels increases the upregulation of *xyr1*, increasing transcription levels of cellulase [54].

3.5 References

[1] Saloheimo M, Pakula TM. The cargo and the transport system: Secreted proteins and protein secretion in *Trichoderma reesei* (*Hypocrea jecorina*). Microbiology 2012;158:46–57. https://doi.org/10.1099/mic.0.053132-0.

[2] Adav SS, Sze SK. *Trichoderma* Secretome. Biotechnol Biol *Trichoderma*, Elsevier; 2014, p. 103–14. https://doi.org/10.1016/b978-0-444-59576-8.00008-4.

[3] Li C, Lin F, Zhou L, Qin L, Li B, Zhou Z, et al. Cellulase hyper-production by *Trichoderma reesei* mutant SEU-7 on lactose. Biotechnol Biofuels 2017;10:228. https://doi.org/10.1186/s13068-017-0915-9.

[4] Noguchi T, Saito H, Nishiyama R, Yoshida N, Matsubayashi T, Teshima Y, et al. Isolation of a cellulase hyperproducing mutant strain of *Trichoderma reesei*. Bioresour Technol Reports 2021;15:100733. https://doi.org/10.1016/j.biteb.2021.100733.

[5] Peterson R, Nevalainen H. *Trichoderma reesei* RUT-C30 - Thirty years of strain improvement. Microbiology 2012;158:58–68. https://doi.org/10.1099/mic.0.054031-0.

[6] Shida Y, Furukawa T, Ogasawara W. Deciphering the molecular mechanisms behind cellulase production in *Trichoderma reesei*, the hyper-cellulolytic filamentous fungus. Biosci Biotechnol Biochem 2016;80:1712–29. https://doi.org/10.1080/09168451.2016.1171701.

[7] Zimmermann C, Till P, Danner C, Mach-Aigner AR. Genetic Regulation Networks in Cellulase and Hemicellulase Production in an Industrially Applied Cellulase Producer *Trichoderma reesei*. Handb Biorefinery Res Technol 2023:1–23. https://doi.org/10.1007/978-94-007-6724-9_25-1.

[8] Gao F, Hao Z, Sun X, Qin L, Zhao T, Liu W, et al. A versatile system for fast screening and isolation of *Trichoderma reesei* cellulase hyperproducers based on DsRed and fluorescence-assisted cell sorting. Biotechnol Biofuels 2018;11:261. https://doi.org/10.1186/s13068-018-1264-z.

[9] Luu XC, Shida Y, Suzuki Y, Sato N, Nakumura A, Ogasawara W. A novel high-throughput approach for transforming filamentous fungi employing a droplet-based microfluidic platform. N Biotechnol 2022;72:149–58. https://doi.org/10.1016/j.nbt.2022.11.003.

[10] Wang G, Jia W, Chen N, Zhang K, Wang L, Lv P, et al. A GFP-fusion coupling

FACS platform for advancing the metabolic engineering of filamentous fungi. Biotechnol Biofuels 2018;11:232. https://doi.org/10.1186/s13068-018-1223-8.

[11] Bleichrodt RJ, Read ND. Flow cytometry and FACS applied to filamentous fungi. Fungal Biol Rev 2019;33:1–15. https://doi.org/10.1016/j.fbr.2018.06.001.

[12] Samlali K, Alves CL, Jezernik M, Shih SCC. Droplet digital microfluidic system for screening filamentous fungi based on enzymatic activity. Microsystems Nanoeng 2022;8:123. https://doi.org/10.1038/s41378-022-00456-1.

[13] Beneyton T, Wijaya IPM, Postros P, Najah M, Pascal L, Couvent A, et al. High-throughput screening of filamentous fungi using nanoliter- range droplet-based microfluidics 2016;6:27223. https://doi.org/10.1038/srep27223.

[14] Kintses B, van Vliet LD, Devenish SRA, Hollfelder F. Microfluidic droplets: New integrated workflows for biological experiments. Curr Opin Chem Biol 2010;14:548–55. https://doi.org/10.1016/j.cbpa.2010.08.013.

[15] Kaminski TS, Scheler O, Garstecki P. Droplet microfluidics for microbiology: Techniques, applications and challenges. Lab Chip 2016;16:2168–87. https://doi.org/10.1039/c6lc00367b.

[16] Beneyton T, Thomas S, Griffiths AD, Nicaud JM, Drevelle A, Rossignol T. Droplet-based microfluidic high-throughput screening of heterologous enzymes secreted by the yeast *Yarrowia lipolytica*. Microb Cell Fact 2017;16:18. https://doi.org/10.1186/s12934-017-0629-5.

[17] Bachmann H, Fischlechner M, Rabbers I, Barfa N, Dos Santos FB, Molenaar D, et al. Availability of public goods shapes the evolution of competing metabolic strategies. Proc Natl Acad Sci U S A 2013;110:14302–7. https://doi.org/10.1073/pnas.1308523110.

[18] Neun S, Zurek PJ, Kaminski TS, Hollfelder F. Ultrahigh throughput screening for enzyme function in droplets. vol. 643. 1st ed. Elsevier Inc.; 2020. https://doi.org/10.1016/bs.mie.2020.06.002.

[19] Agresti JJ, Antipov E, Abate AR, Ahn K, Rowat AC, Baret JC, et al. Ultrahigh-throughput screening in drop-based microfluidics for directed evolution. Proc Natl Acad Sci U S A 2010;107:4004–9. https://doi.org/10.1073/pnas.0910781107.

[20] He R, Ding R, Heyman JA, Zhang D, Tu R. Ultra-high-throughput picoliter-droplet microfluidics screening of the industrial cellulase-producing filamentous fungus *Trichoderma reesei*. J Ind Microbiol Biotechnol 2019;46:1603–1610.

https://doi.org/10.1007/s10295-019-02221-2.

[21] Shida Y, Yamaguchi K, Nitta M, Nakamura A, Takahashi M, Kidokoro SI, et al. The impact of a single-nucleotide mutation of bgl2 on cellulase induction in a *Trichoderma reesei* mutant. Biotechnol Biofuels 2015;8:230. https://doi.org/10.1186/s13068-015-0420-y.

[22] Daranagama ND, Suzuki Y, Shida Y, Ogasawara W. Involvement of Xyr1 and Are1 for Trichodermapepsin Gene Expression in Response to Cellulose and Galactose in *Trichoderma reesei*. Curr Microbiol 2020. https://doi.org/10.1007/s00284-020-01955-y.

[23] Yuan H, Zhou Y, Lin Y, Tu R, Guo Y, Zhang Y, et al. Microfluidic screening and genomic mutation identification for enhancing cellulase production in *Pichia pastoris*. Biotechnol Biofuels Bioprod 2022;15:50. https://doi.org/10.1186/s13068-022-02150-w.

[24] Watanabe M, Serizawa M, Sawada T, Takeda K, Takahashi T, Yamamoto N, et al. A novel flow cytometry-based cell capture platform for the detection, capture and molecular characterization of rare tumor cells in blood. J Transl Med 2014;12:143. https://doi.org/10.1186/1479-5876-12-143.

[25] Bradford MM. A rapid and sensitive method for the quantitation of microgram quantities of protein utilizing the principle of protein-dye binding. Anal Biochem 1976;72:248–54. https://doi.org/https://doi.org/10.1016/0003-2697(76)90527-3.

[26] Mathis H, Margeot A, Bouix M. Optimization of flow cytometry parameters for high-throughput screening of spores of the filamentous fungus *Trichoderma reesei*. J Biotechnol 2020;321:78–86. https://doi.org/10.1016/j.jbiotec.2020.05.015.

[27] Kaminski TS, Scheler O, Garstecki P. Droplet microfluidics for microbiology: techniques, applications and challenges. Lab Chip 2016;16:2168. https://doi.org/10.1039/c6lc00367b.

[28] Nakamura A, Honma N, Tanaka Y, Suzuki Y, Shida Y, Tsuda Y, et al. 7-Aminocoumarin-4-acetic Acid as a Fluorescent Probe for Detecting Bacterial Dipeptidyl Peptidase Activities in Water-in-Oil Droplets and in Bulk. Anal Chem 2021;94:2416–2424. https://doi.org/10.1021/acs.analchem.1c04108.

[29] Saito K, Ota Y, Tourlousse DM, Matsukura S, Fujitani H, Morita M, et al. Microdroplet-based system for culturing of environmental microorganisms using FNAP-sort. Sci Rep 2021;11:9506. https://doi.org/10.1038/s41598-021-88974-2.

[30] Yanakieva D, Elter A, Bratsch J, Friedrich K, Becker S, Kolmar H. FACS-Based Functional Protein Screening via Microfluidic Co-encapsulation of Yeast Secretor and Mammalian Reporter Cells. Sci Rep 2020;10:10182. https://doi.org/10.1038/s41598-020-66927-5.

[31] Yu Z, Geisler K, Leontidou T, Young REB, Vonlanthen SE, Purton S, et al. Droplet-based microfluidic screening and sorting of microalgal populations for strain engineering applications. Algal Res 2021;56:102293. https://doi.org/10.1016/j.algal.2021.102293.

[32] Zheng G, Cui Y, Lu L, Guo M, Hu X, Wang L, et al. Microfluidic chemostatic bioreactor for high-throughput screening and sustainable co-harvesting of biomass and biodiesel in microalgae. Bioact Mater 2023;25:e02111. https://doi.org/10.1016/j.bioactmat.2022.07.012.

[33] Yang Z, Qiao Y, Li J, Wu FG, Lin F. Novel Type of Water-Soluble Photosensitizer from *Trichoderma reesei* for Photodynamic Inactivation of Gram-Positive Bacteria. Langmuir 2020;36:13227–35. https://doi.org/10.1021/acs.langmuir.0c02109.

[34] Schmoll M, Esquivel-Naranjo EU, Herrera-Estrella A. *Trichoderma* in the light of day - Physiology and development. Fungal Genet Biol 2010;47:909–16. https://doi.org/10.1016/j.fgb.2010.04.010.

[35] Alfiky A. Effects of ultraviolet irradiation on the in vitro antagonistic potential of *Trichoderma* spp. against soil-borne fungal pathogens. Heliyon 2019;5. https://doi.org/10.1016/j.heliyon.2019.e02111.

[36] Dos Santos Castro L, Pedersoli WR, Antoniêto ACC, Steindorff AS, Silva-Rocha R, Martinez-Rossi NM, et al. Comparative metabolism of cellulose, sophorose and glucose in *Trichoderma reesei* using high-throughput genomic and proteomic analyses. Biotechnol Biofuels 2014;7. https://doi.org/10.1186/1754-6834-7-41.

[37] Shida Y, Yamaguchi K, Nitta M, Nakamura A, Takahashi M, Kidokoro SI, et al. The impact of a single-nucleotide mutation of *bgl2* on cellulase induction in a *Trichoderma reesei* mutant. Biotechnol Biofuels 2015;8:1–18. https://doi.org/10.1186/s13068-015-0420-y.

[38] Silva JCR, Salgado JCS, Vici AC, Ward RJ, Polizeli MLTM, Guimarães LHS, et al. A novel *Trichoderma reesei* mutant RP698 with enhanced cellulase production. Brazilian J Microbiol 2021;51:39. https://doi.org/10.1007/s42770-019-00167-2.

[39] Han L, Liu K, Ma W, Jiang Y, Hou S, Tan Y, et al. Redesigning transcription factor Cre1 for alleviating carbon catabolite repression in *Trichoderma reesei.* Synth Syst Biotechnol 2020;5:230–5. https://doi.org/10.1016/j.synbio.2020.07.002.

[40] Shibata N, Kakeshita H, Igarashi K, Takimura Y, Shida Y, Ogasawara W, et al. Disruption of alpha-tubulin releases carbon catabolite repression and enhances enzyme production in *Trichoderma reesei* even in the presence of glucose. Biotechnol Biofuels 2021;14:1–16. https://doi.org/10.1186/s13068-021-01887-0.

[41] Li Y, Yu J, Zhang P, Long T, Mo Y, Li J, et al. Comparative transcriptome analysis of Trichoderma reesei reveals different gene regulatory networks induced by synthetic mixtures of glucose and β-disaccharide. Bioresour Bioprocess 2021;8. https://doi.org/10.1186/s40643-021-00411-4.

[42] Li Y, Liu C, Bai F, Zhao X. Overproduction of cellulase by *Trichoderma reesei* RUT C30 through batch-feeding of synthesized low-cost sugar mixture. Bioresour Technol 2016;216:503–10. https://doi.org/10.1016/j.biortech.2016.05.108.

[43] Zhang P, Li Q, Chen Y, Peng N, Liu W, Wang X, et al. Induction of cellulase production in *Trichoderma reesei* by a glucose-sophorose mixture as an inducer prepared using stevioside. RSC Adv 2022;12:17392. https://doi.org/10.1039/d2ra01192a.

[44] Tiina N-S, Marja P, Jarno K, Jari V, Merja P, Markku S. Genetic Modification of Carbon Catabolite Repression in *Trichoderma reesei* for Improved Protein Production. Appl Environ Microbiol 2009;75:4853–60. https://doi.org/10.1128/AEM.00282-09.

[45] He R, Li C, Ma L, Zhang D, Chen S. Effect of highly branched hyphal morphology on the enhanced production of cellulase in *Trichoderma reesei* DES-15. 3 Biotech 2016;6:1–10. https://doi.org/10.1007/s13205-016-0516-5.

[46] Zheng F, Yang R, Cao Y, Zhang W, Lv X, Meng X, et al. Engineering *Trichoderma reesei* for hyperproduction of cellulases on glucose to efficiently saccharify pretreated corncobs. J Agric Food Chem 2020;68:12671–82. https://doi.org/10.1021/acs.jafc.0c04663.

[47] Wang S, Liu G, Wang J, Yu J, Huang B, Xing M. Enhancing cellulase production in *Trichoderma reesei* RUT C30 through combined manipulation of activating and repressing genes. J Ind Microbiol Biotechnol 2013;40:633–41. https://doi.org/10.1007/s10295-013-1253-y.

[48] Zhang J, Chen Y, Wu C, Liu P, Wang W, Wei D. The transcription factor ACE3 controls cellulase activities and lactose metabolism via two additional regulators in the fungus *Trichoderma reesei*. J Biol Chem 2019;294:18435–50. https://doi.org/10.1074/jbc.RA119.008497.

[49] Nitta M, Furukawa T, Shida Y, Mori K, Kuhara S, Morikawa Y, et al. A new Zn(II) 2Cys 6-type transcription factor BglR regulates β-glucosidase expression in *Trichoderma reesei*. Fungal Genet Biol 2012;49:388–97. https://doi.org/10.1016/j.fgb.2012.02.009.

[50] Ilmén M, Onnela M-L, Klemsdal S, Keränen S, Penttilä M. Functional analysis of the cellobiohydrolase I promoter of the filamentous fungus *Trichoderma reesei*. Mol Gen Genet MGG 1998;257:386. https://doi.org/10.1007/s004380050661.

[51] Takashima S, Iikura H, Nakamura A, Masaki H, Uozumi T. Analysis of Cre1 binding sites in the *Trichoderma reesei cbh1* upstream region. FEMS Microbiol Lett 1996;145:361–6. https://doi.org/10.1016/S0378-1097(96)00432-6.

[52] Daranagama ND, Shioya K, Yuki M, Sato H, Ohtaki Y, Suzuki Y, et al. Proteolytic analysis of *Trichoderma reesei* in celluase-inducing condition reveals a role for trichodermapepsin (TrAsP) in cellulase production. J Ind Microbiol Biotechnol 2019;46:831–42. https://doi.org/10.1007/s10295-019-02155-9.

[53] Liu P, Lin A, Zhang G, Zhang J, Chen Y, Shen T, et al. Enhancement of cellulase production in *Trichoderma reesei* RUT-C30 by comparative genomic screening. Microb Cell Fact 2019;18:81. https://doi.org/10.1186/s12934-019-1131-z.

[54] Karimi Aghcheh R, Németh Z, Atanasova L, Fekete E, Paholcsek M, Sándor E, et al. The VELVET A Orthologue VEL1 of *Trichoderma reesei* Regulates Fungal Development and Is Essential for Cellulase Gene Expression. PLoS One 2014;9:e112799.

Chapter 4: General conclusion

The filamentous fungus *Trichoderma reesei* is the most well-known cellulase producer in the biorefinery industry. Droplet-based microfluidic technology is a powerful tool for single-cell cultivation and rapid isolation of bacteria, yeasts, and algae. However, it has been of limited use for studies of filamentous fungi due to the fast growth of their branched hyphae. The long regeneration time for fungal protoplasts and low-throughput screening methods are inherent problems for current genetic transformation techniques. This thesis describes a series of studies that have contributed to developing novel high-throughput workflows for genetic modifications and strain improvements of the filamentous fungus *T. reesei* employing a droplet-based microfluidic platform.

In the first study, a novel high-throughput workflow for the genetic transformation of the filamentous fungus *T. reesei* has been established using a droplet-based microfluidic platform. This strategy enabled the encapsulation of single fungal spores and protoplasts, the induction of gene expression, and the rapid detection and enrichment of either growing fungi or regenerating fungal transformants from a large candidate library. The total time for the approach is about two weeks, with one round of droplet cultivation and screening, two rounds of genomic evaluation, and one round of single-spore separation. The proposed workflow is expected to open up opportunities for accelerating the genetic modification of filamentous fungi in research and practical applications. In this field of research, studies on the molecular mechanisms involved in gene function and expression should become rapid and insightful. By means of this novel method, industrial fungal strains can be generated in a short period and used to produce bioactive compounds, hydrolytic enzymes, or recombinant proteins.

In the second one, the thesis proposes a novel repeated uHTP workflow for the random mutagenesis of the filamentous fungus *T. reesei* by employing a droplet-based microfluidic platform. Using this novel method, the study generated several CCR-releasing T. reesei strains with cellulase production improvements on cellulose with the supplement of a high glucose dosage. Additionally, the study elucidated the regulatory network behind the enhanced enzyme production in the generated mutants under the repression condition. This novel approach can accelerate the industrial strain design and high-throughput screening of *T. reesei* strains capable of carbon catabolite repression release and cellulase hyper-production and help reduce cellulase production costs.

Chapter 5: Published paper

(1) 2022.12.25 New Biotechnology Vol. 72 pp.149-158

"*A novel high-throughput approach for transforming filamentous fungi employing a droplet-based microfluidic platform*"

Xuan Chinh Luu, Yosuke Shida, Yoshiyuki Suzuki, Naomi Sato, Akihiro Nakamura, Wataru Ogasawara

(2) 2023.8.3 Bioscience, Biotechnology and Biochemistry zbad108 (Online)

"*Ultra-high-throughput screening of Trichoderma reesei strains capable of carbon catabolite repression release and cellulase hyper-production using a microfluidic droplet platform*"

Xuan Chinh Luu, Yosuke Shida, Yoshiyuki Suzuki, Daiki Kuwahara, Takeshi Fujimoto, Yuka Takahashi, Naomi Sato, Akihiro Nakamura, Wataru Ogasawara

Acknowledgment

This study was conducted under the supervision of Professor Wataru Ogasawara at the Hakko Science Laboratory, Nagaoka University of Technology. I am grateful for the invaluable guidance and support from Professor Ogasawara, Associate Professors Yosuke Shida and Yoshiyuki Suzuki, and Assistant Professor Akihiro Nakamura. My sincerest thanks to them for their enthusiasm in guiding me throughout my study at Nagaoka University of Technology.

I would like to express my profound appreciation to all the staff and members of the Hakko Science Laboratory for their generous support during the implementation of the study. Special thanks to the members of the laboratory responsible for sequencing and analyzing genomic data in this research. Lastly, my family and friends have always been a strong spiritual support and encouragement for me, and I am thankful for their unwavering support.

Luu Xuan Chinh
October, 2023